University of L'Aquila

Department of Biotechnological and Applied Clinical Sciences

PhD in Experimental Medicine

Curriculum: Biochemistry

XXXII cycle

Title

Biochemical and molecular characterization of GES and NDM engineered variants: interactions with β-lactams and inhibitors

SSD BIO/12

Candidate

Alessandra Piccirilli

Coordinator:

Prof.ssa Mariagrazia Perilli

Tutor:

Prof. Gianfranco Amicosante

A.A. 2018/2019

Table of Contents

Summary

β-lactams resistance occurs when bacteria causing an infection survive after being exposed to a drug that, under normal conditions, would kill it or inhibit its growth. As a result, these surviving strains multiply and spread thanks to the lack of competition from other strains sensitive to the same drug. Carbapenems and 3rd generation cephalosporins resistant-Enterobacteriaceae represent one of the most critical group against which there is an urgent need to develop new antibiotics. These bacteria are common pathogens causing severe infections such as bloodstream infections, pneumonia, complicated urinary tract infections and complicated intra-abdominal infections. According to the Centers for Disease Control and Prevention (CDC) definition, carbapenem-resistant Enterobacteriaceae (CRE) are defined as any Enterobacteriaceae which are resistant to carbapenems or are documented to produce a carbapenemase. There are three major mechanisms by which Enterobacteriaceae become resistant to carbapenems: enzyme production, efflux pumps and porin mutations. Of these, enzyme production is the main resistance mechanism. Gram-negative bacteria generally develop resistances through the production of β-lactam-hydrolyzing enzymes, called β-lactamases. In the present study, two classes of these enzymes were analyzed and characterized also in association with a new molecule with inhibitory activity. In the first part of the thesis, the role of the Ω-loop (159-182 residues) in GES class A β-lactamase is well investigated. Recent studies report that, in these enzymes, carbapenemase activity is attributed to a single amino acid substitution at position 170. In our study, we decided to investigate other positions of the Ω-loop, in particular residue 174, occupied by a proline residue. This residue is well conserved in class A β-lactamases. Our kinetic and computational data have demonstrated that not only 170 residue is important in the carbapenemase activity, but also residue 174. Being Ω-loop a mobile structure of class A β-lactamases, we suppose that any mutation in this region could modify the substrate hydrolysis of the enzyme, not only toward carbapenems. The second part of the thesis is addressed to the involvement of some hydrophobic residues on the β-lactams hydrolysis by NDM-1 (subclass B1 β-lactamase). In particular, our attention was focalized on leucine residues located in the Loop 10 of this enzyme. In NDM-1, residue Y229 (belonging to Loop 10) forms hydrophobic contacts with several amino acids, including L218, L221 and L269 in the top of it and also with residue L209 under it. For this reason, we have pointed the attention on L218, L221 and L269 residues. Our results have demonstrated that the replacement of these leucines reduces the enzyme catalytic activity toward β-lactams. In addition, we studied the effect of Y229W substitution in our laboratory variant (L209F) with a drastic reduction in β-lactamase activity. This substitution is able to restore the catalytic activity in the L209F mutant enzyme.

Actually, one of the most problem is related to the absence of inhibitors for metallo-β-lactamases in clinical therapy. For this reason, in collaboration with VenatoRx Pharmaceuticals (Malvern, PA, USA), we tested a new boronic acid, VNRX-5133, combinated with cefepime (taniborbactam), in NDM-1 and some engineered NDM-1 mutants able to hydrolyze β-lactams very efficiently. Taniborbactam was also tested in NDM-1-producing Enterobacteriaceae clinical strains. Our results revealed that the addition of VNRX-5133 restored cefepime activity in both NDM-1 producing recombinant strains of *E. coli* and clinical isolates of Enterobacteriaceae. The development of new non-β-lactam inhibitors would provide a new opportunity for the treatment of bacterial infections with existing antibiotics.

Chapter 1

General introduction: β-lactams and β-lactamases

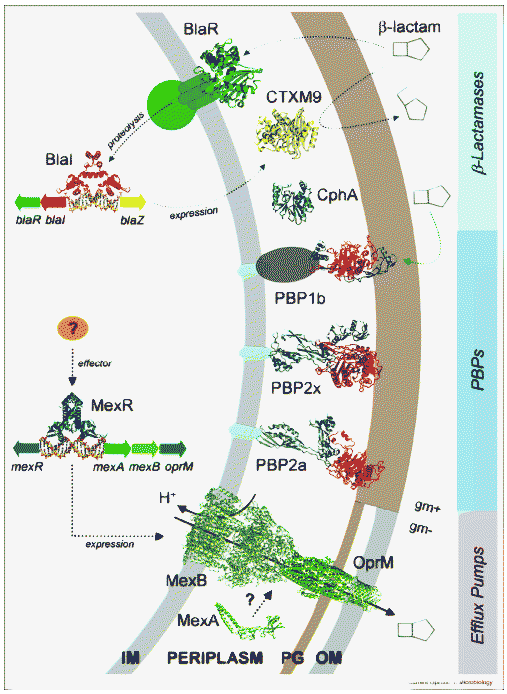

By Wilke MS et al., 2005

1.1 β-lactams

β-Lactam antibiotics are the most frequent prescribed antibacterial agents in the hospital settings due to their safety, efficacy and breadth of spectrum of activity (1). To better understand the mechanisms by which β-lactamases have changed the status of β-lactams in our therapeutic choice, it is important to review how β-lactams kill bacteria. All these antibiotics have a common bacterial killing mechanism that involves the inhibition of penicillin-binding proteins (PBPs), enzymes required for the terminal step of bacterial cell wall synthesis in both Gram-negative and Gram-positive bacteria (2). In the 1960s, Strominger noted that the β-lactam ring is sterically similar to the terminal D-Ala-D-Ala dipeptide of the nascent peptidoglycan in the dividing bacterial cell. The mechanism involves binding of a β-lactam to an active site serine found in all functional PBPs (3). The resulting inactive acyl enzyme may then slowly hydrolyze the antibiotic to form a microbiologically inactive entity (4). Cell death may occur as a result of inhibiting one or more of these PBPs. Based on the structures of the *core* ring and discovery, the four main classes of β-lactams include penicillins, cephalosporins, carbapenems and monobactams (Figure 1).

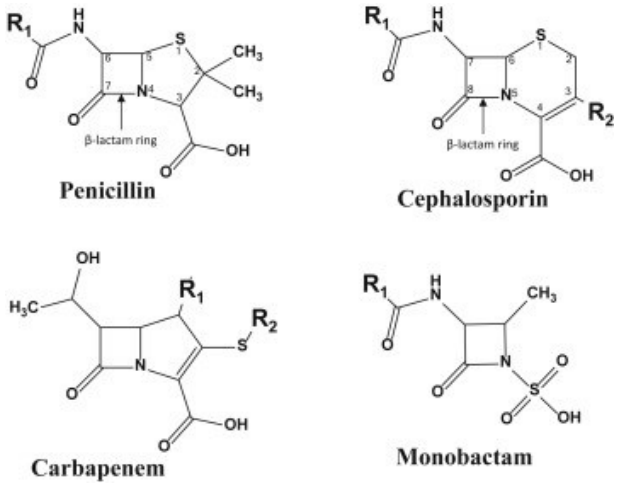

Figure 1: The four main classes of β-lactams

1.1.1 Penicillins

Penicillin G (benzylpenicillin) was the first β-lactam to be used clinically, in particular to treat streptococcal infections for which it had high potency. The selection of penicillin-resistant penicillinase-producing staphylococci in patients treated with penicillin G led to decrease use of this agent, and prompted the search for more penicillins. Penicillins are divided, on the basis of antibacterial activity into the following subclasses: natural penicillins (penicillin G, penicillin V), β-lactamase resistant penicillins (methicillin, oxacillin), aminopenicillins (ampicillin, amoxicillin), carboxypenicillins (carbenicillin, ticarcillin), ureidopenicillins (piperacillin, mezlocillin), penicillin/inhibitor combination (clavulanic acid, tazobactam, sulbactam). The increase of β-lactamases number has compromised the use of penicillins, as single agents, limiting the therapeutic use of these agents as monotherapy (5). Ampicillin, amoxicillin, piperacillin, and ticarcillin have continued to be useful, primarily as a result of their combination with an appropriate β-lactamase inhibitor.

1.1.2 Cephalosporins

Cephalosporins are a subgroup of β-lactams isolated for the first time from *Cephalosporium acremonium* cultures. The natural cephalosporins had modest antibacterial activity but had a stable ring system that made them ideal for chemical modification. For this reason, to date five generations of semisynthetic cephalosporins have been synthetized which are much more potent than their natural counterparts. First-generation cephalosporins (e.g. cefazolin, cephaloridine, and cephalothin) are more effective against Gram-positive bacteria, though they also work against some Gram-negative bacteria. Second-generation cephalosporins (e.g. cefoxitin, cefuroxime and ceftriaxone) have variable activity against Gram-positive bacteria but increased activity against Gram-negative bacteria. Third-generation cephalosporins (e.g. ceftazidime, cefotaxime, and cefixime) have an extended-spectrum of activity against Gram-negative bacilli and most members of Enterobacteriaceae, including some strains that are resistant to previous generations of cephalosporins. They may be used to treat hospital-acquired infections, although increasing levels of extended-spectrum β-lactamases are reducing the clinical utility of this antibiotics (1). These enzymes, in addition to both serine and metallo-carbapenemases, have severely compromised the activity of almost all penicillins and cephalosporins, necessitating the development of combination therapy with other β-lactams, β-lactamase inhibitors, or antibiotics from other classes. These cephalosporins are also able to be effective against *Escherichia coli, Klebsiella pneumoniae, Proteus mirabilis, Neisseria meningitidis, Hemophilus influenzae, Neisseria gonorrhoeae*. Fourth-generation cephalosporins (e.g. cefepime, cefpirome, and cefozopran) work against both Gram-positive and Gram-negative bacteria. They are generally used

for more severe infections or for those with weakened immune systems. Further, fourth-generation cephalosporins remain effective against β-lactamase-overproducing Gram-negative strains resistant to other extended-spectrum cephalosporins. They also possess increased penetration through the porin channels, which is more rapid than that of ceftazidime. Concerning the fifth generation cephalosporins it is important to mention ceftaroline, ceftobiprole and ceftolozane. Ceftaroline and ceftobiprole are a broad-spectrum cephalosporins with bactericidal in vitro activity against common Gram-positive organisms but not against extended-spectrum β-lactamase-producing Enterobacteriaceae. Ceftobiprole has been subjected to various clinical trials that have led to its approval in Spain for the treatment of nosocomial pneumonia, excluding that associated with mechanical ventilation, and community-acquired pneumonia. Ceftolozane-tazobactam is a cephalosporin β-lactam and β-lactamase inhibitor marketed as a fixed-dose combination agent for the treatment of complicated urinary tract and intraabdominal infections.

1.1.3 Carbapenems

Carbapenems are broad-spectrum antibiotics with activity against Gram-positive and Gram-negative bacteria. Carbapenems, in general, bind strongly to PBP2 in Gram-negative bacteria, but may also bind to PBP1a, 1b, and 3, thus providing supplemental killing mechanisms that may serve to lessen the emergence of resistance. Carbapenems are notable for their stability to most β-lactamases, with the exception of the emerging carbapenemases found primarily in Gram-negative bacteria (5). Because of the lability of imipenem to hydrolysis by the human renal dehydropeptidase (DHP) causing inactivation of the drug, it is dosed in combination with cilastatin, a DHP inhibitor that also acts as a nephroprotectant (6). Based on the potent broad-spectrum activity of the early carbapenems, other related agents, including meropenem, ertapenem, and doripenem, have been developed for global use, with generally the same group of organisms included in their activity spectrum. All these carbapenems are more chemically stable than imipenem. Like imipenem, they are stable to most β-lactamases, other than carbapenemases (5).

1.1.4 Monobactams

Unlike the penicillins, cephalosporins and carbapenems, which are bicyclic compounds, the monobactams are monocyclic β-lactam antibiotics. Aztreonam, a total synthetic monobactam, is the only member of this subgroup approved for therapeutic use. It exhibits potent and specific activity against a wide range of β-lactamase-producing and non-producing aerobic Gram-negative bacteria, including *Pseudomonas aeruginosa*. The emergence of extended-spectrum-β-lactamases (ESBLs) and the serine carbapenemases has since rendered it less effective against multidrug-resistant β-

lactamase-producing organisms. However, the monobactam nucleus is not a good substrate for hydrolysis by metallo-β-lactamases (MBLs), thus leading to a unique opportunity for this monobactam to be used in combination therapy with a serine β-lactamase inhibitor to treat infections caused by multi-β-lactamase-producing bacteria (7).

1.2 Mechanisms of resistance to β-lactams

Antibiotic bacterial resistance can be either natural (intrinsic) or acquired. In acquired resistance the bacterial population is initially susceptible to antibacterial agents but the bacteria undergo changes either by acquisition of plasmid and transposon or by chromosome mutation. Intrinsic resistance refers to the existence of genes in bacterial genomes that could generate a resistance phenotype. There are four mechanisms by which bacteria can overcome β-lactam antibiotics (8):

(i) changes in the active site of PBPs can lower the affinity for β-lactam antibiotics and subsequently increase resistance to these agents. Methicillin resistance in *Staphylococcus* spp. is the most known example of this resistance. Although the cause for this resistance is heterogeneous, it is often conferred by acquisition of the *mecA* gene which produces PBP2a (also denoted PBP2') (9). Through natural transformation and recombination with DNA from other organisms, *Neisseria* spp. and *Streptococcus* spp. have acquired highly resistant, altered PBPs (10, 11).

(ii) In order to access PBPs on the surface of the inner membrane, β-lactams must either diffuse through or directly traverse porin channels in the outer membrane of Gram-negative bacterial cell walls. Resistance to β-lactams can occur when these porin proteins are modified such that they are not produced in a fully active form. Some Gram-negative bacteria show resistance to carbapenems based on loss and or reduction of these outer membrane proteins, such as the loss of OprD, which is associated with resistance to imipenem and reduced susceptibility to meropenem in the non-fermenter *P. aeruginosa* (12). Point mutations or insertion sequences in porin-encoding genes can produce proteins with decreased function and thus lower permeability to β-lactams. The disruption of porin proteins alone is not always sufficient for producing the resistance phenotype, and typically this mechanism is found in combination with β-lactamase expression (13).

(iii) Efflux pumps mechanism, as part of either acquired or intrinsic resistance phenotype, is capable of exporting a wide range out of the bacterial cell. These pumps are important to determine multidrug resistance in many Gram-negative pathogens, particularly *P.*

aeruginosa and *Acinetobacter* spp. In *P. aeruginosa*, upregulation of the MexA-MexB-OprD system, in combination with low outer membrane permeability, can contribute to decreased susceptibility to penicillins and cephalosporins, as well as quinolones, tetracycline, and chloramphenicol (14-16).

(iv) Production of β-lactamases is the most common and important mechanism of resistance in Gram-negative bacteria and will be the focus of this thesis.

1.3 β-lactamases: history, function and classification

β-lactamases are the most important enzymes that have driven research in academic laboratories since the early 1940s. β-Lactamases are versatile enzymes with a limited range of molecular structures found in a diversity of bacterial species. They have the ability to hydrolyze chemical compounds containing a β-lactam ring. β-lactamases are ancient enzymes that existed even in the absence of the pressure of therapeutic antibiotics. Modern phylogenetic analyses have estimated the age of serine β-lactamases to be more than 2 billion years old (17), with plasmid-encoded β-lactamases appearing millions of years ago (18). Additional metagenomic analyses of ancient environmental samples identified a novel metallo-β-lactamase, isolated from a 14th century bone sample, with an unusual substrate profile unlike that of other known MBLs. However, there are still organisms with no confirmed β-lactamases, notably *Streptococcus pneumoniae*, *Streptococcus pyogenes*, *Helicobacter pylori*, *Mycoplasma* spp. and the *Chlamydiae*, probably due to the production of homologous enzymes with the ability to inactivate β-lactams (19). In the early to mid-1940s, the first clinically relevant reports of resistant bacteria due to production of β-lactamase described a staphylococcal penicillinase able to hydrolyze penicillin G (20,21). As more β-lactams were introduced into the clinic, resistance to each agent was observed; the growing number of β-lactam antibiotics increased the selective pressure on bacteria, promoting the survival of organisms through the production of β-lactamases (22). Indeed, β-lactamases were discovered in a great number of Gram-negative bacteria including Enterobacteriaceae and non-fermenters strains such as *P. aeruginosa*. At this time, more than 2770 naturally occurring β-lactamases are now identified and they possess a unique amino acid sequence and characteristic hydrolysis profile (23). These enzymes are both encoded by chromosome and plasmids. In Gram-positive bacteria, β-lactamases are either bound to the cytoplasmic membrane or excreted into the extracellular space, whereas in Gram-negative bacteria they are located in the periplasmic space (24). β-lactamases have been classified biochemically into two broad families, serine-β-lactamases (SBLs) and metallo-β-lactamases (MBLs), according to the mechanism by which they perform hydrolysis. Serine-β-lactamases hydrolyze β-lactams by the formation of an acyl

enzyme with an active-site serine (25). Metallo-β-lactamases need one or two essential zinc ions for β-lactam hydrolysis (26). As shown in table 1, two major classification schemes are currently used for β-lactamases: Ambler molecular classification, which divides β-lactamases into four molecular classes (A, B, C and D) on the basis of their amino acid sequence, and the Bush–Jacoby–Medeiros functional classification scheme, based on substrate and inhibitor profiles. This classification has recently been updated in order to accommodate newly discovered β-lactamses (27-29). Enzymes are still differentiated with respect to the relative hydrolysis of the β-lactam substrates, or on reactions with inhibitors (clavulanic acid, avibactam, metal ion chelator EDTA) (30-32). β-lactamases of Ambler classes A, C and D, are all SBLs with a structural similarity, whereas class B includes MBLs (Figure 2).

Ambler class[8]: catalytic site (spectrum)	Bush–Jacoby–Medeiros group[9]: catalytic site (spectrum)	Substrates	Inhibited by	Examples
A: serine (variable)	2a: serine (penicillinases)	Penicillins	Clavulanate, avibactam and other newer inhibitors[a]	Penicillinases from Gram-positive bacteria
	2b: serine (penicillinases)	Penicillins and narrow-spectrum cephalosporins	Clavulanate, avibactam and other newer inhibitors	TEM-1, TEM-2 and SHV-1
	2be: serine (ESBLs)	Penicillins and cephalosporins, including extended-spectrum	Clavulanate, avibactam and other newer inhibitors	SHV-2, TEM-10, CTX-M and GES-1
	2br: serine (inhibitor-resistant)	Penicillins	Avibactam and other newer inhibitors	TEM-30 and SHV-72
	2c: serine (penicillinases)	Penicillins and carbenicillin	Clavulanate, avibactam and other newer inhibitors	PSE (CARB)
	2f: serine (carbapenemases)	Penicillins, cephalosporins and carbapenems	Avibactam and other newer inhibitors	KPC, SME, NMC-A and GES-2
B: metallo (carbapenemase)	3: metallo (carbapenemases)	Most β-lactams, including carbapenems, but not monobactams	Chelating agents (EDTA) and ANT431	IMP, VIM and NDM
C : serine (cephalosporinases)	1: serine (cephalosporinases)	Penicillins and cephalosporins	Cloxacillin, avibactam and other newer inhibitors	Chromosomal AmpC, CMY, ACT-1 and DHA
D : serine (oxacillinases)	2d: serine (oxacillinases)	Penicillins and cloxacillin; some include cephalosporins and/or carbapenems	Sodium chloride; some by clavulanate, avibactam and other newer inhibitors	OXA-1/30, OXA-10, OXA-23 and OXA-48

Table 1: Molecular and functional classification of β-lactamases.

[a]The term ‘newer inhibitors‘ refers to the diazabicyclooctanone and boronic acid inhibitors.

(a)

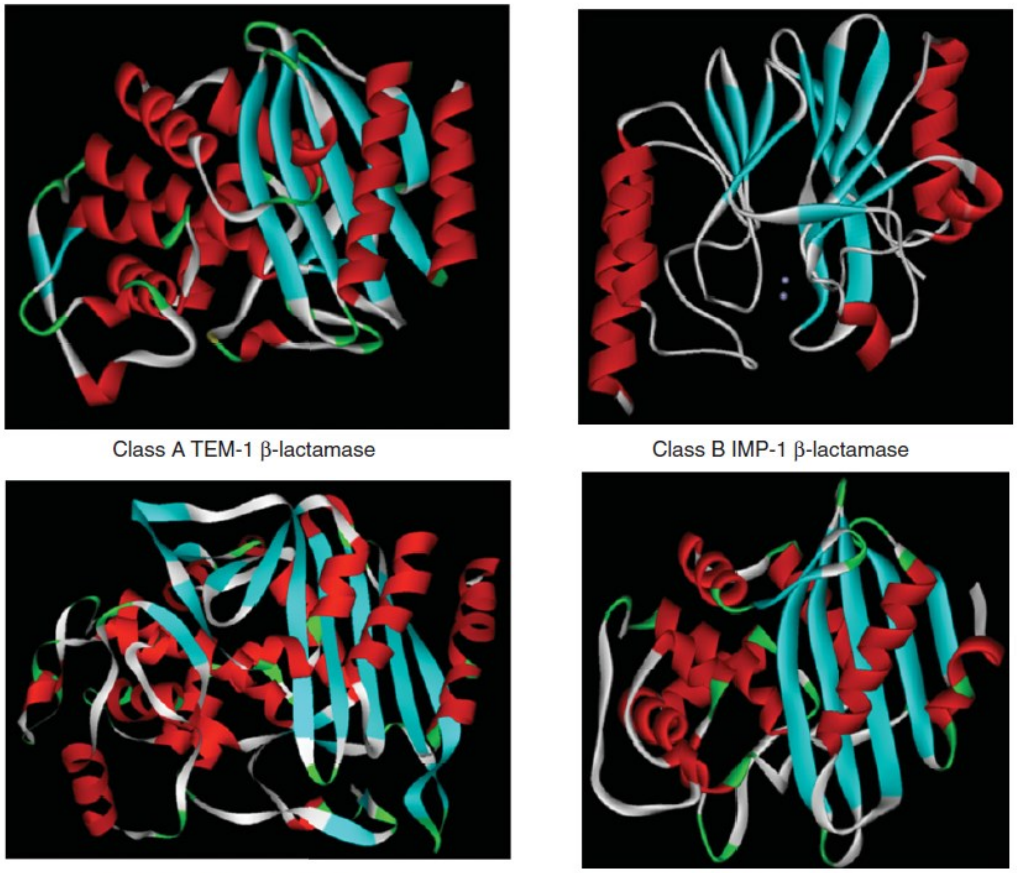

(b)

ENZYME	1st ELEMENT	2nd ELEMENT	3rd ELEMENT
Class A	^{70}Ser-X-X-Lys^{73}	^{130}Ser-Asp-sn(Ser)^{132}	^{234}Lys-Thr-Gly^{236} ^{234}Lys-Ser-Gly^{236} ^{234}Arg-Ser-Gly^{236}
Class C	^{64}Ser-X-X-Lys^{67}	^{150}Tyr-X-Asn^{152}	^{315}Lys-Thr-Gly^{317}
Class D	^{70}Ser-X-X-Lys^{70}	^{144}Tyr-Gly-Asn^{146}	^{214}Lys-Thr-Gly^{216}
DD peptidase	^{62}Ser-X-X-Lys^{65}	^{159}Tyr-Ser-Asn^{161}	^{298}His-Thr-Gly^{300}

Figure 2: (a) “Family portrait” of β-lactamases (b) Structural elements that limit the active site in most serine-β-lactamases.

The functional classification scheme divides β-lactamases into four groups and multiple major subgroups: groups 1, 2 (with the major subgroups 2a, 2b, 2br, 2d, 2be, 2c and 2f) and 3.

Group 1 are cephalosporinases not inhibited by clavulanic acid, belonging to the molecular class C. AmpC-type β-lactamases confer resistance to most cephalosporins, including extended-spectrum cephalosporins such as ceftazidime, cefotaxime, ceftriaxone and cephamycins like cefoxitin. They are also able to hydrolyze penicillins and some monobactams. Chromosomal β-lactamases are produced by many species of Gram-negative bacteria and are especially important in clinical isolates of *Citrobacter freundii*, *Enterobacter aerogenes*, *Enterobacter cloacae*, *Serratia marcescens* and *P. aeruginosa* because the enzymes can be inducible in these species. AmpC β-lactamases can also be expressed from plasmids, which have now become widely disseminated. Plasmid-encoded AmpC-type enzymes are also called cephamycinases because they hydrolyze cefoxitin and other cephamycins very efficiently. The loss of porin proteins in clinical isolates of *K. pneumoniae* and *Salmonella enterica* with plasmid-encoded AmpC enzymes results in resistance to carbapenems.

Group 2 are penicillinases, cephalosporinases, or both inhibited by clavulanic acid, belonging to the molecular classes A and D related to the original TEM, SHV and OXA genes. However, because of the increasing number of TEM and SHV derived β-lactamases, they were divided into two subclasses, 2a and 2b. The 2a subgroup contains penicillinases, whereas 2b are broad spectrum β-lactamases, able to inactivate penicillins and cephalosporins at the same ratio. Moreover, subgroup 2b has been divided into new subgroups:

-subgroup 2be (with “e” for extended spectrum of activity), includes serine β-lactamases. These enzymes hydrolyze penicillins and cephalosporins that have both narrow- and extended spectrum of activity. Most ESBLs are susceptible to inhibitors approved by the Food and Drug Administration (FDA). These ESBLs are TEM and SHV derived, with amino acid substitutions resulting in an ’extended’ substrate profile. The importance of TEM and SHV variants have diminished, to be replaced by the CTX-M-family of ESBLs. In general, CTX-M β-lactamases hydrolyze cefotaxime and ceftriaxone better than ceftazidime. CTX-M-type enzymes are inhibited by tazobactam and by newer BLIs, such as avibactam, relebactam and vaborbactam. CTX-M β-lactamases are commonly found in *E. coli* and *K. pneumoniae* but have also been found in other species of Enterobacteriaceae, including *Salmonella* spp., *Shigella* spp., *C. freundii*, *Enterobacter* spp. and *S. marcescens* as well as some non-fermenting bacteria (33). Other clinically important ESBL families include GES, PER, VEB, BES, BEL, SFO and TLA, but they are found with lower prevalence than CTX-M types.

- subgroup 2br, with the letter "r" denoting reduced binding to clavulanic acid and sulbactam, contains inhibitor-resistant β-lactamases, also known as inhibitor-resistant TEM and SHV-types; nevertheless, they are still susceptible to tazobactam and avibactam.

-subgroup 2c was segregated from group 2 because these enzymes inactivate carbenicillin more than benzylpenicillin, with some activity also on cloxacillin.

-subgroup 2d enzymes inactivate cloxacillin more than benzylpenicillin, with some effect against carbenicillin; these enzymes are poorly inhibited by clavulanic acid, and some of them are ESBLs. The OXA-type enzymes have a large variability in their substrate profiles and sequences. They hydrolyze oxacillin very efficiently, and some variants are able to inactivate cephalosporins or carbapenems. OXA enzymes are poorly inhibited by most BLIs with the exception of avibactam (34). OXA-type enzymes with a carbapenemase spectrum include OXA-48 and related enzymes such as OXA-162, OXA-163, OXA-181 and OXA-232. These enzymes have been identified in various species of Enterobacteriaceae and are most prevalent in the Mediterranean region and southern Europe.

-subgroup 2e enzymes are cephalosporinases that can also hydrolyze monobactams, and they are inhibited by clavulanic acid.

-subgroup 2f was added to distinguish serine based carbapenemases, in contrast to the zinc based carbapenemases (group 3). β-lactamases incorporated in this group are KPC, SME, NMC-A, IMI and some GES-variants. KPC-2 and KPC-3 variants are the most spread worldwide. These enzymes can appear in almost Gram-negative pathogen, although they are mainly detected in *K. pneumoniae* (35). KPC-type enzymes are not inhibited by clavulanate or tazobactam; however, they are inhibited by avibactam and vaborbactam. GES enzymes were initially considered ESBLs, but a single point mutation confers activity against carbapenems in some GES variants (36). NMC-A and IMI enzymes are chromosomally encoded carbapenem-hydrolyzing β-lactamases found in *E. cloacae*. Similarly, SME is a chromosomal enzyme exclusively from *S. marcescens* showing greatest amino acid sequence similarity (70%) with NMC-A. SME enzymes are able to hydrolyze carbapenems, but they have only limited activity against extended-spectrum cephalosporins.

Group 3 includes metallo β-lactamases, corresponding to the molecular class B. They are able to hydrolyze penicillins, cephalosporins, and carbapenems, but they do not show activity against monobactams. Thus, carbapenems are hydrolyzed by both group 2f (serine based mechanism) and group 3 (zinc based mechanism). These enzymes can be inhibited by chelating agents such as EDTA; however, they are not inhibited by β-lactamase inhibitors combinations approved by FDA. Plasmid-

encoded MBLs are located in mobile genetic elements that can disseminate and harbour resistance genes to other antimicrobial classes (37). Plasmid-encoded MBLs, IMP, VIM and NDM variants are the most widespread worldwide (38). They have been identified in various Gram-negative clinical isolates, including several species of Enterobacteriaceae, *P. aeruginosa* and *Acinetobacter* spp. IMP-1 was detected in an isolate of *P. aeruginosa* from Japan in 1988 but is now detected in other Gram-negative bacteria including *E. coli* and *K. pneumoniae*. VIM-1 was described 1999 in a multidrug-resistant *P. aeruginosa* isolate from Verona, Italy (39). VIM-type enzymes have become widespread and are especially prevalent in the Mediterranean region.

1.4 General Aims

Carbapenemases are the most common β-lactamases causing serious infections, especially in hospitalized patients. In the present thesis we focalized the attention on two β-lactamases with carbapenemase activity: the enzyme NDM-1 (MBL) and GES-type (SBL). These two enzymes are able to hydrolyze meropenem, imipenem and ertapenem with different catalytic mechanism. The NDM-1 is a definite carbapenemase whereas GES enzymes are ESBLs that, thanks to some point of mutation in the active site, have developed, over time, the ability to hydrolyze carbapenems. In this context, we analyzed two enzyme models by site-directed mutagenesis, in order to explore the role of some specific residues involved or not in the catalytic machinary. Site-directed mutagenesis was performed to presume what will be the future evolution of these β-lactamases. Detailed kinetic and dynamic studies have been performed on laboratory mutants to evaluate the possible therapeutical options. In this context we have studied the interaction of a new molecule named taniborbactam, a combination of cefepime and VNRX-5133 (a cyclic boronic acid), with NDM-1 and its laboratory mutants.

In detail:

-GES-1 enzyme was used as template for site-directed mutagenesis in two residues of the Ω-loop: G170 and P174. For GES-1, five mutants have been generated;

- regarding NDM-1, the role of the hydrophobicity of L218, L221 and L269 in the substrate hydrolysis was investigated. A double mutant L209F/Y229W was generated to ascertaine if the effect of two amino acids replacement is able to restore the activity of the mutant L209F;

-to date, clinical inhibitors of MBLs are not available. Thus, a new boronic acid (VNRX-5133) in combination with cefepime, was tested “in vitro” on NDM-1 and its laboratory mutants.

Chapter 2

Kinetic and biochemical characterization of GES-1 and GES-5 laboratory mutants

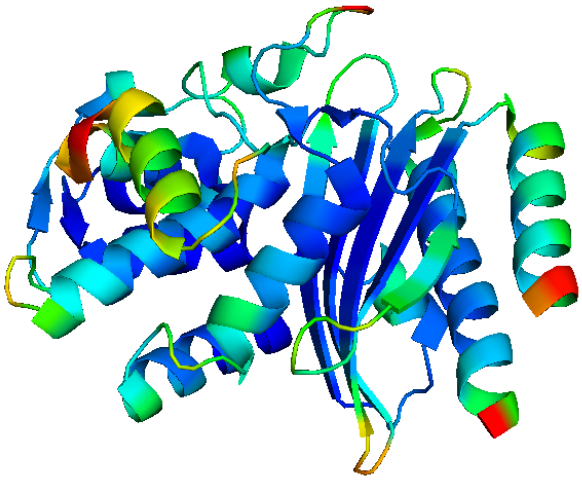

2.1 Background

Class A β-lactamases are enzymes with a very wide spectrum of activity and represent the most studied β-lactamases. The prototypical class A TEM-1 and SHV-1 were the first β-lactamases identified in Gram-negative bacteria. These enzymes, could be considered narrow-spectrum β-lactamases able to hydrolyze first generation penicillins and cephalosporins approved for clinical use. Progressive introduction of subsequent generations of β-lactam antibiotics leds to an inexorable emergence of new enzymes with enhanced catalytic activity. Particularly worrisome β-lactamases are found among the extended-spectrum β-lactamases, named ESBLs (functional group 2be). These enzymes were recognized shortly after the introduction in clinical theraphy of 'β-lactamase-stable' cephalosporins (i.e. cefotaxime and ceftazidime) and aztreonam. ESBLs were initially identified as variants of the common SHV-1 or TEM-1 β-lactamase, often differing from the parent enzymes by only one or two amino acids. After their recognition in the late 1980s concomitantly in Europe and the US, they became associated with major outbreaks of cephalosporin-resistant infections caused by ESBL-producing *E. coli* and *K. pneumoniae*. The genes encoding for these enzymes were generally found on plasmids that conferred resistance to multiple antibiotic classes and that were readily transferable among species. Even during the first reported outbreaks, other Enterobacteriaceae such as *C. freundii, E. aerogenes*, and *S. marcescens* were identified as ESBL producers. ESBLs are still associated with major outbreaks of β-lactam resistance. However, the early SHV and TEM variants have been largely replaced by the CTX-M family. The first two CTX-M enzymes were identified in the early 1990s in western Europe and South America in individual clinical isolates (41). Within a decade, the CTX-M β-lactamases became the most common ESBLs in many medical centers such that they have largely replaced TEM- and SHV-derived ESBLs throughout the world (Figure 2) (41).

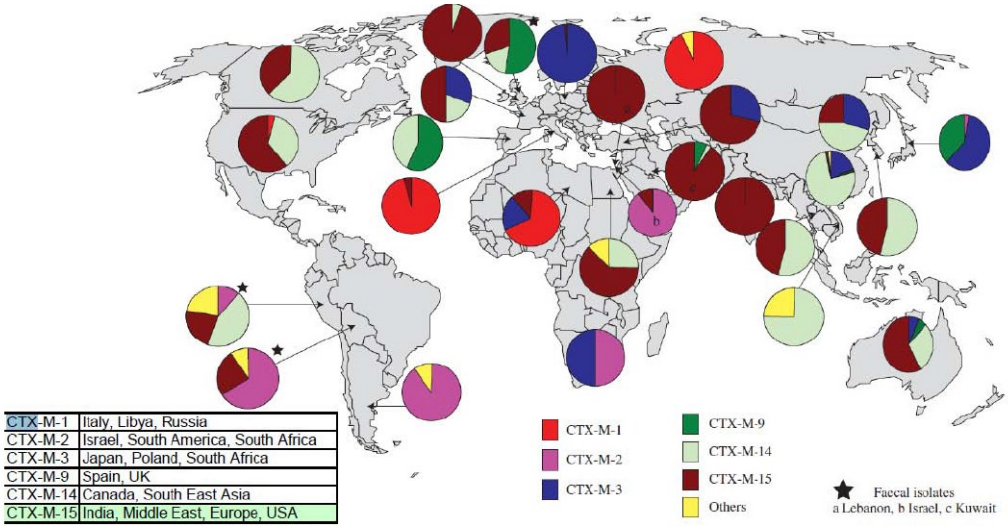

Figure 2: Epidemiology of CTX-M β-lactamases (41).

In response to the challenge of organisms with class A β-lactamases, the first carbapenem, imipenem, was brought to the clinic in the mid-1980s. Shortly thereafter newer carbapenems, meropenem, doripenem and ertapenem, were introduced. Carbapenems rapidly became antibiotics of last resort, because of their exceptional breadth of activity and potency. Carbapenemases represent the most versatile family of β-lactamases, with a breadth of spectrum unrivaled by other β-lactam-hydrolyzing enzymes. Although known as "carbapenemases," many of these enzymes recognize almost all hydrolyzable β-lactams, and most are resilient against inhibition by all commercially β-lactamase inhibitors. Class A serine carbapenemases of functional group 2f have appeared sporadically in clinical isolates since their first discovery over 20 years ago (37). These β-lactamases have been detected in *E. cloacae*, *S. marcescens*, and *Klebsiella* spp. as single isolates or in small outbreaks. Bacteria expressing these enzymes are characterized by reduced susceptibility to imipenem. Three major families of class A serine carbapenemases include the NMC/IMI, SME, and KPC enzymes. Their hydrolytic mechanism requires an active-site serine at position 70 in the Ambler numbering system for class A β-lactamases. All of these enzymes have the ability to hydrolyze a broad variety of β-lactams, including carbapenems, cephalosporins, penicillins, and aztreonam. These β-lactamases are inhibited by clavulanic acid and tazobactam, placing them in the 2f functional subgroup. A fourth member of this class, the GES β-lactamases, was originally identified as an ESBL family, but over time, variants were discovered that had low, but measurable, imipenem hydrolysis. This subgroup of GES enzymes is also classified as functional group 2f carbapenemases. With the notable exception of KPCs and GES, the clinical distribution of the types of carbapenemases is relatively limited (42).

2.2 Active site and catalytic mechanism of class A β-lactamases

Class A β-lactamases react with β-lactam antibiotics through the following pathway:

- Michaelis complex formation;
- acyl-enzyme formation;
- deacylation of the acyl-enzyme as shown in Scheme 1.

Scheme 1

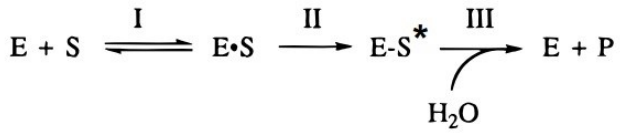

where E is the enzyme, S the β-lactam, E•S the Michaelis complex, E-S* the acyl-enzyme, and P the product of hydrolysis.

Sequence alignment of class A β-lactamases revealed highly conserved motifs, consisting of three polar regions: the tetrad S70-X-X-K73, the triad S130-D131-N132, and the triad K234-T(S)235-G236. There are important hydrogen-bond between this three polar region, stabilized by water molecules.

A crucial role in the catalytic mechanism of class A β-lactamases is played by serine active residue. Crystallographic studies and molecular modeling have shown that the structures of enzymes belonging to A, C and D have the similar “oxyanion holes” including the main chain NH-groups of S70 and A237 in the class A enzymes. The nucleophilic attack of the active site serine γ-O atom on the carbonyl carbon of the β-lactam bond, leads to a negatively charged tetrahedral transition state. The interaction of the β-lactam carbonyl oxygen with the oxyanion hole and by the dipole of the buried helix is necessary in order to stabilize the tetrahedral transition state. The lysine at position 73 has been ascertained in the orientation of the serine proton towards the nitrogen of the leaving group (43). The mechanism of catalysis is based on the presence of a proton park in the catalytic pocket represented by three residues: K73, S130 and E166. For class A enzymes two distinct residues have been proposed for the role of general base. In one hypothesis, this role is played by the conserved E166. This residue in class A β-lactamases is part of a structural element called **Ω**-loop. Crystallographic data have highlighted the presence of a tightly bound water molecule, forming a bridge between the S70 hydroxyl group and the E166 carboxylate side chain. This water molecule is

found at the same position in all class A structures solved by X-ray (44,45). Although site-directed mutagenesis experiments suggested that E166 might play the role of general base in the acylation reaction, it seems too far from the S70 OH group (46). Molecular modeling studies have suggested that the conserved water molecule might act as a relay molecule in the transfer of the proton between the S70 and E166 side chains. Alternatively, the flexibility of the Ω-loop might allow the distance between the two residues to be shortened during the acylation process. Both cases require the presence of a second water molecule, the ε-amino groups of K73 and K234 and the hydroxyl group of S130, which acts as the last proton donor. On the contrary, Mobashery and co-workers, suggested that S130 can decrease the energy barrier for hydrolysis of substrates by merely hydrogen-bonding to the nitrogen atom of the β-lactam ring in the course of S70 acylation (47,48). In the second hypothesis formulated on the structural properties of the E166N mutant of the TEM-1 β-lactamase the authors argued that E166 is expendable for acylation and thus proposed an unsymmetrical mechanism, with two different general bases, K73 and E166, participating in acylation and deacylation respectively (49).

2.3 GES β-lactamases

2.3.1 Epidemiology and genetic structure

The first representative enzyme of the GES family (Guiana extended-spectrum; named after the country of origin of the first isolate) was GES-1, isolated in 1998 from a clinical strain of *K. pneumoniae* (50). GES-1 was found to confer resistance to penicillins and broad-spectrum cephalosporins, but not to monobactams or carbapenems. A few years later GES-5 (G170S), a single amino acid derivative of GES-1, was shown to confer resistance to carbapenems in clinical bacterial isolates (51,52). To date, 30 GES variants, differing from each other by one to three amino acid substitutions, have been discovered (ftp://ftp.ncbi.nlm.nih.gov/pathogen/betalactamases/Allele.tab). In table 2 are indicated the main GES-variants.

Name	Protein accession	Definition
GES-1	AF156486.1	class A extended-spectrum beta-lactamase GES-1
GES-2	AF326355.1	class A extended-spectrum beta-lactamase GES-2
GES-3	AB113580.1	class A extended-spectrum beta-lactamase GES-3
GES-4	AB116260.1	carbapenem-hydrolyzing class A beta-lactamase GES-4
GES-5	AY494717.1	carbapenem-hydrolyzing class A beta-lactamase GES-5
GES-6	AY494718.1	carbapenem-hydrolyzing class A beta-lactamase GES-6
GES-7	AF208529.2	class A beta-lactamase GES-7
GES-8	AF329699.1	class A extended-spectrum beta-lactamase GES-8
GES-9	AY920928.1	class A beta-lactamase GES-9
GES-10	FJ820124.1	class A beta-lactamase GES-10
GES-11	FJ854362.1	class A extended-spectrum beta-lactamase GES-11
GES-12	FN554543.1	class A beta-lactamase GES-12
GES-13	GU169702.1	class A beta-lactamase GES-13
GES-14	GU207844.1	carbapenem-hydrolyzing class A beta-lactamase GES-14
GES-15	GU208678.1	carbapenem-hydrolyzing class A beta-lactamase GES-15
GES-16	HM173356.1	carbapenem-hydrolyzing class A beta-lactamase GES-16
GES-17	HQ874631.1	class A beta-lactamase GES-17
GES-18	JQ028729.1	carbapenem-hydrolyzing class A beta-lactamase GES-18
GES-19	JN596280.1	class A beta-lactamase GES-19
GES-20	JN596280.1	carbapenem-hydrolyzing class A beta-lactamase GES-20
GES-21	JQ772478.1	carbapenem-hydrolyzing class A beta-lactamase GES-21
GES-22	JX023441.1	class A beta-lactamase GES-22

GES-23	KF179354.1	class A extended-spectrum beta-lactamase GES-23
GES-24	AB901141.1	carbapenem-hydrolyzing class A beta-lactamase GES-24
GES-25	KT732289.1	class A beta-lactamase GES-25
GES-26	KP096411.1	class A beta-lactamase GES-26
GES-27	KT151556.1	class A beta-lactamase GES-27
GES-28	KT626944.1	class A beta-lactamase GES-28
GES-29	KT997885.1	class A beta-lactamase GES-29
GES-30	LC126615.1	class A beta-lactamase GES-30
GES-31	KX034181.1	class A beta-lactamase GES-31

Table 2: GES-variants from clinical isolates. Data from ftp://ftp.ncbi.nlm.nih.gov/pathogen/betalactamases/Allele.tab

These enzymes have been identified worldwide in several Gram-negative bacteria, including Enterobacteriaceae and non-fermenting strains such as *P. aeruginosa* and *A. baumannii* (53-57). Their rapid spread among different bacterial species and countries is largely due to the localization of *bla*$_{GES}$ genes in mobile genetic elements such as integrons and plasmids. Most of them are localized in a complex structure. For example, *bla*$_{GES-6}$ and *bla*$_{GES-7}$ have been found in IncL/M plasmids harboring various β-lactamase genes (Figure 3) (58).

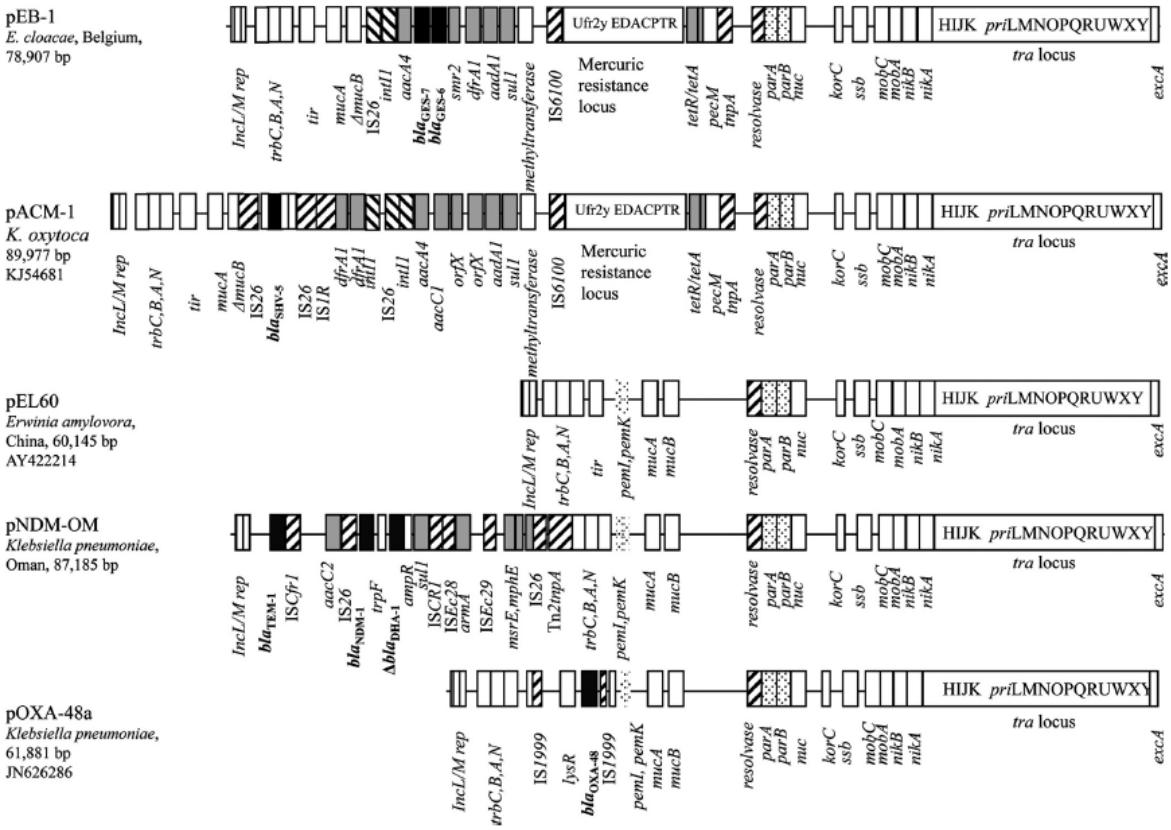

Figure 3. Schematic representation of plasmid pEB-1 carrying *bla*$_{GES-6}$ and *bla*$_{GES-7}$ genes and comparison with four other IncL/M plasmids harboring various β-lactamases, pACM-1 (GenBank accession number KJ541681), pEL60 (GenBank accession number AY422214), pNDM-OM (GenBank accession number JX988621), and pOXA-48a (GenBank accession number JN626286). White boxes indicate plasmid scaffold regions that are common to all of the plasmids or are of unknown function. Resistance genes are indicated by gray boxes, except for the β-lactamase genes, which are indicated by black boxes. Transposon-related genes (*tnpA*, *tnpR*, and *tnpM*), insertion sequences, and integrase genes are indicated by hatched boxes. Replicase genes are indicated by boxes with vertical lines. Genes encoding mobilization and partition systems are indicated by dotted boxes (58).

2.3.2 Biochemical structure of GES enzymes

Like all class A β-lactamases, GES enzymes are folded into two domains comprising α-helixes, β-sheet, and loops (Figure 4a) (59). The active site of GES consists of several highly conserved residues, including S70, K73, S130, N132, E166, and residues 159 to 182 (Ω-loop), which are strictly conserved in all class A β-lactamases (Figure 4b) (59). Within the Ω-loop, the E166 residue acts as a general base to activate a water molecule for the acyl-enzyme deacylation yielded by the reaction between S70 and β-lactam ring (59,60). In addition, in class A β-lactamases, the side chain of N170 plays an important role in enzyme catalysis; in fact, it could be considered the third ligand of the

hydrolytic water molecule (60). In GES β-lactamases, position 170 is occupied by glycine (i.e., GES-1, GES-3, GES-7), serine (i.e., GES-4, GES-5, GES-6, GES-8, GES-14, GES-18, GES-20), or asparagine (i.e., GES-2, GES-13). GES-1 is able to confer resistance to penicillins and broad-spectrum cephalosporins, but it has reduced activity against carbapenems. Carbapenemase activity was demonstrated only in GES variants that have replaced glycine 170 with serine or asparagine (60,61).

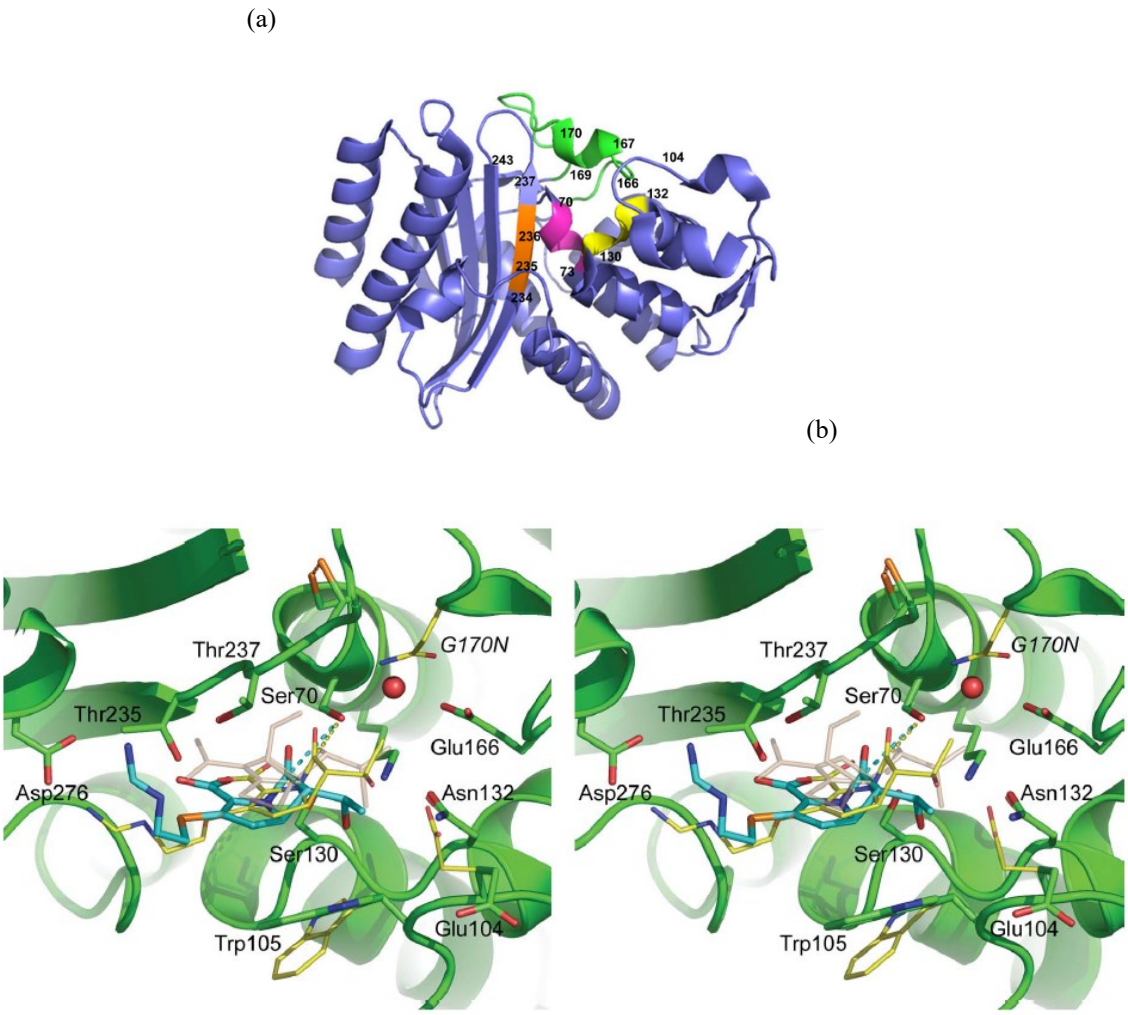

Figure 4: (a) Overall structure of GES-1. The conserved element 1 (S70-K73) is in magenta, conserved element number 2 (S130-N132) is in yellow, conserved element number 3 (K234-G236) is in orange and the omega loop (residues E166, P167, M169 and G170) is in green. G243, T237, E104 and G170 are important residues in substrate selectivity of GES-type β-lactamases. (PDB: 3V3R). (b) Stereoview of the 'GES-1' simulation active site (green) with the imipenem from 'GES-1' (cyan bonds) and 'GES-2' (thinner yellow bonds) superimposed (59).

All known class A carbapenemases contain a disulfide bond (C69-C238) important for stability and, in some cases, for carbapenemase activity (62,63). Even if in GES-1 a disulfide bond is present, it does not show carbapenemase activity. Most likely, the disulfide bond in GES enzymes is not particularly essential for enzyme activity. Unlike NMCA and SME-1 enzymes, the disruption of the C69-C238 disulfide bridge in GES-5 yielded an enzyme that was still active against carbapenems (64). GES enzymes are in continuous evolution, which is proven by the identification of several variants with improving hydrolytic activity against carbapenems.

2.4 Aim of the study

Catalytic mechanism of class A serine-β-lactamases has been well studied and the role of catalytic and/or non-catalytic residues has been well investigated. The appearance of class A enzymes able to hydrolyze carbapenems has represented for most researchers an interesting challenge. Differently to other class A carbapenemases, such as KPC-variants, only some GES-variants showed carbapenemase activity. In detail, only GES enzymes with G170S or G170N amino acid substitutions have developed the ability to hydrolyze carbapenems. Furthermore, carbapenemase activity by GES enzymes is attributed to a single amino acid substitution at position 170.

The goal of this study was to investigate the role of the Ω-loop (residues 159-182) in GES-1 and GES-5 enzymes and, possibly, to highlight its effect on β-lactamase activity. In GES carbapenemases, as well as in class A β-lactamases, position 174 is well conserved and occupied by a proline residue. Thus, in this study we studied positions 170 and 174 by design the following mutants:

- GES-1^{P174E} and GES-5^{P174E}: the role of residue 174 was explored in GES-1 enzyme, a prototype enzyme unable to hydrolyze carbapenems, and in GES-5 which has evolved its substrate profile *versus* carbapenems. In GES-5 we can find the G170S mutation.
- GES-1^{G170L}, GES-1^{G170K} and GES-1^{G170H}.

This aim has been achieved by the combined application of experimental and computational techniques.

2.5 Materials & methods

2.5.1 Strains and vector. The *bla*$_{GES-5}$ gene was isolated from *Enterobacter cloacae* AQ-1 clinical strains (University of l'Aquila collection). *E. coli* BL21(DE3) competent cells were used as recipient for recombinant plasmids. The vector pET-24a(+) (Novagen, Milan, Italy) was used for cloning and enzyme expression.

2.5.2 Site-directed mutagenesis and cloning. Site-directed mutagenesis was performed on *bla*$_{GES-5}$ gene using the overlap extension method (65). PCR is used to generate two fragments which have their ends modified by *mispriming* and a region of homology. The external primers are the following :5'-GGGG**CATATG**CGTTTCATACATGCG and 5'-GGGG**AAGCTT**ATTTATCGGTGGACAGG (with the *Nde*I and *HindIII* restriction sites, respectively, indicated in bold) The primers for site-saturation mutagenesis are 5'-CGGAGATGNNNGACAACACANNNGGCGA-3' and 5'-TCGCCNNNTGTGTTGTCNNNCATCTCCG-3'. The codons encoding glycine (GGC) and proline 174 (CCT) were exchanged with a degenerated codon NNN, where N represents all four bases (A, T, C, G). *bla*$_{GES-1}$ was generated by site-directed mutagenesis from *bla*$_{GES-5.}$ The *bla*$_{GES-1}$ and *bla*$_{GES-5}$ genes and mutated amplicons were cloned into pET-24a (+) vector using the *Nde*I and *HindIII* restriction sites. The recombinant plasmids were transferred into *E. coli* BL21(DE3) and selected on LB agar plates supplemented with kanamycin (50 μg/mL), ampicillin (50 μg/mL) and cefotaxime (1 μg/mL). The authenticity of the cloned mutant genes was confirmed by sequencing, on both strands, of the recombinant plasmids using an automated sequencer (ABI PRISM3500; Life Technologies, Monza, Italy).

2.5.3 Antibiotics. Meropenem was from AstraZeneca (Milan, Italy). Imipenem, ertapenem, and cefoxitin were from Merck Sharp & Dohme (Rome, Italy). Nitrocefin was kindly provided by Shariar Mobashery (Notre Dame University, South Bend, IN, USA). Tazobactam was from Wyeth-Lederle (Catania, Italy) and clavulanic acid was from GlaxoSmithKline (Verona, Italy). The other antimicrobial agents used were purchased from Sigma-Aldrich (Milan, Italy). The wavelengths expressed in nanomolar (nm) for each β-lactam and the molar extinction coefficients of the β-lactams (Δε) used to analyze the kinetic properties of the enzyme were as follows: ampicillin ($\Delta\varepsilon_{235nm}$ = -820 M^{-1} cm^{-1}), benzylpenicillin ($\Delta\varepsilon_{235nm}$ = -775 M^{-1} cm^{-1}), carbenicillin ($\Delta\varepsilon_{235nm}$=-780 M^{-1} cm^{-1}), piperacillin ($\Delta\varepsilon_{235nm}$ = -822 M^{-1} cm^{-1}), cefazolin ($\Delta\varepsilon_{260nm}$ = -7400 M^{-1} cm^{-1}), cefotaxime ($\Delta\varepsilon_{260nm}$ = -7500 M^{-1} cm^{-1}), cefoxitin ($\Delta\varepsilon_{261nm}$ = -7775 M^{-1} cm^{-1}), nitrocefin ($\Delta\varepsilon_{482nm}$ = 15000 M^{-1} cm^{-1}), imipenem

($\Delta\varepsilon_{300nm}$ = -9000 M^{-1} cm^{-1}), meropenem ($\Delta\varepsilon_{297nm}$ = -6500 M^{-1} cm^{-1}), ertapenem ($\Delta\varepsilon_{298nm}$ = -7500 M^{-1} cm^{-1}).

2.5.4 Antimicrobial susceptibility tests. The phenotypic profile has been characterized by a microdilution method using a bacterial inoculum of 5 × 10^5 CFU/ml according to Clinical and Laboratory Standards Institute (CLSI) performance standards (66). Tazobactam was used at fixed concentration of 4 µg/mL. Clavulanic acid was used in association with amoxicillin at a 2:1 ratio (amoxicillin-clavulanic acid). IPTG (isopropyl-β-D-thiogalactopyranoside) at 0.4 mM was added to the medium used for the MIC assay. MIC experiments were performed in triplicate.

2.5.5 Expression and purification of GES-1, GES-5, GES-1^{P174E}, and GES-5^{P174E}enzymes. GES-1, GES-5, GES-1^{P174E}, and GES-5^{P174E} were extracted from 1.2 liters of culture of *E. coli* BL21(DE3) /pET-GES-1, *E. coli* BL21(DE3) /pET-GES-5, *E. coli* BL21(DE3) /pET-GES-1^{P174E}, and *E. coli* BL21(DE3) /pET-GES-5^{P174E}, respectively. The cultures were grown at 37°C until an A_{600} of approximately 0.7 was achieved; at this stage, IPTG was added at a final concentration of 0.4 mM. The cultures were incubated for 16 h at 22°C under aerobic conditions. The bacterial suspension was pelleted, resuspended in 20 mM Tris-HCl buffer (pH 7.6) (buffer A), and disrupted by sonication on ice (5 cycles at 60 W for 1 min with a 2-min break). The lysate was centrifuged at 100,000 x *g* for 30 min, and the cleared supernatant was then dialyzed against buffer A and loaded onto a Q-Sepharose FF column equilibrated with the same buffer. The proteins were eluted by a linear NaCl gradient (0 to 1 M) in 20 mM Tris-HCl buffer (pH 7.6) (buffer B). The fractions with β-lactamase activity were pooled and dialyzed overnight against buffer A at 4°C. This partially purified enzyme was loaded onto a Mono Q column (Pharmacia Biotech) equilibrated with the same buffer. The proteins were eluted with buffer B. The fractions with β-lactamase activity were pooled and dialyzed overnight against 25 mM Bis-Tris buffer (pH 7.1) (buffer C) at 4°C. Chromatofocusing was performed on a Mono P 5/50 GL column (GE Healthcare, Milan, Italy) equilibrated with buffer C. The proteins were eluted with 100% Polybuffer 74 (GE Healthcare, Milan, Italy). Fractions with the highest β-lactamase activities were pooled and dialyzed overnight at 4°C against 25 mM sodium phosphate buffer (pH 7.1) (buffer D), frozen at -80°C, and used for further experiments. The purity of the enzymes was evaluated by SDS-PAGE (67) with a fixed 12.5% (wt/vol) polyacrylamide gel in the presence of 0.1% SDS, using a Mini-Protean III apparatus (Bio-Rad Laboratories, Milan, Italy). After electrophoresis, the proteins bands were stained with Coomassie brilliant blue R-250. Protein content was determined by the Bradford method, with bovine serum albumin as the standard (68).

2.5.6 Determination of kinetic parameters. Steady-state kinetic experiments were performed following the hydrolysis of each substrate at 25°C in 20 mM sodium phosphate buffer (pH 7.0), containing 0.2 M KCl to prevent enzyme instability. The data were collected with a Perkin-Elmer Lambda 25 spectrophotometer (Perkin-Elmer Italia, Monza, Italy). Each kinetic value is the mean of five different measurements; the error was below 5%. Kinetic parameters were determined under initial-rate conditions as described by De Meester et al. (69) and Segel (70). For K_m values lower than 10 μM and higher than 1 mM, K_m was determined as K_i using nitrocefin as the reporter substrate. Inhibition experiments with clavulanic acid and tazobactam were monitored directly by using 100 μM nitrocefin as the reporter substrate. Competitive inhibition assays were performed using the following equation: $v_0/v_i = 1 + [(K_m \text{ x } I) / (K_m + S) \text{ x } K_i]$, where v_i and v_0 represent the initial rates of hydrolysis of nitrocefin with and without inhibitor, respectively, I is the concentration of inhibitor or poor substrate, K_i is the inhibition constant, K_m is the Michaelis constant, and S is the concentration of the reporter substrate. The plot v_0/v_i versus I yielded a straight line of slope, $K_m / (K_m + S) \text{ x } K_i$.

2.5.7 Temperature stability. The effect of temperature on enzyme stability was evaluated by measuring the residual activity of the enzymes incubated at 25°C, 35°C, and 45°C. At several times (0, 15, 30, 60, 90, and 120 min), the residual activity was measured following the hydrolysis of nitrocefin at 300 μM for GES-1 and GES-1^{P174E}, 150 μM for GES-5, and 50 μM for GES-5^{P174E}.

2.5.8 CD. Far-UV circular dichroism (CD) spectra (190 to 260 nm) were recorded with a Jasco J-810 spectropolarimeter at 20°C in 25 mM sodium phosphate buffer, pH 7.0, using a 1-mm-pathlength quartz Suprasil cell (Hellma), with protein concentrations of about 0.1 mg/ml. Four scans (20 nm/min, 1-nm bandwidth, 0.1-nm data pitch, and 2-s digital integration time) were averaged, baselines were subtracted, and no smoothing was applied. Data are presented as the molar residue ellipticity ([Θ]MRW), calculated using the molar concentration of protein and number of residues (MRW=108.6).

2.5.9 MD simulations. Molecular dynamic (MD) simulations of GES-1, GES-5, GES-1^{P174E}, and GES-5^{P174E} complexed with imipenem and meropenem were performed with the GROMACS package, version 4.5.5 (71), with the GROMOS force-field (gromos54a7) (72). The simulations of GES-1 and GES-5 complexed with imipenem were started using the crystal structure of the acyl-enzyme complexes (PDB codes 4GOG and 4H8R). The mutants were generated with the program MOLDEN (73). The simulations with meropenem were initiated by taking the same initial structures of the complexes with imipenem and changing the substrate. The structures were inserted into a cubic box of 369 nm3 and filled with water molecules (11,245 molecules) using the water-simple point

charge (SPC) model and the proper number of counterions for ensuring electrical neutrality of the system. For all the simulations, we adopted the same protocol: (i) energy minimization, (ii) thermalization from 10 K to 298 K using short simulations of 20 ps, and (iii) productive runs. The length of the productive runs was 100 ns (only 80 ns was used for the analysis) with a time step of 2.0 fs, the NVT ensemble was adopted at a density of 1 atm, long-range electrostatic interactions were computed by the particle mesh Ewald (PME) method (74), and the temperature was kept constant at 298 K using a velocity rescaling algorithm (75). A LINCS algorithm was adopted for constraining bond lengths (76). For imipenem and meropenem, we adapted the GROMOS force-field calculating the atomic charges using quantum chemical calculations with the Gaussian 09 package (77). Overall fluctuations of the enzymes were calculated as the trace of the positional covariance matrix as widely described in the literature (78).

2.6 Results

2.6.1 Characterization of P174E mutants

Mutation at position 174 was performed by site saturation mutagenesis using *bla*$_{\text{GES-1}}$ and *bla*$_{\text{GES-5}}$ as the template (79). PCR products obtained by mutagenesis were cloned into pET-24a(+) overexpression vector and inserted by transformation in *E. coli* BL21(DE3) competent cells in the presence of kanamycin 50 µg/ml. The mutants *bla*$_{\text{GES-1}}^{\text{P174E}}$ and *bla*$_{\text{GES-5}}^{\text{P174E}}$ were recovered after antibiotic selection in the presence of ampicillin (50 µg/ml) and cefotaxime (1 µg/ml). Compared to GES-1 prototype enzyme, in GES-5$^{\text{P174E}}$ two mutations appeare in the Ω-loop of the enzyme: G170S and P174E. Microbiological and biochemical effects of these mutations were studied in both GES-1$^{\text{P174E}}$ and GES-5$^{\text{P174E}}$ β-lactamases.

Antimicrobial susceptibility

Antimicrobial susceptibility testing was carried out on *E. coli* BL21(DE3) harboring GES-1, GES-5, GES-1$^{\text{P174E}}$, and GES-5$^{\text{P174E}}$ enzymes toward a large panel of β-lactams including piperacillin, piperacillin-tazobactam combination, amoxicillin, amoxicillin-clavulanate combination, 2$^{\text{nd}}$, 3$^{\text{rd}}$ and 4$^{\text{th}}$ generation cephalosporins, carbapenems and aztreonam (monobactam). As shown in Table 3, the GES-1, GES-1$^{\text{P174E}}$, GES-5, and GES-5$^{\text{P174E}}$ β-lactamases were able to confer resistance to penicillins, cefazolin, ceftazidime, and aztreonam. All the recombinant strains showed low MIC values for carbapenems except *E. coli* BL21(DE3) /pET-GES-5 and *E. coli* BL21(DE3) /pET-GES-5$^{\text{P174E}}$,

which had MIC values of 8 µg/ml. Tazobactam and clavulanic acid were able to restore the susceptibility of piperacillin and amoxicillin, respectively.

Antibiotics	*E. coli* pET-24 GES-1	*E. coli* pET-24 GES-5	*E. coli* pET-24 GES-1^{P174E}	*E. coli* pET-24 GES-5^{P174E}	*E. coli* pET-24
Piperacillin	>256	>256	>256	>256	1
Piperacillin/tazobactam	16	16	16	16	1
Amoxicillin	1024	1024	512	1024	0.5
Amoxicillin/clavulanic acid	32	32	8	8	0.5
Imipenem	0.5	8	0.5	8	0.0625
Ertapenem	0.0625	1	0.5	1	0.0625
Meropenem	0.0625	0.50	0.25	1	0.0625
Cefazolin	>128	>128	64	128	0.125
Cefotaxime	16	4	2	4	0.0625
Ceftazidime	16	16	16	16	<0.0625
Cefepime	8	8	8	8	0.125
Cefoxitin	1	16	2	16	0.125
Aztreonam	>128	>128	32	32	0.0625

Table 3: Antimicrobial susceptibility of *E. coli* BL21(DE3) carrying *bla*GES-1, *bla*GES-5, *bla*GES-1^{P174E} and *bla*GES-5^{P174E}. MIC were determined on microdilution plates using an inoculum of 5x10^5 CFU/mL as reported by CLSI (22). Tazobactam was used at fixed concentration of 4 µg/mL and the amoxicillin-clavulanic acid combination was used at ratio 2:1.

Thermostability of P174E mutants

Thermostability of the four enzymes was evaluated at 25°C, 35°C, and 45°C after 120 min of preincubation. Residual activity, calculated at 25°C and 35°C, shows the same values for the four enzymes (from 90% to 94%). In contrast, at 45°C, in GES-1 and GES-1^{P174E}, the activity gradually decreased to 45% and 68%, respectively (Figure 5). In contrast, in GES-5 and GES-5^{P174E}, the residual activity rose to 50% after 15 min of preincubation but dropped to 37 to 38% after 120 min of preincubation (Figure 5).

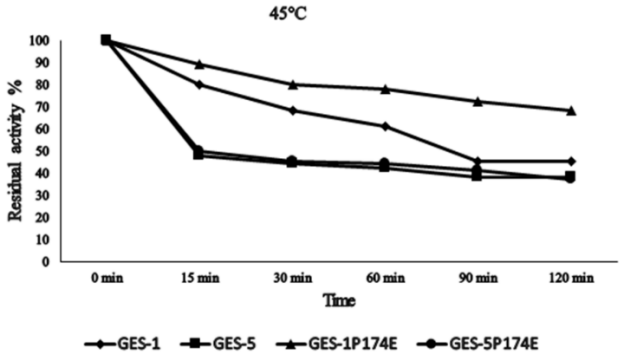

Figure 5: Thermal stability of GES-1, GES-5, GES-1^{P174E}, and GES-5^{P174E} calculated at 45°C. Data are mean values of three measurements. The standard deviation was always lower than 10%.

Kinetic parameters

Steady-state kinetic parameters were calculated by measuring the initial rate of the reaction using purified GES-1, GES-1^{P174E}, GES-5, and GES-5^{P174E} (enzymes pure at >95%). All the enzymes were tested against benzylpenicillin, ampicillin (aminopenicillin), piperacillin (ureidopenicillin), and carbenicillin (carboxypenicillin). As shown in table 4, GES-1 and GES-5 very efficiently hydrolyzed benzylpenicillin and ampicillin. In comparison with GES-1, GES-1^{P174E} showed low k_{cat} values toward both benzylpenicillin and ampicillin. With respect to benzylpenicillin and ampicillin, GES-5 and GES-5^{P174E} exhibited K_m and k_{cat} values similar to those of GES-1. In comparison to GES-1, GES-1^{P174E} showed a decreased k_{cat}/K_m value for piperacillin due to a lower k_{cat} value. Carbenicillin was a poor substrate for GES-1^{P174E} (high K_m value, 2,300 μM). Concerning cefazolin, GES-1^{P174E} showed a 10-fold-lower K_m value than GES-1, whereas its catalytic efficiency was slightly increased (Table 4). Indeed, a high k_{cat} value was calculated for GES-5 (844 s^{-1}), which makes it the most active enzyme toward cefazolin in terms of catalytic efficiency. GES-5^{P174E} exhibited a k_{cat} value lower than that of GES-5. Cefoxitin was hydrolyzed only by GES-5 and GES-5^{P174E}, with k_{cat} values of 30 s^{-1} and 15 s^{-1}, respectively. Cefoxitin was not hydrolyzed by GES-1 and GES-1^{P174E}, and the K_m values were

calculated as K_i using nitrocefin as the reporter substrate. All four enzymes hydrolyzed cefotaxime very efficiently, even though it was impossible to estimate the k_{cat} values because of their low affinity (high K_m values). In comparison with GES-1, GES-1^{P174E} showed a slight increase in k_{cat} values for imipenem, meropenem, and ertapenem (Table 4). The P174E substitution in GES-1 and GES-5 increased k_{cat}/K_m values for imipenem 100-fold and about 3-fold, respectively. Regarding meropenem, GES-1^{P174E} showed a k_{cat} value about 14-fold higher than that of GES-1, whereas GES-5^{P174E} exhibited a k_{cat} value similar to that of GES-5. The K_m of GES-5^{P174E} for meropenem was less than that calculated for GES-5.

Antibiotics	GES-1			GES-1^{P174E}			GES-5			GES-5^{P174E}		
	K_m (μM)	k_{cat} (s^{-1})	k_{cat}/K_m (μM^{-1} s^{-1})	K_m (μM)	k_{cat} (s^{-1})	k_{cat}/K_m (μM^{-1} s^{-1})	K_m (μM)	k_{cat} (s^{-1})	k_{cat}/K_m (μM^{-1} s^{-1})	K_m (μM)	k_{cat} (s^{-1})	k_{cat}/K_m (μM^{-1} s^{-1})
Benzylpenicillin	210±15	117	0.557	190±10	5	0.027	310±25	254	0.822	300±20	199	0.654
Ampicillin	260±20	236	0.908	230±8	30	0.130	148±5	53	0.358	106±6	62	0.585
Piperacillin	1400±150	184	0.131	610±30	23	0.038	>3000*	N.D.	N.D.	>3000*	N.D.	N.D.
Carbenicillin	1250±35	41	0.033	2300*±500	N.D.	N.D.	>3000*	N.D.	N.D.	1700±250	N.D.	N.D.
Cefazolin	1440±35	375	0.26	140±10	103	0.72	500±20	844	1.70	670±25	98	0.15
Cefoxitin	50*±5	N.H.	N.D.	10*±1	N.H.	N.D.	380±20	30	0.078	227±15	15	0.066
Cefotaxime	12000*±150	N.D.	N.D.	37000*±350	N.D.	N.D.	9600*±220	N.D.	N.D.	1840*±180	N.D.	N.D.
Nitrocefin	330±20	168	0.52	350±20	122	0.35	170±25	769	4.47	46±8	290	6.3
Imipenem	0.8*±0.1	0.006	0.0075	0.013*±0.001	0.01	0.77	0.4*±0.1	0.7	1.75	0.1*±0.05	0.5	5.0
Meropenem	0.08*±0.01	0.007	0.0875	0.1*±0.05	0.1	1.0	0.3*±0.02	0.15	0.5	0.08*±0.01	0.12	1.5
Ertapenem	0.25*±0.02	0.003	0.012	0.1*±0.05	0.008	0.08	0.26*±0.01	0.1	0.384	0.09*±0.002	0.077	0.875

Table 4: Determination of k_{cat}, K_m and k_{cat}/K_m of GES-1, GES-1^{P174E}, GES-5 and GES-5^{P174E} towards β-lactams. *K_m was calculated as K_i using nitrocefin as reporter substrate (31). N.D., Not Determined; N.H., No Hydrolisis. Each kinetic value is the mean of five different measurements; the error was below 10%.

Tazobactam was the best inhibitor for all GES enzymes examined (Table 5). However, clavulanic acid was able to inhibit GES-1^{P174E} and GES-5^{P174E} efficiently, with K_i values about 10-fold lower than those calculated for GES-1 and GES-5.

Enzymes	Clavulanic Acid	Tazobactam
	K_i (µM)	K_i (µM)
GES-1	21±1	2.0±0.5
GES-1^{P174E}	2.3±0.1	2.0±0.2
GES-5	17±1	1.7±0.2
GES-5^{P174E}	3.7±1	0.6±0.1

Table 5: Determination of K_i for clavulanic acid and tazobactam. K_i values were determined using nitrocefin as reporter substrate at concentration of 300 µM for GES-1 and GES-1^{P174E}, 150 µM for GES-5 and 50 µM for GES-5^{P174E}.

Circular dicroism

With four enzymes, possible conformational changes resulting from the mutation were estimated by circular dichroism (CD) spectroscopy in the far UV. Thus, spectra (Figure 6) recorded in the 260- to 190-nm range indicate that the signal is dominated by the contribution of α-helices, with negative bands at ~222 and ~208 nm, and, most importantly, comparison of the four spectra shows no significant differences in both their shapes and relative magnitudes, thus indicating that the mutation has no major effect on the secondary structural content of the enzymes.

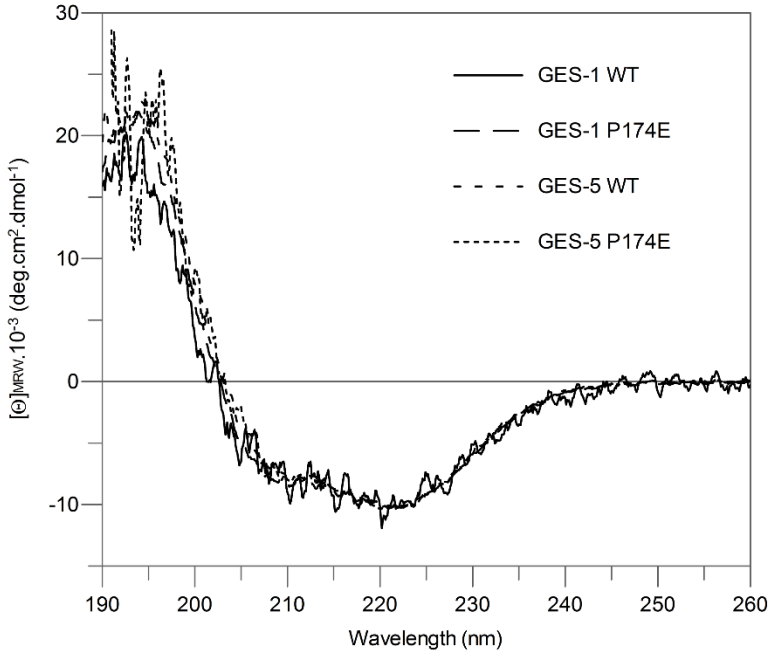

Figure 6: Far-UV spectra of GES-1 and GES-5 wild-type β-lactamases and their corresponding P174E mutants. Data were obtained at 20°C, in sodium phosphate buffer, pH=7.

MD simulations

Molecular dynamic (MD) atomistic simulations were carried out to explain the kinetic behavior of the four enzymes. Eight MD simulations were performed with GES-1, GES-5, GES-1^{P174E}, and GES-5^{P174E} complexed with imipenem and meropenem. The difference between the position of each residue (more precisely the C-α position) along the trajectory and the position of the same residue within the crystal structure of GES-1 was evaluated by calculating the root mean square deviation (RMSD). The result of these simulations reveals that all the systems undergo a sharp, although not dramatic, structural reorganization with respect to the crystal structure of GES-1, even though the native secondary structure was basically unaltered (Figure 7). Most of the relevant deviations are localized in solvent-exposed regions and appear as quantitatively independent of the presence of imipenem or meropenem. By changing the two substrates, differences in deviations were appreciated in the following specific regions: (i) the region comprising residues 78 to 84 (region 78−84) only in the GES-5^{P174E}-meropenem complex; (ii) the loop comprising residues 90 and 99 (loop 90-99); (iii) the α-helix comprising residues 101 to 110 (α-helix 101−110); (iv) α-helix 138−145 only in GES-1 meropenem and GES-1^{P174E}-meropenem complexes; and (v) α-helix 264−274 only in GES-5^{P174E}-meropenem and GES-1-imipenem complexes (Figure 7). The mechanical stability of the investigated systems was evaluated by calculating the fluctuation of the enzyme backbone and the fluctuation of the substrate with respect to the enzyme. Interestingly, results reported in Table 4 show that all the backbones present a relatively low fluctuation in values, confirming a high mechanical stability, in line with the RMSD data (Figure 7). The P174E substitution induces a sharp increase in the internal mobility of the enzyme in all the systems analyzed, with the exception of the GES-1^{P174E}-meropenem complex. We also monitored the fluctuation of each residue (root mean square fluctuation [RMSF]) in the four enzymes complexed with imipenem (Figure 8a) and meropenem (Figure 8b). In detail, a very high fluctuation was observed in the following regions of GES-5^{P174E} complexed with substrates: (a) the solvent-exposed loop 91−100 (both with imipenem and meropenem); (b) the solvent exposed α-helix region 203−211 (only with imipenem), and (c) in the solvent exposed loop 103−113 (only with imipenem). Interestingly, a high mechanical stability in the Ω-loop region, observed for GES-1 and GES-5 complexed with imipenem, was partially lost in the GES-1^{P174E} and GES- 5^{P174E} mutants. When the enzymes were complexed with meropenem, the Ω-loop fluctuation was lower. This effect was explained by monitoring the local contacts between the two substrates and the active-site residues. In Table 6, the average values and the corresponding standard deviations are reported. Both

imipenem and meropenem have contact with active-site residues (S70, K73, S130, N132, E166, P167, G/S170, T237, C238). Moreover, meropenem has a high number of contacts with respect to imipenem. In addition, meropenem also has contacts with residues T235, G236, and R244.

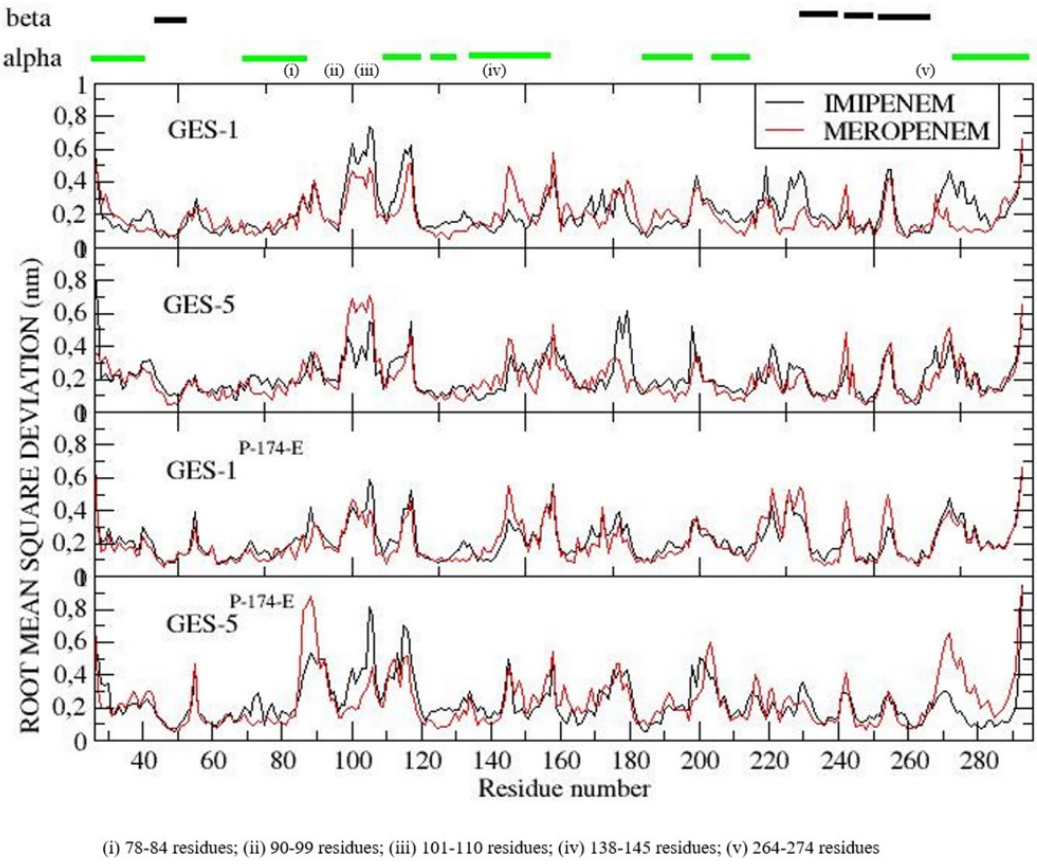

Figure 7. Root Means Square Deviation with respect GES-1 cristal structure for the four investigated systems, i.e., GES-1, GES-5, GES-1^{P174E} and GES-5^{P174E} complexed with imipenem (black curves) and with meropenem (red curves). Above the graph, the structured regions are represented by green (alpha-helix) and black (beta-strands) lines.

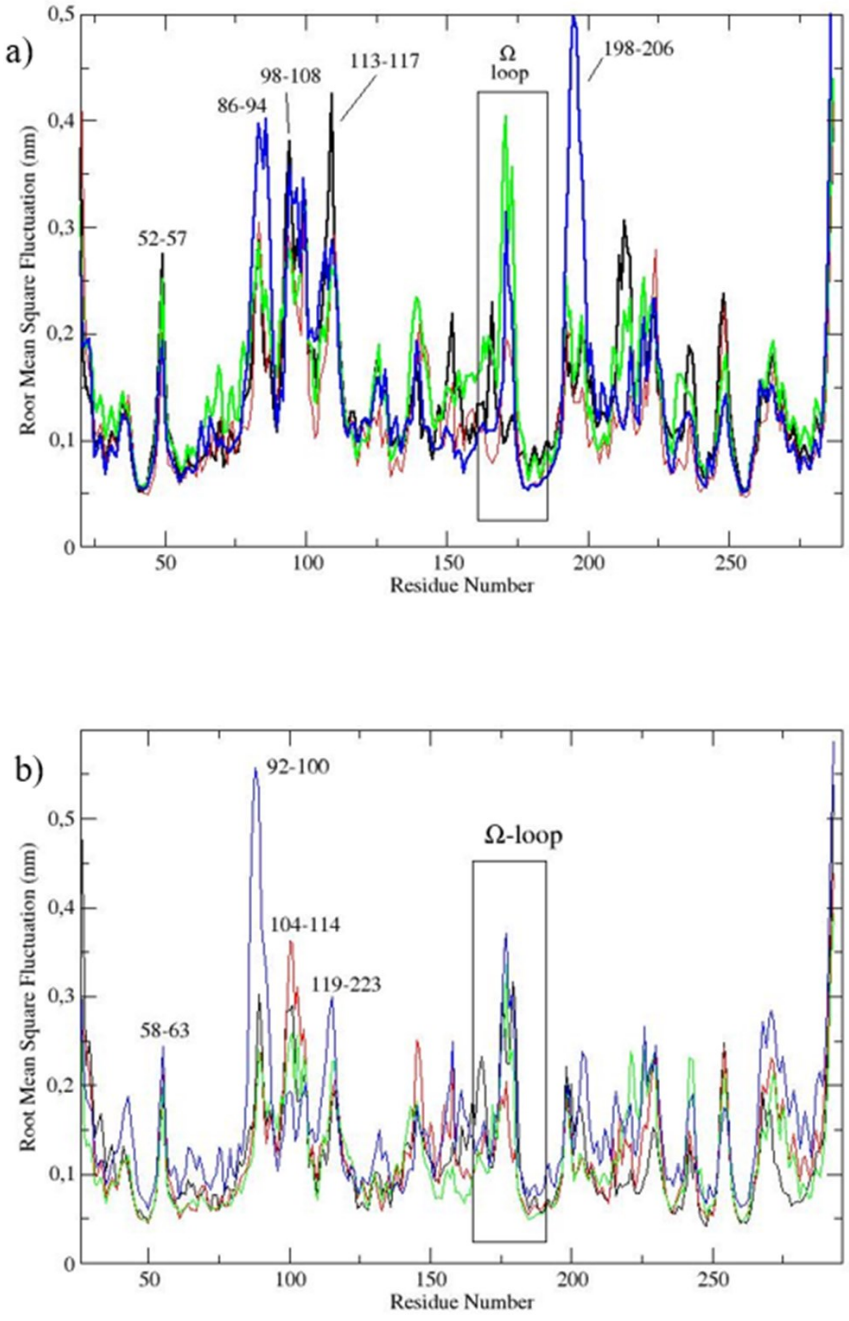

Figure 8: Root Mean Square Fluctuation per residue of the four systems (GES-1, black; GES-5, red; GES-1^{P174E}, green; GES-5^{P174E}, blue) complexed with imipenem (a) and meropenem (b). Note that the numbers in the abscissa refer to the residues according to the sequence reported in PDB records 4GOG and 4H8R.

Antibiotic and residue	Distance (Å) (mean ± SD)[a]			
	GES-1	GES-5	GES-1^{P174E}	GES-5^{P174E}
Imipenem				
S70	**2.5 ± 0.6**	3 ± 1	3 ± 1	3.1 ± 0.6
F72	3 ± 1	5.8 ± 0.7	4 ± 1	4 ± 1
K73	**2.3 ± 0.7**	3 ± 1	4 ± 2	3 ± 1
S130	3 ± 2	4 ± 2	3 ± 2	3 ± 1
N132	4 ± 2	**2.8 ± 0.7**	3 ± 1	4 ± 2
E166	**1.5 ± 0.1**	**1.5 ± 0.2**	**1.5 ± 0.1**	**1.5 ± 0.1**
P167	5 ± 1	3.9 ± 0.6	4.3 ± 0.9	4.5 ± 0.8
G/S170	3.2 ± 0.9	3.2 ± 0.5	3.6 ± 0.5	3.9 ± 0.4
T237	**2 ± 1**	3 ± 1	**2 ± 1**	**2 ± 1**
C238	4 ± 1	6 ± 1	4 ± 1	4 ± 1
Meropenem				
S70	**1.8 ± 0.2**	1.8 ± 0.2	1.8 ± 0.2	2.5 ± 0.1
K73	**3 ± 1**	2.2 ± 0.3	2.5 ± 0.5	3.1 ± 0.9
S130	**1.7 ± 0.2**	1.7 ± 0.2	1.7 ± 0.2	1.6 ± 0.5
N132	**2.8 ± 0.9**	3.0 ± 0.3	3.1 ± 0.5	4.2 ± 0.2
E166	**7 ± 2**	5.7 ± 0.9	5.8 ± 0.8	5 ± 1
P167	**6 ± 2**	7.6 ± 0.8	7.6 ± 0.8	8 ± 1
G/S170	**7.0 ± 0.8**	7 ± 1	7 ± 1	5 ± 1
T235	**1.8 ± 0.2**	1.8 ± 0.2	1.8 ± 0.2	2.8 ± 0.3
G236	**3.9 ± 0.2**	3.9 ± 0.3	3.8 ± 0.3	4.7 ± 0.2
T237	**1.7 ± 0.2**	1.7 ± 0.1	1.7 ± 0.1	2.0 ± 0.6
C238	**5.7 ± 0.2**	5.6 ± 0.3	5.7 ± 0.3	5.5 ± 0.9
R244	**3 ± 1**	2.4 ± 0.9	5 ± 2	5 ± 1

[a]Bold indicates all distances that, considering their fluctuation, were found to reach values below 2.0 Å along the simulation.

Table 6: Distances and related fluctuations (evaluated as SDs) between imipenem and meropenem and the closest residues.

2.6.2 Deciphering the role of position 170 in GES enzymes

The *bla*$_{GES170H}$, *bla*$_{GES170L}$ and *bla*$_{GES170K}$ mutants were prepared by site-directed mutagenesis and cloned into pET-24a (+) vector. The recombinant plasmids were transferred into *E. coli* BL21(DE3) for enzymes expression following the protocol described in the methods section. Purified enzymes were used to determine the kinetic parameters for some β-lactam substrates (Table 7). Compared to GES-1 and GES-5, the three mutants GES-1^{G170H}, GES-1^{G170L} and GES-1^{G170K} showed a reduction of k_{cat} and K_m values towards benzylpenicillin and cephalosporins. Benzylpenicillin was not hydrolyzed by GES-1^{G170K} and the K_m value was calculated as K_i, using nitrocefin as the reporter substrate. GES-1^{G170L} exhibited low K_m and k_{cat} values with a 10-fold-higher catalytic efficiency than GES-1 and GES-5. In comparison with GES-1 and GES-5, all mutants showed an increase in k_{cat}/K_m values for cefotaxime due to lower K_m values. Imipenem was hydrolyzed only by GES-1^{G170L} and GES-1^{G170H}, with k_{cat} values of 0.16 s^{-1} and 3 s^{-1}, respectively. Imipenem was not hydrolyzed by GES-1^{G170K}.

Antibiotics	GES-1			GES-1^{G170L}			GES-1^{G170K}			GES-1^{G170H}			GES-5		
	K_m (μM)	k_{cat} (s^{-1})	k_{cat}/K_m ($\mu M^{-1}\ s^{-1}$)	K_m (μM)	k_{cat} (s^{-1})	k_{cat}/K_m ($\mu M^{-1}\ s^{-1}$)	K_m (μM)	k_{cat} (s^{-1})	k_{cat}/K_m ($\mu M^{-1}\ s^{-1}$)	K_m (μM)	k_{cat} (s^{-1})	k_{cat}/K_m ($\mu M^{-1}\ s^{-1}$)	K_m (μM)	k_{cat} (s^{-1})	k_{cat}/K_m ($\mu M^{-1}\ s^{-1}$)
Benzylpenicillin	210±15	117	0.557	0.07*±0.01	0.4	5.7	6*±1	N.H.	N.D.	31*±2	6	0.19	310±25	254	0.822
Cefazolin	1440±35	375	0.26	117±10	58	0.5	86±8	5	0.06	35±3	9	0.25	500±20	844	1.70
Cefoxitin	50*±5	N.H.	N.D.	3*±1	8	2.7	2*±1	N.H.	N.D.	22*±2	0.68	0.031	380±20	30	0.078
Cefotaxime	12000*±150	N.D.	N.D.	102±10	5	0.05	5*±1	1	0.2	910±80	14	0.015	9600*±220	N.D.	N.D.
Nitrocefin	330±20	168	0.52	91±8	8	0.09	171±10	0.9	0.005	127±9	9	0.07	170±25	769	4.47
Imipenem	0.8*±0.1	0.006	0.0075	25±4	0.16	0.0064	0.0094*± 0.001	N.H.	N.D.	24±3	3	0.125	0.4*±0.1	0.7	1.75

Table 7: Determination of k_{cat}, K_m and k_{cat}/K_m of GES-1, GES-1^{G170L}, GES-1^{G170K}, GES-1^{G170H} and GES-5 towards β-lactams

Steady-state kinetic experiments were performed following the hydrolysis of each substrate at 25°C in 25 mM sodium phosphate buffer (pH 7.0), containing 0.2 M NaCl.

*K_m was calculated as K_i using nitrocefin as reporter substrate. N.D., Not Determined; N.H., No Hydrolysis

2.7 Discussion

In GES enzymes, the Ω-loop seems to play an important role in the catalytic efficiency of carbapenems. As previously reported, the carbapenemase activity in GES enzymes was particularly attributed to position 170. In these enzymes, the replacement of glycine with serine or glutamine enhances the activity against carbapenems (22). Therefore, in our opinion, other Ω-loop residues could also affect the substrate binding and hydrolytic activity toward β-lactams (i.e., carbapenems). For this reason, we focused our attention on proline 174, which is well conserved in several class A β-lactamases (i.e., TEM, SHV, CTX-M), including class A carbapenemases (i.e., SME, KPC, IMI, BIC). Site saturation mutagenesis and consequent selective antibiotic pressure were able to select only the GES-1^{P174E} and GES-5^{P174E} mutants. A single amino acid substitution at position 174 in GES-1 and GES-5 seems to effectively change the catalytic behavior of these enzymes toward some β-lactams. The GES-1^{P174E} and GES-5^{P174E} mutants showed k_{cat} and k_{cat}/K_m values for penicillins and cephalosporins that were lower than those reported for GES-1 and GES-5 prototypes. Instead, the replacement of proline 174 with glutamic acid in GES-1 (G170) and GES-5 (S170) increases the affinity for all carbapenems tested even if the turnover (k_{cat} value) improves slightly. The P174E substitution enhanced the catalytic efficiency of GES-1 and GES-5 for imipenem about 100- and 3-fold, respectively. This behavior seems not to be in agreement with the MIC values, which are the same for GES-1 and GES-1^{P174E}. However, it is possible to compare MIC values only with k_{cat} values. Concerning imipenem, the k_{cat} values were 0.006 s^{-1} for GES-1 and 0.01 s^{-1} for GES-1^{P174E}, in perfect accordance with the MIC values. The high k_{cat}/K_m value for GES-1^{P174E} is due to the lower K_m value. In comparison with GES-1, GES-5^{P174E} showed a 660-fold enhancement in the k_{cat}/K_m value. The combination of S170 and E174 clearly increases the catalytic efficiency toward imipenem. As previously reported, imipenem is a good substrate for GES-5, and this was attributed to the substitution G170S (20,21). Crystal structures of GES-5 complexed with imipenem indicate that the substrate makes several hydrogen bonds with some conserved catalytic residues, such as S70, S130, N132, E166, S170, T235, and T237 (21,22). In comparison with GES-1, the presence of serine 170 has an evident effect on the conformation of the GES-5 active site, moving the E166 toward S70, with consequences for the position of the water molecule involved in the deacylation step. The specific role of residue 170 is to anchor the deacylation water molecule in the active site. In the main class A β-lactamases, this role is played by asparagine, whereas in some GES enzymes, it is played by glycine or serine. In this study, we have attempted a systematic investigation of the Michaelis complexes by performing a comparative analysis of the structural/dynamic differences in eight different systems investigated by means of MD simulations with a long time scale (100 ns). In our

calculations, we cannot find any direct answer concerning the catalytic step, but our results give useful information about the stability of the Michaelis complexes. MD simulations carried out in complexes with two different substrates are in good agreement with the CD spectra. All systems undergo a relatively low deviation from the crystal structure, indicating that the overall shape and the secondary structure elements are systematically conserved. On the other hand, insertion of glutamic acid at position 174 modifies the mechanical stability of the enzymes. In particular, all the mutants systematically show an increase in fluctuation pattern. This effect might be related to the observed reduction in the K_m values calculated for the mutants. Another important effect is related to the substrate size. When imipenem was concerned, we observed a loss of substrate-enzyme contacts with a consequent loss of rigidity of the active site, including the Ω-loop, and a sharp increase in water permeability. In addition, imipenem has stable contacts only with E166 and, minimally, with T237. This finding well explains the higher fluctuation of the backbone and of the enzyme itself. Unlike imipenem, meropenem has a systematically higher number of contacts with catalytic residues. This could be due to the larger size of meropenem than of imipenem. Interestingly, regardless of the nature of the substrate, P174E leads to a reduction in the number of close contacts for both substrates, imipenem and meropenem. This is not in disagreement with the observed increase in fluctuation. All these data correlate well with the level of substrate hydration evaluated by counting the average number of H-bonds formed with the solvent (Table 5). The increase in fluctuation and the loss of substrate-enzyme contacts nicely fit the increase in the average number (and fluctuation) of H-bonds with water. Concerning the inhibitors, tazobactam could be considered the best inhibitor for all the enzymes examined in this study. Clavulanic acid is a good inhibitor for GES-1 and GES-5 variants that showed the same K_i values reported in literature. Interestingly, GES-1^{P174E} and GES-5^{P174E} have K_i values for clavulanic acid that are about 10-fold lower than that of their prototype. The K_i values determined for the two mutants are comparable with that reported for other class A carbapenemases, such as NMCA (clavulanic acid K_i =3.2 μM, tazobactam K_i =2 μM) and KPC-2 (clavulanic acid K_i =1.5 μM, tazobactam K_i= 0.18 μM). The G170 substitution seems to change the behavior of GES-1 enzyme toward some β-lactams. The GES-1^{G170L} and GES-1^{G170H} enzymes showed K_m and k_{cat} values for benzylpenicillin and cephalosporins, that were lower than those for GES-1 and GES-5. The replacement of glycine 170 with leucine in GES-1 (G170L) enhanced the catalytic efficiency for benzylpenicillin about 10-fold. Regards cefotaxime, GES-1^{G170L} and GES-1^{G170K} showed a better hydrolytic efficiency than the other enzymes due to lower K_m and k_{cat} values. The GES-1^{G170L} and GES-1^{G170H} showed an increased turnover (k_{cat} value) for imipenem.

Chapter 3

Kinetic and biochemical characterization of NDM-1 laboratory mutants

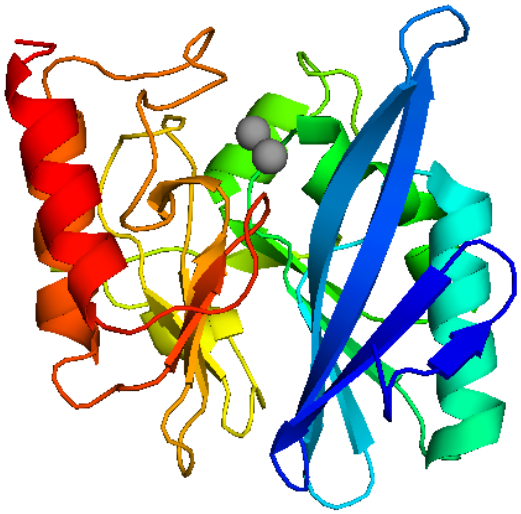

3.1 Metallo-β-lactamases: a significant public health problem

Metallo-β-lactamases (MBLs) are Zn^{2+}-dependent β-lactamases able to hydrolyze most β-lactams, including carbapenems, but not monobactams. These enzymes are members of Ambler class B and belonging to group 3 of Bush–Jacoby–Medeiros classification. MBLs (discovered in the mid-1960s) were not initially considered a serious problem for antibiotic therapy because they were found chromosomally encoded and in non-pathogenic organisms (80,81). This situation changed in the 1990s, when they have been identified in various Gram-negative pathogens, including several species of Enterobacteriaceae, *P. aeruginosa* and *Acinetobacter* spp. (82). MBL *bla* genes are located on the chromosome, plasmids, and integrons. When the integrons are associated with transposons or plasmids, they can readily be transferred among species (83). The more geographically widespread MBLs include IMP, VIM, and NDM (84). Other more geographically confined MBLs include: (a) SPM-1 (Sao Paulo MBL), which has been associated with hospital outbreaks in Brazil; (b) SIM-1 (Seoul imipenemase), from *A. baumannii* isolates in Korea; (c) AIM-1 (Australian imipenemase), isolated from *P. aeruginosa* in Australia;(d) FIM-1 (Florence imipenemase), from a clinical isolate of *P. aeruginosa* in Italy. With the exception of SPM-1, which has been found also in Europe, these MBLs have remained limited to their countries/cities of origin (Figure 9).

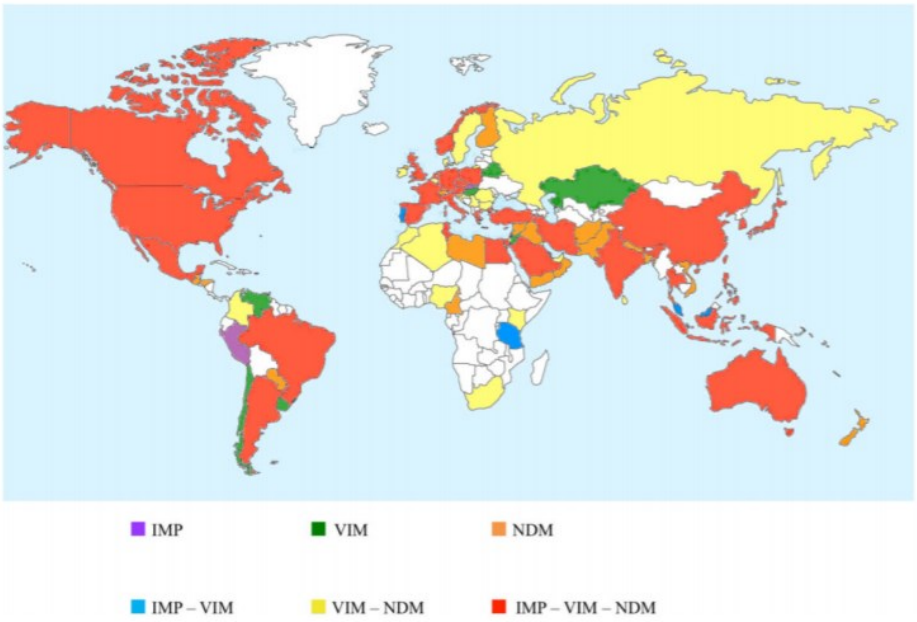

Figure 9: Global distribution of IMP, VIM and NDM MBLs.

3.2 MBLs: biochemistry and classification

X-ray structures of MBLs showed a common αβ/βα sandwich structure, with a central β-sheet sandwich flanked on either side by α-helices, called MBL-fold. The active site, with the two zinc ions, is located at the interface between domains (85,86). On the basis of the sequences, three subclasses of class B β-lactamases (B1, B2 and B3) were identified (Figure 10 and 11). The standard numbering scheme (BBL numbering) of class B β-lactamases allow easy comparisons of the sequences of these enzymes (87). There is a relatively low sequence identity (<20%) between the subclasses. Enzymes of subclasses B1 and B3 are broad spectrum enzymes that hydrolyze most β-lactam antibiotics including carbapenems and the active site contains two zinc ions. The subclass B2 enzymes are strictly carbapenemases and their active site contains only one zinc (88,89). Each subclass is described below.

3.2.1 Subclass B1 MBLs

Subclass B1 contains the largest number of known MBLs, including chromosomal encoded enzymes *Bacillus cereus* BcII (80), CcrA from *Bacteroides fragilis* (90), BlaB from *Chryseobacterium meningosepticum* (91), and the clinically important and transferable IMP-, VIM-, and NDM-type enzymes. These enzymes show broad-spectrum activity towards most β-lactams including carbapenems (92) with the exception of SFB-1 from *Shewanella frigidi* which shows reduced activity towards benzylpenicillin, ticarcillin, meropenem, and third generation cephalosporins (93).

3.2.2 Subclass B2 MBLs

Subclass B2 MBLs differ from B1 and B3 enzymes in their characteristic of harbouring one Zn^{2+} ion in the active site required for β-lactam hydrolysis and exhibit a narrow substrate spectrum focused exclusively on carbapenems hydrolysis (94). The subclass B2 MBLs have similarities in the amino acid sequences with the B1 subclass, probably due to a common ancestor (95). The overall fold is the same of the other MBLs, but the active site cavity is deeper and narrower, perhaps contributing to the substrate profile of these enzymes. The α3 helix (residues R140-L161) is elongated relative to the corresponding helix in B1 enzymes, and has an unusual kink (around W150) enabling it to follow the curvature of the enzyme's surface in the proximity of the active-site groove and provide a surface which contributes to substrate binding. On the other hand, subclass B2 enzymes lack the mobile loop (residues 60–66) observed in B1 members, which is involved in the substrate binding (96,97). The enzymes of subclass B2 show only 11% of identity with subclass B1 members. This subclass includes the enzymes produced by different species of *Aeromonas* (the most studied are CphA produced by *A.*

hydrophila (98) and ImiS produced by *A. veronii* (99) as well as the Sfh-I enzyme produced by *Serratia fonticola* (100). The genes coding for subclass B2 enzymes are located on the chromosome.

3.2.3 Subclass B3 MBLs

Most of the subclass B3 MBLs producing bacteria are environmental inhabitants and non-pathogenic. Subclass B3 enzymes are generally found to be intrinsically located on the chromosome, with the exception of bla_{L1} which was found also in a plasmid of *Strenotrophomonas malthophilia* (101) and, AIM-1 and SMB-1, which have been found to be acquired by *P. aeruginosa* and *S. marcescens*, respectively (102) With the exception of L1, that showed a tetrameric structure, all members of this subclass are monomeric enzymes. In L1, tetramerization is achieved by three defined sets of interactions. The two most striking sets of interactions involve the N-terminus region. The last set of interactions is made by the M175 side-chain, which penetrates into a hydrophobic pocket defined by L154, P198 and Y236. The differences from subclass B1 enzymes include an elongated C-terminal helix and longer α3–β7 and β12–α5 loops. By contrast, the equivalent of the β3–β4 (residues 60–66) loop in subclass B1 enzymes is a significantly shorter (by 7–8 residues) β2–β3 loop and supporting β-sheets. In subclass B3 enzymes there is an intramolecular disulphide bridge, which restricts the elongated β12–α5 loop and stabilises the elongated C-terminal helix. Subclass B3 metallo-β-lactamases have only nine conserved residues when compared with the other metallo β- lactamases.

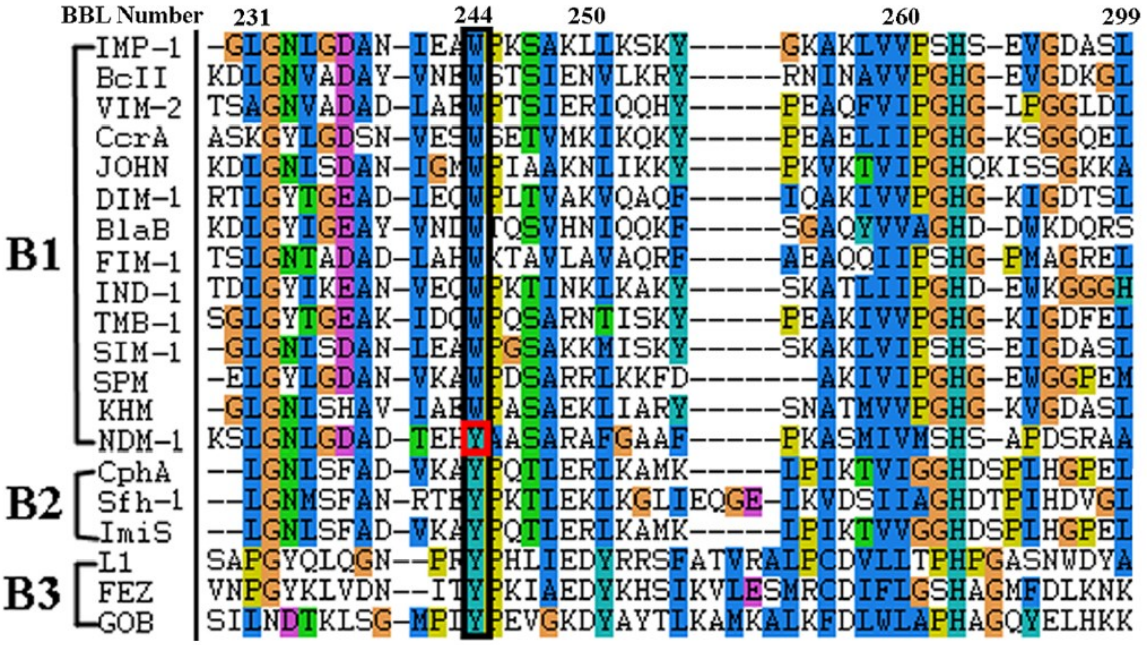

Figure 10: The sequence alignment of MBLs around position 244 (BBL numbering), parallel with position 229 in NDM-1. In bold is highlighted residue Y229 in NDM-1.

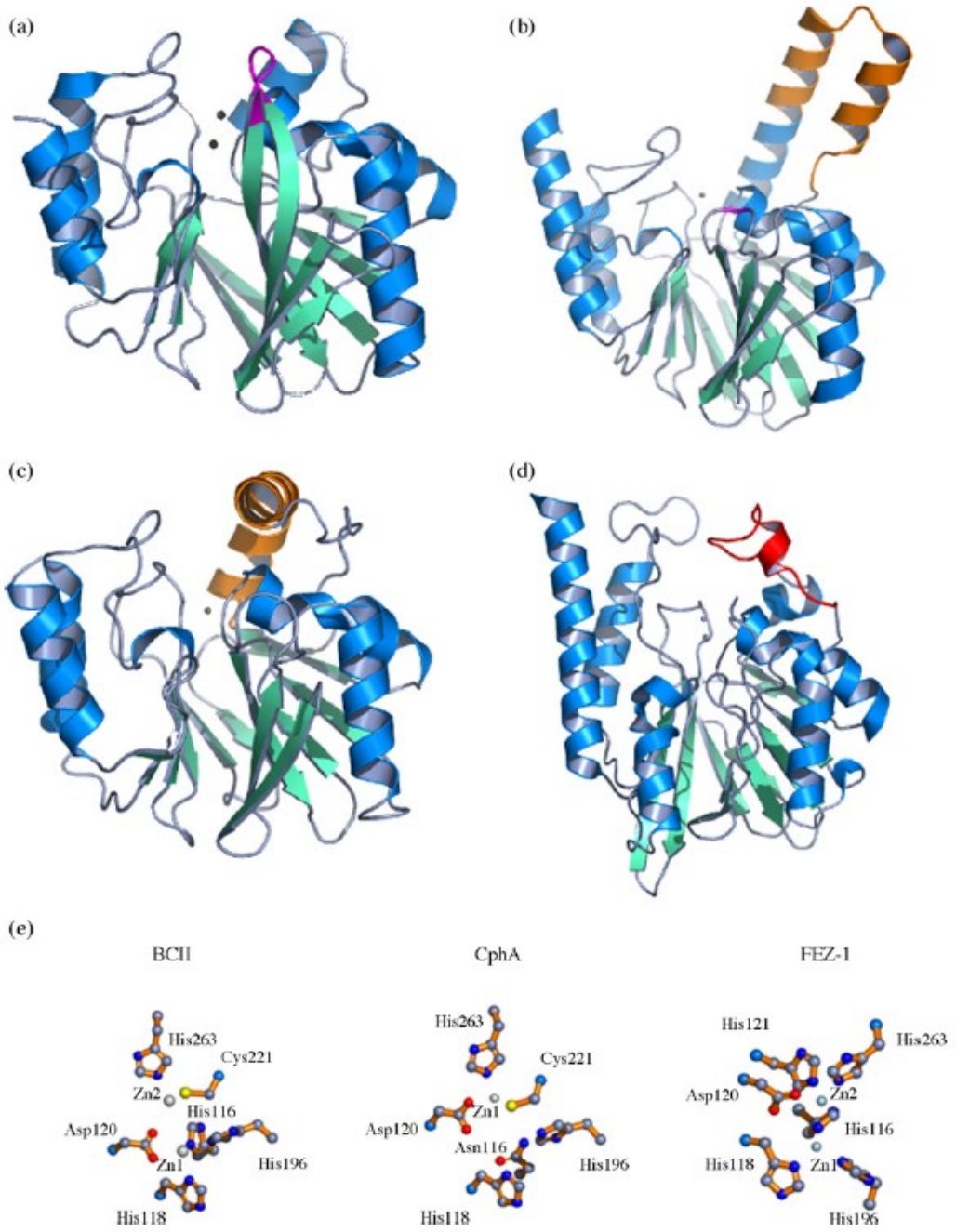

Figure 11: Metallo-β-lactamases overall structures. The helices are represented in blue, strands in green and loops in grey. (a) Subclass B1 BcII enzyme with the mobile 61–65 loop in magenta. (b) Subclass B1 SPM-1 enzyme with residues 61–65 in magenta and the extended α3-α4 region in orange. (c) Subclass B2 CphA enzyme with the elongated α3 helix in orange. (d) Subclass B3 FEZ-1 enzyme with the 151–166 loop in red. (e) Representation of the zinc binding sites of subclass B1 (BcII), B2 (CphA), and B3 (Fez-1) β-lactamases (92).

3.3 Catalytic mechanism of MBLs and metal coordination

MBLs require zinc as a metal cofactor and have two zinc binding sites in close proximity to one another; these are often referred to as Zn1 or the 3H site and Zn2 or the DCH site, although there are variations in the coordinating residues, particularly between the different subclasses. In a number of cases crystal structures have been obtained with a single zinc ion bound (particularly when crystallised at low pH), but all the evidence indicates that all MBLs can bind two zinc ions under the right conditions. Representative coordination structures are shown in Figure 12. There has been controversy about the number of zinc ions required for catalysis and the mechanism of metal binding; this is discussed below in the context of the individual subclasses. However, MBLs possess two potential Zn^{2+} binding sites. In the case of B1 enzymes, Zn1 possesses a tetrahedral coordination sphere and is coordinated by H116, H118, H196 and a water molecule or hydroxide ion. The Zn2 has a trigonal-pyramidal coordination sphere which involves D120, C221, H263 and two water molecules. One water/hydroxide molecule serves as a ligand for both metal ions. The two binding sites are named the ‘‘histidine’’ and ‘‘cysteine’’ sites, respectively. In the mononuclear BcII, VIM-2 and SPM-1 enzymes, the sole metal ion was shown to be located in the ‘‘histidine’’ site. Enzymes of subclass B2 are inhibited in a non-competitive manner by the binding of a second zinc ion (103). As shown in Figure 11, the structure of the di-zinc CphA enzyme shows that the second zinc ion is bound in a modified Zn1 site; H118 and H196 are conserved, but the third ligand H116 is not conserved and is replaced by an asparagine residue, which is not involved in metal binding. It has been proposed that the binding of the second zinc ion inhibits B2 enzymes by immobilizing H118 and H196 and preventing them from playing their roles in the postulated catalytic mechanism (104). For subclass B3, in the Zn1 (3H) site the metal ion is coordinated by the same conserved residues (H116, H118 and H196, BBL numbering) as subclass B1 enzymes, and by a bridging water (or hydroxide ion). By contrast, while the distorted trigonal bipyramid geometry of the Zn2 site is retained, the ligands comprise aspartate (D120) and histidine (H263), equivalent to those seen in subclass B1 enzymes, together with a second, non-conserved, histidine residue (H121), the bridging water molecule and a second, apical, water. The serine (S221) which replaces the cysteine ligand in B1 enzymes is not involved in metal binding.

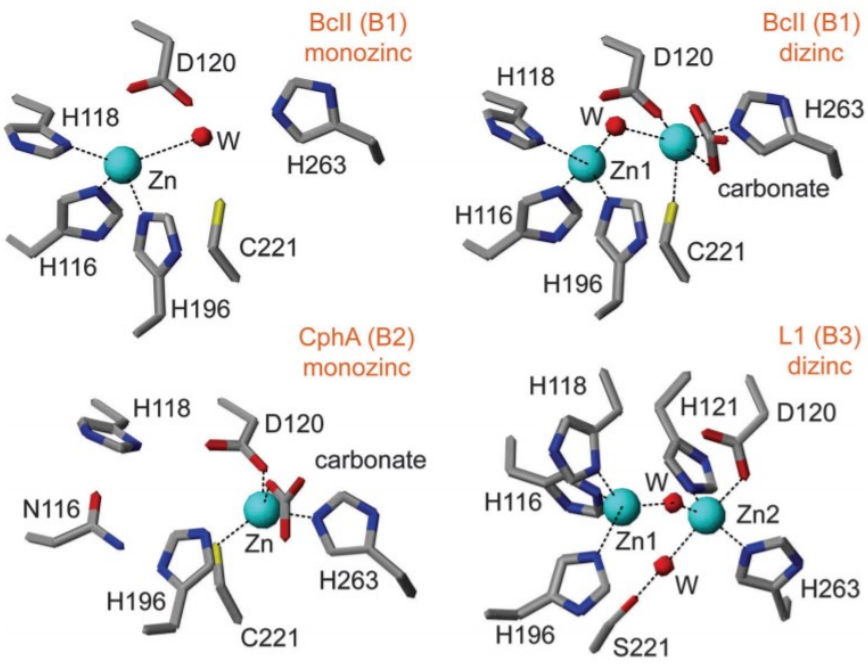

Figure 12: Representative zinc coordination in the active site of B1, B2 and B3 MBLs. BBL numbering is used for all examples.

The zinc acts as a Lewis acid by co-ordination to the amide carbonyl oxygen giving a more electron deficient carbonyl carbon which facilitates nucleophilic attack by the zinc-bound hydroxide and/or it stabilizes the negative charge developed on the carbonyl oxygen of the tetrahedral intermediate anion. Coordination to the metal ion will lower the pKa of the co-ordinated water, increasing the concentration of the hydroxide species. However, the hydroxide ion formed by this ionization, while it may become the dominant species, will be stabilized by simultaneous coordination to two zinc ions and hence will be more weakly nucleophilic. Finally, breakdown of the tetrahedral intermediate could be facilitated by direct co-ordination of the departing amine nitrogen to the metal ion or, alternatively, a metal-bound water could act as a general acid catalyst, protonating the amine nitrogen leaving group. Different mechanisms of hydrolysis have been proposed for the three different subclasses of MBLs and a briefly explanation is given below.

Two zinc mechanism – subclasses B1 and B3

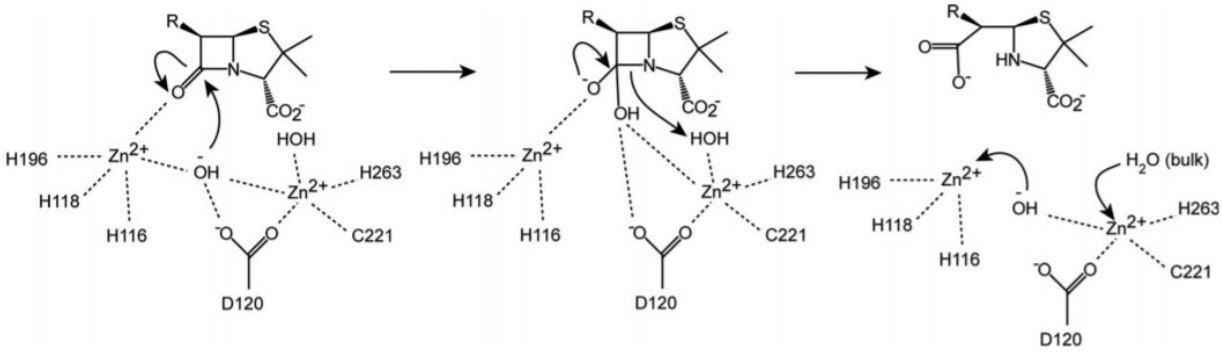

Scheme 1: Catalytic mechanism for di-zinc B1 MBLs (105).

As suggested by Zheng & Xu (105), this mechanism involves the bridging hydroxide performing the nucleophilic attack on the β-lactam carbonyl carbon, transfer of its proton to D120 and C–N bond cleavage occurring together.

One zinc mechanism in subclasses B1

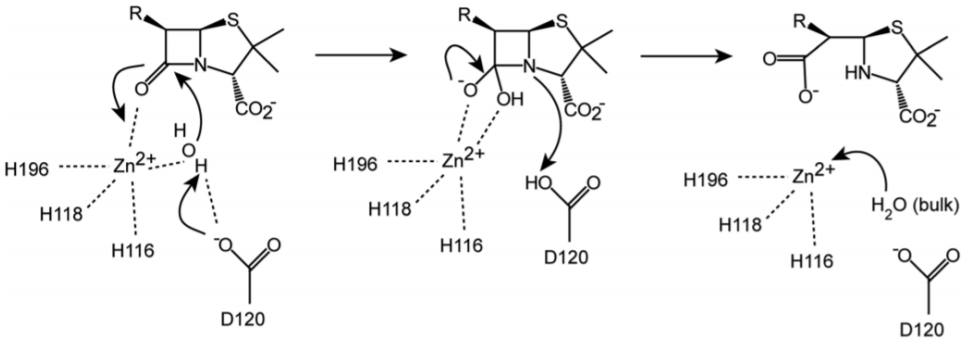

Scheme 2: Proposed hydrolysis mechanism for mono-zinc B1 MBLs (105).

This proposed mechanism involves deprotonation of a Zn-bound water molecules by D120, forming a hydroxide ion which performs the nucleophilic attack on the carbonyl carbon, the zinc ion stabilizing the anionic tetrahedral intermediate, and the β-lactam nitrogen receiving back the proton from D120.

One zinc mechanism – subclass B2

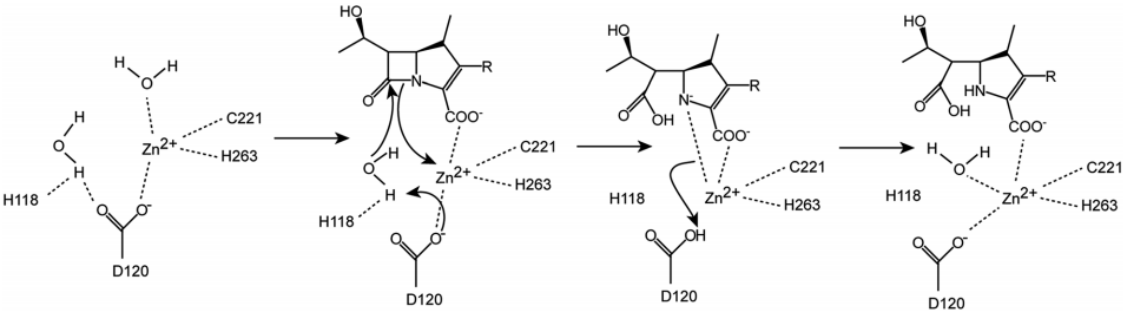

Scheme 3: Proposed hydrolysis mechanism for mono-zinc B2 MBLs (105).

In contrast to the mechanism proposed for mono-zinc B1 enzymes, where the zinc ion is in the Zn1 (3H) site, the nucleophilic attack is carried out by a water molecule which is not zinc-bound and which is activated by D120. The zinc ion coordinates the β-lactam nitrogen and promotes the ring opening reaction by stabilizing the negative charge on nitrogen during the transition state; it is not involved in the interacting with the anionic transition state, which is stabilized by H196, D120 and H118. After a rotation about the C5–C6 bond, the newly formed carboxyl interacts with T119 and T157 and a water molecule protonates the lactam nitrogen, followed by release of the substrate.

3.4 New Delhi Metallo-β-lactamase-1: epidemiology and genetic

The New Delhi Metallo-β-lactamase-1 (NDM-1) was first identified in a multidrug-resistant *K. pneumoniae* strain isolated from a Swedish patient (106). To date, NDM-1 and its variants have been found in Enterobacteriaceae, including *E. coli*, *P. mirabilis*, *K. pneumoniae*, and *Citrobacter koseri* (107-110), as well as in nonfermenters such as *P. aeruginosa* and *A. baumannii.* NDM-1-producing bacteria have been identified from both nosocomial and community-acquired infections, including urinary and pulmonary tract infections, peritonitis, septicemia, and osteomyelitis, throughout the world. NDM-1-positive strains can degrade almost all β-lactam antibiotics, including penicillins, cephalosporins, and the highly potent carbapenems (111). Instead, NDM-1 does not conferred resistance to monobactam, aztreonam, and the amidinopenicillin, mecillinam (112). NDM-1 genes are encoded on plasmids, facilitating their transmission across different bacterial strains. In addition, the widespread use of β-lactams has created selective pressure that promotes the dissemination of

MBLs genes. An increase in population exchange at global level and enhanced medical tourism could play a significant role in spreading uncontrolled NDM-1 related resistance worldwide. In fact, in these bacteria, NDM-1 is secreted in outer membrane vesicles, which increases the stability of the enzyme. Asian continent is the major reservoir of NDM-producers, with around 58.15% abundance of NDM-1 variant distributed mostly in China and India. Europe shows around 16.8% of the total producers, with the maximum spread of NDM-1 variant in Bulgaria, Romania, Poland, France, Italy, Turkey, Germany, Greece, Serbia, London, Ukraine, Croatia, Azerbaijan and Ireland. NDM-4 is also reported to be distributed in European subcontinent in Italy, while NDM-5 and NDM-7 are prevalent in Denmark and France. American continent shows around 10.8% abundance of the total NDM-1 producers as reported globally, of which subcontinent Brazil serves as the major reservoir. Africa carries around 10.8% pool of the total NDM-1 producers scattered globally. Australia serves as the 1.6% reservoir of the total NDM-1 producers. However, the clinical success of NDM enzymes is attributed as well to the fact that NDM-1, in Gram-negative bacteria, is a lipidated membrane-anchored enzyme (113). The *bla*$_{\text{NDM}}$ genes have evolved over time, and 26 NDM variants, differing from each other by a few amino acids, have been identified. In clinical isolates, the most frequent amino acid substitution found in NDM variants is M154L, present in a single or double mutant (NDM-4, NDM-5, NDM-7, NDM-8, NDM-12, NDM-13, and NDM-15). In many variants, D130 is replaced by a residue of asparagine (NDM-7) or glycine (NDM-8 and NDM-14) also in combination with M154L (NDM-7 and NDM-8). Single substitutions P28A, D95N, A233V, and R264H are present in NDM-2, NDM-3, NDM-6, and NDM-16, respectively. A wide range of antibiotic resistance genes have been found to be co-harbored by the plasmids carrying *bla*$_{\text{NDM-1}}$, resulting in additional resistance mechanisms against β-lactams (e.g., due to the presence of ESBLs and AmpC cephalosporinases), macrolides (due to erythromycin esterase), tetracyclines (due to increased efflux) and sulfonamides (due to altered dihydropteroate synthases) (114). The presence of the ESBLs and cephalosporinases as a result of these co-harbored resistance genes accounts for the resistance of many NDM-1 producers to aztreonam, which is not hydrolyzed by NDM-1 enzyme (115). This particular resistance pattern is governed by a set of genes that can move easily from one bacterium to another. *bla*$_{\text{NDM-1}}$ was associated with different plasmid scaffolds (IncFII, IncL/M, IncN, IncR, IncHIB-M/FIB-M), IncF type being the prevalent one. Bonnin RA et al. have characterized the IncFII plasmid carrying the *bla*$_{\text{NDM-1}}$ gene from *E. coli* ST131 (116). The *bla*$_{\text{NDM-1}}$ gene was localized in a multidrug resistance (MDR) region of 20,181 bp. This region was bracketed by two copies of insertion sequence IS*26* in opposite orientations creating an IS*26*-made compound transposon that was not bracketed by a target site duplication. Immediately upstream of the *bla*$_{\text{NDM-1}}$ gene, a remnant of IS*Aba125* insertion sequence was identified. This truncated IS*Aba125* contained the −35 promoter

sequence leading to the *bla*$_{NDM-1}$ gene expression. Upstream of the ΔIS*Aba125*, two IS*26* were identified bracketing the *aacC2* aminoglycoside resistance gene. Then, three gene cassettes being part of a remnant of a class 1 integron, namely *aacC4*, *bla*$_{OXA-1}$ and a truncated *catB4* genes were identified, that latter gene being truncated by another IS*26* element (Figure 13).

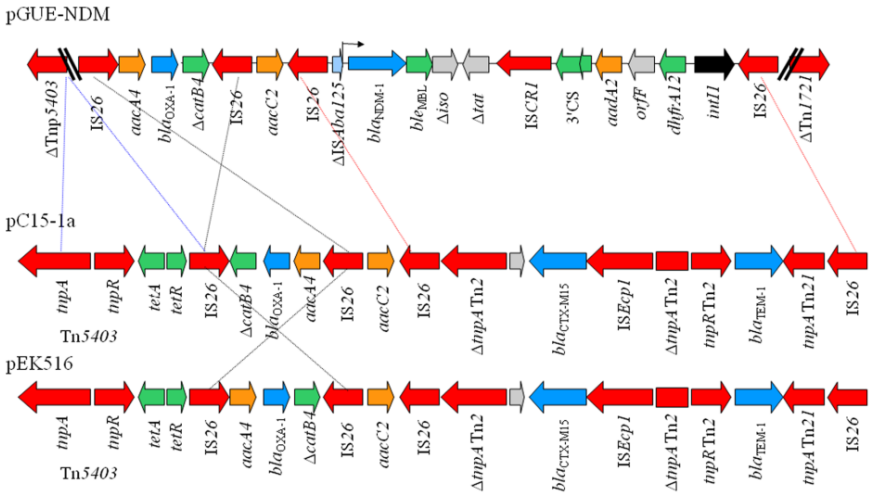

Figure 13: Schematic representation of multi-drug resistance regions of pGUE-NDM, pC15-1a and pEK516 incFII plasmids. The genes and their corresponding transcriptional orientations are indicated by horizontal arrows: green, tetracycline resistance; azure, β-lactams resistance genes; orange, aminoglycosides resistance genes; dark green, trimethoprim resistance gene. Transposon-related genes and insertion sequences are indicated in red arrows. Class 1 integrase gene is indicated by black arrow. Deletion is indicated by blue dashed lines. Homologous recombination event leading to inversion is indicated by black dashed lines. Homologous recombination event leading to allelic exchange of *bla*$_{CTX-M-15}$ locus by *bla*$_{NDM-1}$ locus is indicated by red dashed lines. The accession numbers were: pC15-1a (genbank n°AY458016) and pEK516 (genbank n°EU935738) (116).

Downstream of the *bla*$_{NDM-1}$ gene, the *ble*$_{MBL}$ gene encoding resistance to bleomycin was identified followed by a truncated phosphorybosilanthranilate isomerase gene (*Δiso*), and then by a truncated twin-arginine translocation pathway signal protein gene (*Δtat*), as previously found on other plasmid scaffolds. Then, the IS*CR1* insertion sequence was identified, followed by a class 1 integron structure containing three gene cassettes, namely *aadA2* encoding resistance to streptomycin and spectinomycin, *orfF* of unknown function, and *dfrA12* encoding resistance to trimethoprim, and then the class 1 integrase gene. Finally, an additional copy of IS*26* truncating the Tn*1721* transposase gene was identified.

3.5 Structure and catalytic mechanism of NDM-1

NDM-1 is a single-chain polypeptide consisting of 270 amino acids with an N-terminal signal peptide of 28 amino acids. NDM-1 is actively present as a monomer in solution. NDM-1 adopts a characteristic αββα fold with two twisted β-sheets packed together, each flanked on its outer face by two α-helices, and a fifth helix bridging these two β-sheets, which is a common feature to all MBLs. However, the overall structure of NDM-1 shows some difference to other MBLs. NDM-1 shows lower sequence identity with other MBLs, and the most closely related MBLs are VIM-2 and IMP-1, which show about 32% sequence identity with NDM-1. Figure 14 is a cartoon representation of NDM-1 with VIM-2 and IMP-1 superimposed onto it. As shown in figure 14A, it is clear that the N-terminus of NDM-1 is much longer than that of VIM-2 or IMP-1, forming two more β-strands (labelled as β1 and β1" in Figure 14A) but not part of the N-terminal β-sheet. The tip of these extra strands packs to loop L3 through residue I35 (Figure 14B), which may strengthen or extend the hydrophobicity of loop L3 and contribute to substrate binding or specificity. A close examination shows that the substrate binding face of this loop in NDM-1 is more hydrophobic than others, which may contribute to tight substrate binding strand β8. In other MBLs this loop is replaced by a twisted β turn in NDM-1 moving away from strand β9. This configuration is probably attributed to the two proline residues in this fragment (P171 and P175), which disrupt the β-strand conformation (26). The active site of NDM-1 is located at the bottom of a shallow groove enclosed by two important loops, L3 and L10. Consistent with other subclass B1 MBLs, two zinc ions are also located at the active site, with Zn1 coordinated by three histidine residues (H120, H122, and H189) and Zn2 coordinated by D124, C208, and H250 (117).

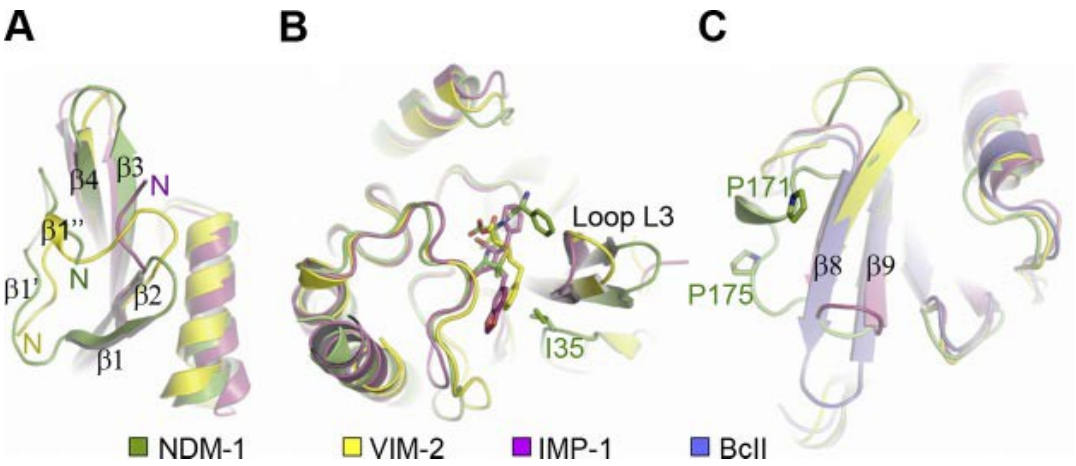

Figure 14: Ribbon representation of VIM-2, IMP-1, and BcII superimposed onto NDM-1. NDM-1, VIM-2, IMP-1, and BcII are shown in green, yellow, magenta, and blue, respectively (26).

As mentioned above, Loop L3 in MBLs is flexible, which enables the active site of MBLs to accommodate different substrates. To facilitate substrate hydrolysis, the active site needs both stability and flexibility. The flexibility of the active site loops (L6 and L10) might assist the structural rearrangement of the metal sites during catalytic turnover. By structural comparison with other MBLs, 2 residues in NDM-1 might play critical roles in stabilizing the conformation of the active site, which are residue Y229 and residue K125. In subclass B1 MBLs (BcII, CcrA, IMP-1, VIM-2 and VIM-4), a tryptophan residue is conserved at position 229 (NDM-1 numbering), while in subclass B2 MBL (CphA) and in subclass B3 (L1), it is a tyrosine residue. In contrast to other subclass B1 MBLs, NDM-1 also has a tyrosine residue at 229 instead of a tryptophan residue, which makes it look like subclass B2 or B3 MBLs. A close examination shows that this residue forms extensive hydrophobic interactions with neighbouring residues both on top and bottom (Figure 15). On top of this residue, residue L269 in helix α5, and residues L218 and L221 in loop L10, form strong hydrophobic interactions with it. It is worth nothing that the 2 residues between L218 and L221 (i.e., residues G219 and N220) are conserved in subclass B1 MBLs, which are proposed to participate in the catalysis reaction (118). Although the aforementioned three leucine residues are not fully conserved in other subclass B1 MBLs, the two leucine residues in Loop L10 are always occupied by hydrophobic residues, such as in BcII, in which they are leucine and valine, respectively (119). Besides forming hydrophobic interactions with upper residues, residue Y229 also forms hydrophobic interactions with residues below it, one of which is residue L209, the one just following the Zn2 binding ligand C208 in NDM-1. In addition, the hydroxyl group of residue Y229 forms a hydrogen bond with the main chain carboxyl oxygen of residue L209. These hydrophobic and hydrophilic interactions appear to stabilize or orient the Loop L10 with respect to the C-terminal β-sheet restricting the flexibility of

N220 conferred by G219.

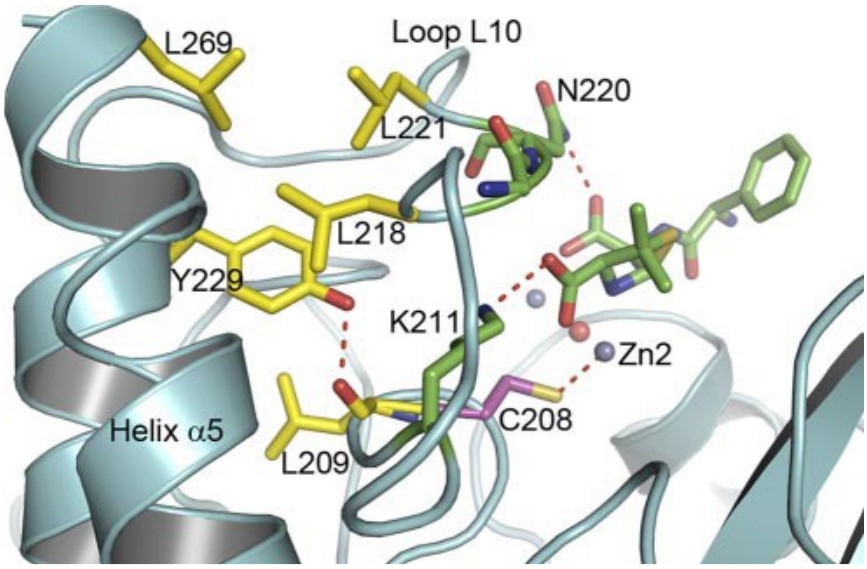

Figure 15: Interactions between residue Y229 and loop L10. Residues in loop L10, including C208, L209, K211, L218, G219, N220, and L221, and residue L269 in helix α5 are shown as stick models. Hydrolyzed ampicillin is also shown as a stick model with green carbons (26).

Loop L6 in subclass B1 MBLs contains 3 important zinc ligands, i.e., H120 and H122 for Zn1 and D124 for Zn2. The role of D124 in subclass B1 MBLs has been studied extensively. Although this residue is not conserved in some enzyme of subclass B1 MBLs (arginine in BcII and VIM-2, serine in CcrA and IMP-1), the position of this residue is too important to be ignored, and with residue Q123, they play important roles for substrate binding, catalysis and inhibition through H-bond interaction. Through these hydrogen bond networks, residue K125 links loop L6 to the N-terminal β-sheet, restricting the flexibility of loop L6 and hence the conformations of 3 zinc ligands (H120, H122 and D124).

Based on the crystal structure of NDM-1 enzyme, Zhang and Hao (26), investigated a hypothetical catalytic mechanism. The structure of NDM-1 in complex with a hydrolyzed ampicillin revealed the tight binding of NDM-1 to penicillin and ampicillin through hydrophobic interactions with the more hydrophobic loop L3 and insight into the lower activity by disclosing a longer distance between the 2 zinc ions at the active site. The proposed catalysis mechanism should be applicable to all three subclasses of MBLs, with a proton coming from the newly formed carboxyl group in the β-lactam ring (Scheme 4).

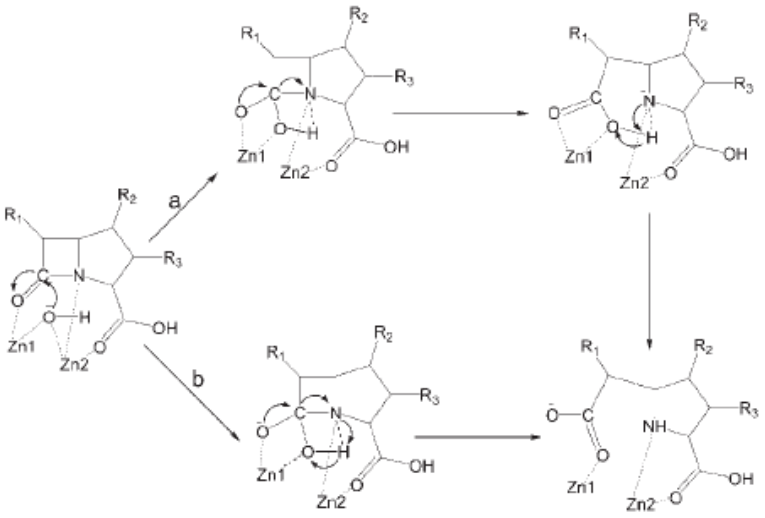

Scheme 4: Drawing of the proposed hydrolysis mechanism of β-lactams by NDM-1 (26).

During hydrolysis of β-lactams, the shared hydroxide between the two zinc ions attacks the carbonyl carbon of β-lactam ring as a nucleophile. Two pathways have been proposed: (a) the C-N bond breaks immediately on the nucleophile attacking resulting in a nitrogen anion intermediate (120); (b) the break of the C-N bond is concerted with the protonation of the nitrogen atom and no nitrogen anion intermediate is generated. In either path, the nitrogen atom of the β-lactam ring gets a proton from the attacking hydroxide.

3.6 Specific aims of the study

In this chapter we focused the attention on NDM-1 metallo-β-lactamase and, in particular, on the role of some hydrophobic residues (leucines) in the hydrolytic activity of the enzyme.

The specific aims of the present study were:

1.Elucidate the role of hydrophobicity in NDM-1 enzyme through the replacement of leucine residues at position 218, 221 and 269 and kinetic analysis of these laboratory mutants.

Leucines 218 and 221 were replaced by threonine, that contains an α-amino group, a carboxyl group, and a side chain with a hydroxyl group. Threonine is a polar, uncharged amino acid. Instead, leucine

at position 269 was substituted with a histidine residue, as in VIM-4 MBL.

2. Evaluate, by kinetic analysis and molecular dynamic (MD) simulations, the effect of the Y229W substitution on the L209F laboratory variant.

Y229W mutant was described by Chen et al. to have an increase of the activity toward meropenem and other cephalosporins (121). On the contrary, L209F mutant showed a drastic reduction of activity toward all β-lactams tested (122). The objective was to verify if the substitution Y229W, in combination with L209F, was able to restore the activity of L209F mutant.

NDM numbering is used in order to facilitate the comparison with other NDM-1 studies.

3.7 Materials & methods

3.7.1 Site-directed mutagenesis and cloning. The NDM-1^{L218T}, NDM-1^{L221T}, NDM-1^{L269H} and NDM-1^{Y229W} mutants were generated by site-directed mutagenesis (65) from pFM-NDM-1. Site-directed mutagenesis was also performed to obtain NDM-1$^{L209F-Y229W}$ mutant from pET-24-L209F. The *bla*$_{NDM}$ was used without N-terminal lipidation signal (first 35 amino acids) (123). In order to amplify the entire gene, the NDM_for (5'-GGGGG**CATATG**GGTGAAATCCGCCCGA) and NDM_rev (5'-GGGGG**CTCGAG**TCAGCGCAGCTTGTCGGC) primers were used (restriction site sequences are in bold). The primers for site-directed mutagenesis are listed below:

L218T_for (5'- GCCAAGTCGACCGGCAAT)

L218T_rev (5'- ATTGCCGGTCGACTTGGC)

L221T_for (5'- GGCAATACCGGTGATGCC)

L221T_rev (5'- GGCATCACCGGTATTGCC)

L269H_for (5'- ATGGCCGACAAGCATCGCTGA)

L269H_rev (5'- TCAGCGATGCTTGTCGGCCAT)

Y229W_for (5'-ACTGAGCACTGGGCCGCGTCA)

Y229W_rev (5'-TGACGCGGCCCAGTGCTCAGT)

DNA sequences coding for NDM variants were cloned into the pET-24a (+) overexpression vector digested with *NdeI* and *XhoI* restriction enzymes. The authenticity of NDM variants was confirmed by sequencing recombinant plasmids using an automated sequencer (ABI Prism 3500; Life Technologies, Monza, Italy). The *E. coli* NovaBlue strain was used for the initial cloning as a nonexpression host. The *E. coli* BL21(DE3) - CodonPlus strain was used for overexpression of the

bla$_{NDM}$ mutants.

3.7.2 Expression and purification of L218T, L221T, L269H, Y229W and L209F-Y229W enzymes. *E. coli* BL21(DE3) -CodonPlus cells harboring *bla*$_{L218T}$, *bla*$_{L221T}$, *bla*$_{L269H}$, *bla*$_{Y229W}$ and *bla*$_{L209F-Y229W}$ were grown in 1 liter of tryptic soy broth (TSB) medium with 50 µg/ml kanamycin at 37°C in an orbital shaker (180 rpm). Each culture was grown to achieve an A_{600} of approximately 0.5, and 0.4 mM isopropyl-β-$_D$-thiogalactoside (IPTG) was added. After the addition of IPTG, the cultures were incubated for 16 h at 22°C under aerobic conditions. Cells were harvested by centrifugation at 8,000 rpm for 10 min at 4°C and washed twice with 25 mM Tris-HCl buffer (pH 7.6) (buffer A). Crude enzymes were obtained by sonication in ice (5 cycles at 60W with 2 min of break). The lysate was centrifuged at 100,000 g for 30 min, and the cleared supernatant was recovered and loaded onto a Q Sepharose Fast Flow column (GE Healthcare, Milan, Italy) equilibrated with buffer A. The column was extensively washed to remove unbound proteins, and the metallo-β-lactamase was eluted with a linear gradient of 25 mM Tris-HCl (pH 7.6) plus 1 M NaCl (buffer B). The fractions containing β-lactamase activity were pooled, concentrated 20-fold using an Amicon concentrator (YM 10 membrane; Millipore, Bedford, MA, USA), dialyzed in 30 mM morpholineethanesulfonic acid (MES [pH 5.9]), and loaded onto a Mono S column (GE Healthcare, Milan, Italy) equilibrated with the same buffer. The active fractions were collected during the elution process and then dialyzed in 20 mM HEPES buffer (pH 7.0) for kinetic experiments.

3.7.3 Antibiotics. Meropenem was obtained from AstraZeneca (Milan, Italy). Imipenem was obtained from Merck Sharp & Dohme (Rome, Italy). The other antimicrobial agents used in this study were purchased from Sigma-Aldrich (Milan, Italy). The molar extinction coefficients and wavelengths used in the assay were imipenem ($\Delta\varepsilon_{300nm}$ = -9000 M^{-1} cm^{-1}); meropenem ($\Delta\varepsilon_{297nm}$ = -6500 M^{-1} cm^{-1}) ; cefepime ($\Delta\varepsilon_{260nm}$ = -10,000 M^{-1} cm^{-1}; cefazolin ($\Delta\varepsilon_{260nm}$ = -7400 M^{-1} cm^{-1}); carbenicillin ($\Delta\varepsilon_{235nm}$=-780 M^{-1} cm^{-1}); benzylpenicillin ($\Delta\varepsilon_{235nm}$ = -775 M^{-1} cm^{-1}); cefotaxime ($\Delta\varepsilon_{260nm}$ = -7500 M^{-1} cm^{-1}), cefoxitin ($\Delta\varepsilon_{261nm}$ = -7775 M^{-1} cm^{-1}); and ceftazidime ($\Delta\varepsilon_{260nm}$ = -7500 M^{-1} cm^{-1}).

3.7.4 Determination of kinetic parameters. Steady-state kinetic experiments were performed following the hydrolysis of the β-lactams at 25°C in HEPES 20 mM (pH 7.0) plus 20 µM $ZnCl_2$. The data were collected with a Lambda 25 spectrophotometer (Perkin-Elmer Italia, Monza, Italy). Kinetic parameters were determined under initial-rate conditions using the GraphPad Prism 6 software to generate Michaelis- Menten curves or by analyzing the complete hydrolysis time courses (124,125). Each kinetic value represents the mean of the results from three different measurements;

the error rate was below 10%. To calculate k_{cat} values, we used the theoretical molecular weight of 25,605.87 Da, assuming cleavage of signal peptide at residue G29 (G24 according to BBL standard numbering), as predicted from SignalP 4.0 (126).

3.7.5 Antimicrobial susceptibility. The phenotypic profile has been characterized by a microdilution method using a bacterial inoculum of $5x10^5$ CFU/ml according to Clinical and Laboratory Standards Institute (CLSI) performance standards (66). The *E. coli* BL21(DE3) - CodonPlus strains used for MIC experiments were those with recombinant plasmids without signal peptide. Resistance breakpoints were determined according to CLSI guidelines (127).

3.7.6 Computational details. All the simulations were carried out using the Gromacs package, version 4.5.5 (71). The charges of the substrate (benzylpenicillin) and active site were calculated using standard fitting procedures with the program Gaussian 09 (77). For the simulations, the enzyme was inserted in a cubic box filled with 7,965 molecules of water described with the simple point charge (spc) model (128). The dimensions of the box were adjusted to correctly reproduce the density of the system at 298 K and 105 Pa of pressure, as previously described (129). The simulations were performed in the NVT ensemble and extended for 100.0 ns. A time step of 2.0 fs was employed in conjunction with a standard protocol, where after an initial energy minimization, the system was gradually heated from 50 to 250 K using short (20-ps) MD simulations. Finally, a further preequilibration of the system, arrived at 298 K, was carried out by running 5.0 ns of MD simulation in all the systems. Note that all these equilibration trajectories were only utilized for obtaining the initial configuration and hence disregarded by the following analysis. The temperature was kept constant using the velocity rescaling procedure. The LINCS algorithm was employed to constrain all bond lengths (76). Long-range electrostatic interactions were computed by the Particle mesh Ewald method with 34 wave vectors in each dimension and a fourth-order cubic interpolation, and a cutoff 1.1 nm was used (74). The starting coordinates of the simulations were obtained by modifying the crystal structure of NDM-1 coordinated to hydrolyzed benzylpenicillin (here termed BzP) taken from the Protein Data Bank (PDB ID 4EYF) (130). Based on previous experimental and computational studies, we explicitly bound the BzP carbonyl group to Zn1 and the BzP amide nitrogen and carboxylate group to Zn2. The mutants were obtained with the program Molden (73).

3.8 Results

3.8.1 Role of hydrophobicity in NDM-1 enzyme activity

The NDM-1^{L218T}, NDM-1^{L221T} and NDM-1^{L269H} mutants were obtained by site-directed mutagenesis using NDM-1 as the template. The NDM-1 enzyme is unstable when it is produced with its native signal peptide. For this reason, *bla*$_{NDM-1}$, *bla*$_{NDM-1}^{L218T}$, bla$_{NDM-1}^{L221T}$, and *bla*$_{NDM-1}^{L269H}$ genes were cloned into pET-24(a) vector without signal peptide for protein expression and purification. The wild-type and mutant enzymes were purified from *E. coli* BL21(DE3) -CodonPlus/pET-24-NDM-1, *E. coli* BL21(DE3)-CodonPlus/pET-24-L218T, *E. coli* BL21(DE3)-CodonPlus/pET-24-L221T and *E. coli* BL21(DE3)-CodonPlus/pET-24-L269H by two chromatographic steps which yielded the enzyme as more than 95% pure, as evaluated by SDS-PAGE analysis. All the enzymes were tested versus several β-lactams and kinetic parameters were calculated (Table 8).

3.8.2 Kinetic analysis of NDM mutants

Penicillins. All laboratory mutants were analyzed toward two penicillins: benzylpenicillin and carbenicillin. Concerning benzylpenicillin, the mutants L218T, L221T and L269H showed a consistent increase of K_m values respect to NDM-1. The variants L218T and L269H exhibited also an increase of k_{cat} value. The L221T showed a reduction of k_{cat} value that, in combination with high K_m value, leads to a diminished catalytic efficiency.

Cephalosporins. Among cephalosporins, in the present study were analyzed 2nd generation (cefazolin and cefoxitin), 3rd generation (cefotaxime and ceftazidime) and 4th generation (cefepime) cephalosporins. The K_m values of the mutants were quite similar to that of NDM-1, with the exception of L269H that exhibited a K_m value for cefoxitin 5-fold higher than NDM-1. The k_{cat} values of L218T and L221T toward cefazolin and cefoxitin were less than that of NDM-1. On the contrary L269H showed a k_{cat} value for cefazolin 2-fold higher than that of NDM-1. The k_{cat} calculated for cefotaxime and ceftazidime for the three mutants were quite similar to that calculated for NDM-1. In addition, in mutants L218T and L221T we observed a decrease of the hydroloytic activity toward cefepime.

Carbapenems. Regarding carbapenems, L218T and L221T exhibited lower k_{cat} and k_{cat}/K_m values toward imipenem and meropenem. Different behavior was observed for L269H, which showed k_{cat} and K_m values higher than NDM-1.

Antibiotics	NDM-1			L218T			L221T			L269H		
	K_m (μM)	k_{cat} (s^{-1})	k_{cat}/K_m ($\mu M^{-1} s^{-1}$)	K_m (μM)	k_{cat} (s^{-1})	k_{cat}/K_m ($\mu M^{-1} s^{-1}$)	K_m (μM)	k_{cat} (s^{-1})	k_{cat}/K_m ($\mu M^{-1} s^{-1}$)	K_m (μM)	k_{cat} (s^{-1})	k_{cat}/K_m ($\mu M s^{-1}$)
Benzylpenicillin	250±10	105	0.42	832±20	294	0.35	937±25	78	0.08	541±12	549	1.01
Carbenicillin	285±5	108	0.38	265±10	59	0.22	398±15	48	0.12	339±9	347	1.02
Cefazolin	20±1	42	2.10	74±5	9	0.12	25	8	0.32	41±2	83	2.02
Cefoxitin	26±1	23	0.88	31±3	3	0.1	31±3	1.5	0.05	100±5	11	0.11
Cefotaxime	14±1	20	1.43	24±2	30	1.25	9±1	2	0.22	37±2	37	1.0
Ceftazidime	50±4	18.5	0.37	19±1	45	2.37	32±1	19	0.59	81±4	10	0.12
Cefepime	35±5	13	0.37	39±2	3	0.07	40±3	2	0.05	64±3	11	0.17
Imipenem	35±1	64	1.83	13±1	2	0.15	59±4	8	0.13	149±9	40	0.27
Meropenem	80±2	75	0.94	22±2	1	0.04	20±1	9	0.45	117±7	109	0.93

Table 8: Kinetic parameters of the NDM-1, L218T, L221T and L269H enzymes toward β-lactams.

3.8.3 Evaluation of Y229W substitution on the L209F variant

Site-directed mutagenesis and antimicrobial susceptibility testing

Y229W and L209F-Y229W mutants were generated by site-directed mutagenesis using pFM-NDM-1 and pET-24-L209F plasmids as the templates, respectively. In order to obtain a large amount of these enzymes, both mutated genes (bla_{Y229W} and $bla_{L209F\text{-}Y229W}$), without signal peptide, were cloned into pET-24a(+) vector. First, the antimicrobial susceptibilities of the four enzymatic systems (NDM-1, L2019F, Y229W, and L209F/Y229W) were investigated versus a large panel of β-lactams (Table 9). MIC data obtained for *E. coli*/pET-24-Y229W and *E. coli*/pET-24-L209F/Y229W were compared with those of *E. coli*/pET-24-NDM-1 and *E. coli*/pET-24-L209F. As with NDM-1 and L209F mutant enzymes, the Y229W mutation confers resistance to all β-lactams tested, with the exception of cefoxitin (MIC, 8 μg/ml). Similarly, *E. coli*/pET-24-L209F-Y229W was resistant to all β-lactams, with MIC values slightly lower than those observed for *E. coli*/pET-24-NDM-1 and *E. coli*/pET-24-Y229W. Compared with *E. coli*/pET-24-NDM-1, the *E. coli*/pET-24-L209F strain showed susceptibility to carbapenems and cephalosporins, and it was resistant only to benzylpenicillin and carbenicillin (123).

B-Lactams	*E. coli* pET-24 NDM-1	*E. coli* pET-24 L209F	*E. coli* pET-24 Y229W	*E. coli* pET-24 L209F/Y229W	*E. coli* pET-24
Imipenem	>64	0.25	>64	64	0.5
Meropenem	>64	<0.0625	>64	>64	0.5
Cefazolin	>128	4	>128	64	<0.0625
Cefotaxime	128	1	>128	32	<0.0625
Ceftazidime	>128	16	>128	32	<0.0625
Cefoxitin	8	8	8	4	0.125
Cefepime	32	<0.0625	16	16	<0.0625
Benzylpenicillin	>256	64	>256	>256	0.5
Carbenicillin	>256	64	>256	128	0.5

Table 9: Antimicrobial susceptibility of *E. coli* BL21 Codon Plus(DE3) carrying *bla*NDM-1, *bla*NDML209F, *bla*NDMY229W and *bla*NDML209F/Y229W (123).

MIC values are expressed in µg/ml

Kinetic analysis of Y229W and L209F/Y229W enzymes

The Y229W (single mutant) and L209F/Y229W (double mutant) enzymes were purified (> 95% pure) and used to determine the steady-state kinetic parameters toward several β-lactams. Table 10 shows the K_m, k_{cat}, and k_{cat}/K_m values for the NDM-1, L209F, Y229W, and L209F/Y229W enzymes. Kinetic data reported for NDM-1 and L209F enzymes were from our previous study (122). Compared with NDM-1, the Y229W single mutant showed a remarkable increase in k_{cat} values for benzylpenicillin, carbenicillin, meropenem, and cefazolin but not for imipenem and cefepime. For all β-lactams reported, in the case of Y229W mutant, the K_m values were higher than that calculated for NDM-1. Indeed, k_{cat}/K_m values for imipenem and cefepime were 4- and 18-fold lower than that of NDM-1 due to a reduction of k_{cat} and an increase in K_m values. Regarding imipenem, the Y229W mutant showed k_{cat} and k_{cat}/K_m values lower than those of NDM-1. On the contrary, meropenem exhibited k_{cat} and k_{cat}/K_m values 11- and 3-fold higher than that of NDM-1. With respect to the NDM-1 wild type, the Y229W mutant showed an increase in k_{cat} and k_{cat}/K_m values for cefazolin. Concerning cefepime, the Y229W mutant exhibited lower k_{cat} value but higher k_{cat}/K_m values than those for NDM-1 (Table 10). In the L209F mutant, a drastic reduction in activity toward penicillins, cefazolin, and carbapenems was measured (122). The K_m values of L209F/Y229W for penicillins were higher than that of L209F single mutant but comparable to the values calculated for NDM-1. The L209F/Y229W mutant showed k_{cat} values higher than those calculated for L209F and, in the case of benzylpenicillin and meropenem, even higher than those of NDM-1. Indeed, k_{cat} values for carbenicillin and benzylpenicillin increased 70- and 250-fold, respectively. The catalytic efficiencies of the L209F/Y229W double mutant for carbenicillin and benzylpenicillin were similar to those of NDM-1 but about 5-fold higher than those for the L209F variant (Table 11). Concerning imipenem, the K_m values were about 3-fold higher than those calculated for NDM-1 and the L209F mutant. In Table 11, we compared the k_{cat} and k_{cat}/K_m values of the L209F/Y229W mutant versus the L209F mutant. A remarkable increase in these values was observed in all β-lactams tested. In particular, compared to the L209F mutant, the L209F/Y229W double mutant showed for imipenem and meropenem increases of about 100- and 240-fold in the k_{cat} values and 27- and 140-fold in the k_{cat}/K_m values, respectively.

Substrates	NDM-1			L209F[a]			Y229W			L209F/Y229W		
	K_m (μM)	k_{cat} (s^{-1})	k_{cat}/K_m ($\mu M^{-1} s^{-1}$)	K_m (μM)	k_{cat} (s^{-1})	k_{cat}/K_m ($\mu M^{-1} s^{-1}$)	K_m (μM)	k_{cat} (s^{-1})	k_{cat}/K_m ($\mu M^{-1} s^{-1}$)	K_m (μM)	k_{cat} (s^{-1})	k_{cat}/K_m ($\mu M^{-1} s^{-1}$)
Benzylpenicillin	210±15	105	0.42	7±0.5	1.00	0.14	841±35	552±5	0.66	378±20	250±4	0.66
Carbenicillin	285±5	108	0.38	20±3	1.40	0.07	1219±200	1258±8	1.03	285±16	94±2	0.33
Cefazolin	20±1	42	2.10	16±2	0.34	0.021	48±2	191±4	3.98	15±1	25±1	1.66
Imipenem	35±1	64	1.83	33±5	0.55	0.017	81±3	38±1	0.47	120±9	55±3	0.46
Meropenem	80±2	75	0.94	50±1	0.86	0.017	259±18	820±6	3.17	88±4	208±7	2.36
Cefepime	35±5	13	0.37	99±3	0.019	$1.9x10^{-4}$	117±8	2.5±0.2	0.02	113±7	8±0.5	0.07

Table 10: Determination of kinetic parameters of NDM-1, L209F, Y229W and L209F/Y229W enzymes. Each kinetic value represents the mean of the results of three different measurements; the error rate was below 10%.

[a] Data from Reference 122.

Substrates	k_{cat} Ratio L209F/Y229W L209F	k_{cat}/K_m Ratio L209F/Y229W L209F
Benzylpenicillin	250	5
Carbenicillin	70	5
Imipenem	100	27
Meropenem	240	140
Cefazolin	75	80
Cefepime	420	370

Table 11: k_{cat} and k_{cat}/K_m ratio calculated for L209F/Y229W double mutant versus L209F mutant enzyme.

Molecular dynamic simulations

The identification of the key factors at the molecular level of the positive effects of the Y229W substitution in the L209F mutant enzyme is a prohibitive task from a computational point of view. In fact, the complexity of the enzyme systems is too high to reduce the experimental observation (i.e., the result of many events distributed in huge time and space domain at atomistic level) to a single and point-like origin. For this reason, we performed molecular dynamics (MD) simulations on the L209F and L209F/Y229W enzymes complexed with benzylpenicillin, focusing attention on the overall mechanical features and on the differences between the two systems. In Figure 16, a comparison of Cα root mean square fluctuation (RMSF) of the two complexed enzymes is depicted. The RMSF pattern is not dramatically different in the systems, indicating that, as expected, both of the enzymes maintain the overall structural features without undergoing unfolding processes at least within the 100.0-ns simulations. At the same time, three sharp and important differences were observed. In particular, the L209F/Y229W double mutant compared to the L209F mutant revealed (i) mechanical destabilization (i.e., RMSF increase) of the region 149 to 154, (ii) mechanical stabilization (i.e., RMSF decrease) of the loop 10 and N-terminal regions, and (iii) mechanical destabilization of the C-terminal region. These mechanical differences, concerning crucial regions of the enzymes, could be related to what was observed experimentally. Subsequently, we have undergone a more detailed

analysis of the local interactions experienced by the residues F209 and W229 in both mutants (L209F and L209F/Y229W). This analysis does not reveal dramatic differences. In fact, in the L209F/Y229W enzyme, the contacts appear, within the margin of error, similar to those of the L209F mutant. However, we also observe a systematic increase in the standard deviation, indicating that Y229W replacement induces a local mechanical stabilization also in the region near the 209 residue.

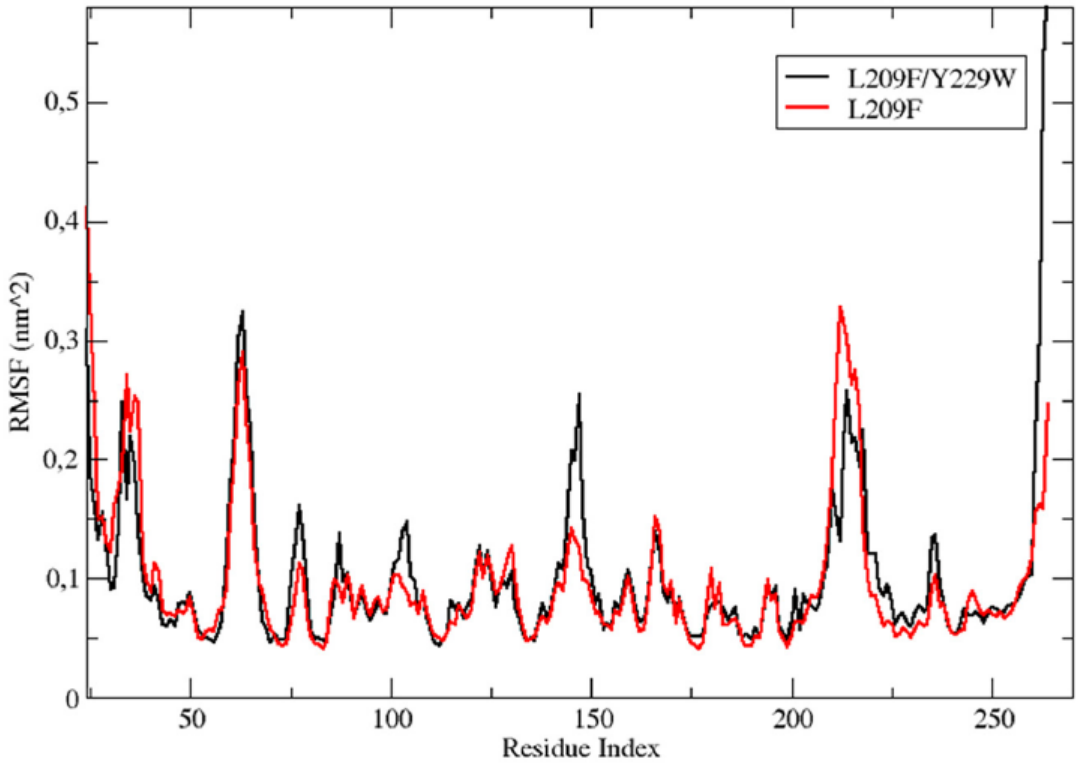

Figure 16: Comparison of the Cα root mean square fluctuation (RMSF) of the L209F/Y229W mutant (black) with that of the L209F mutant (red).

3.9 Discussion

The subclass B1 enzymes have emerged as the most clinically significant MBLs with two zinc ions in the active site. Most MBLs of subclass B1 efficiently hydrolyze penicillins, cephalosporins and carbapenems This broad spectrum may be attributed to the strong electrostatic interactions between zinc ions and the negatively charged groups of the antibiotics and to the relatively unspecific hydrophobic interactions between a flexible loop covering the active site and hydrophobic parts of the antibiotics. NDM-1 is grouped into subclass B1 and has been investigated by several structural studies. The functional significance of several residues in the active site has been studied, including D124 (NDM-1 numbering), which plays a critical role in the catalytic reaction with its exact function remains controversial (117). The rapid evolution of NDM MBLs revealed that non-active-site residue mutations can also influence the enzyme activity. Several studies showed the increased hydrolytic activities of NDM-4 and NDM-5, which differ from NDM-1 by non-active-site amino acid substitutions (M154L for NDM-4, V88L and M154L for NDM-5), toward carbapenems and several cephalosporins (131,132). The M154 side chain interacts with the backbone of Loop 7, which contains the three zinc ligands, so it is likely that this mutation impacts on the metal site structure. This is a second sphere mutation. Molecular dynamics studies (117, 133-135) showed the role of the dynamics of Loop L3 and Loop L10 upon substrate binding in the picosecond-nanosecond time scale. Second sphere residues involve a network of hydrogen bonds below the active side base, which indirectly affect the electronic structure and geometry of the Zn(II) ions (136).

The active site of NDM-1 is a hydrophobic cavity which includes five loops playing an important role in the coordination of zinc ions, stability, and substrate binding of the enzyme. Two loops, Loop 3 (roughly residues M67 to G73) and Loop 10 (roughly residues I210 to A230) are able to correctly orient substrates within the active site (26, 137). However, to make possible substrate hydrolysis, the active site needs both stability and flexibility. Residues within Loop 6 and Loop 10 are involved in the flexibility of the NDM-1 active site. Specifically, Y229 and K125 residues play an important role in stabilizing Loop 10 and Loop 6, respectively. Especially, Y229 forms hydrophobic contacts with several amino acids, including L218, L221 and L269 in the top of it and also with residue L209 under it. In addition, the hydroxyl group of residue Y229 forms a hydrogen bond with the main-chain carboxyl oxygen of residue L209. Through these interactions, residue Y229 stabilizes the conformation of loop 10.

In this study we evaluated the role of hydrophobicity of leucines (218, 221 and 269 residues) localized on the Loop 10 of the NDM-1 structure. Our kinetic data confirmed that the substitution of even just one leucine at this position decrease the hydrolytic activity of the mutants toward most β-lactams tested. Only L269H showed a β-lactamase activity similar to NDM-1. In addition, L218T, L221T and

L269H residues forming hydrophobic interactions with Y229 residue. These hydrophobic interactions contribute to stabilize and orient the Loop 10 with respect to the C-terminal β-sheet.

In a previously study, the attention was focused on residue L209 located in the "second sphere" outside the enzyme active site. Site-directed mutagenesis was used to replace leucine 209 to phenylalanine. This substitution was chosen on the basis of the alignment of NDM-1 with the most common B1 MBLs. Leucine at this position is present in NDM-1, BcII and GIM-1 enzymes but is not a conserved residue. In order to inspect the role of L209, both L209F variant and NDM-1 were investigated under various aspects: thermal stability, kinetic features, molecular dynamics (MD) and antimicrobial susceptibilities. As shown in Table 12, the replacement of L209F causes a drastic reduction in β-lactamase activity toward penicillins, cephalosporins, and carbapenems (122).

Substrates	NDM-1			L209F		
	K_m (μM)	k_{cat} (s^{-1})	k_{cat}/K_m ($\mu M^{-1} s^{-1}$)	K_m (μM)	k_{cat} (s^{-1})	k_{cat}/K_m ($\mu M^{-1} s^{-1}$)
Imipenem	35±1	64	1.83	33±5	0.55	0.017
Meropenem	80±2	75	0.94	50±1	0.86	0.017
Biapenem	120±4	30	0.25	109±4	0.52	0.0047
Cefazolin	20±1	42	2.1	16±2	0.34	0.021
Loracarbef	40±2	42	1.05	20±3	0.78	0.039
Benzylpenicillin	250±10	105	0.42	7±0,5	1.00	0.140
Carbenicillin	285±5	108	0.38	20±3	1.40	0.070

Table 122: Kinetic parameters of NDM-1 and L209F enzymes (122).

In other subclass B1 MBLs, such as VIM-2, VIM-4 or IMP-1, the position 229 is occupied by a tryptophan residue (W229). It is known that, substitution Y229W leads to a more active NDM-1. For this reason, we have decided to make Y229W substitution on L209F mutant which completely lost its activity toward penicillins, cephalosporins and carbapenems (123). Our aim was to verify if will be interactions between F209 and W229 and if this interaction will be able to restore the hydrophobic activity of L209F mutant. Crystal studies on NDM-1 have established that L209 forms hydrophobic interactions with the Y229 residue (26, 117,137,138). Leucine 209 in NDM-1 is located in Loop 10, in the "second-sphere residues" outside the active site of the enzyme. Residue 209 is positioned just before Zn2 binding ligand C208 (C221 in BBL numbering). In the case of the L209F mutant, was demonstrated that the presence of F209 perturbs the interactions of this residue with neighboring residues, and a major fluctuation of loop 10 was observed with respect to NDM-1 (122). In particular, in the NDM-1 enzyme, the L209 residue interacts with Y229 by hydrogen bonds. Chen et al. demonstrated that the Y229W substitution in NDM-1 improves the catalytic efficiency toward some

β-lactams, especially benzylpenicillin, cefuroxime, and meropenem (121). Our kinetic results showed that the replacement Y229W changes substantially the kinetic behavior of the L209F enzyme. Compared with L209F, in the L209F/Y229W enzyme, we observed a remarkable increase in k_{cat} values of 100-, 240-, 250-, and 420-fold for imipenem, meropenem, benzylpenicillin, and cefepime, respectively. The K_m values for benzylpenicillin and carbenicillin calculated for the double mutant were 54- and 14-fold higher than that of L209F but similar to that for NDM-1. Compared to the L209F mutant, the L209F/Y229W double mutant seems to have lower affinity for penicillins. When introduced into the L209F single mutant, the Y229W mutation was able to restore the activity of the enzyme that showed high catalytic efficiency values. This is particularly true for cefepime, meropenem, and cefazolin, to which we observed an increase in k_{cat}/K_m values of 370-, 140-, and 80-fold, respectively. Molecular dynamics simulations were performed on the L209F and L209F/Y229W mutants, complexed with benzylpenicillin, in order to observe structural and dynamic differences induced by these amino acid substitutions. The enzyme internal mobility, based on root mean square fluctuation (RMSF), is characterized by fluctuations in different regions, including the Loop 10, N-terminal, C-terminal, and 149 to 154 regions. An evident effect was observed at loop 10. Compared to the single mutant, the L209F/Y229W double mutant showed a decrease in RMSF peak resulting in better mechanical stabilization of loop 10. Fluctuations observed in the two enzymes complexed with benzylpenicillin could probably affect the affinity (K_m values) versus some β-lactams. In the L209F/Y229W double mutant, we noticed a decrease in RMSF peak in Loop 10 (residues F209 to A230), resulting in better mechanical stabilization of loop 10. Undoubtedly, these fluctuations could perturb the zinc ion geometry, resulting in an improvement in hydrolytic activity. In a recent paper, Zhang and coworkers demonstrated that the modulation of Zn1-to-Zn2 distance affects the enzymatic activity of NDM-1 (139). In particular, they have been underlined that a bigger fluctuation of the active site corresponds to a shorter distance between Zn1 and Zn2, favoring higher enzymatic activity. However, the mechanism through which NDM-1 hydrolyzes substrate is complex. As demonstrated by several authors, the enzyme-substrate reaction proceeds by almost two reactive intermediates (140,141). In MBLs, the main “protagonist” of substrate binding is Zn2. We speculate that the enhancement of enzymatic activity of the L209F/Y229W double mutant with respect to the L209F mutant enzyme could be due to fluctuations generated in non-active-site regions, which might modify the Zn1-to-Zn2 distance and the reactivity of Zn2. Moreover, the enhancement of the hydrolytic activity of the L209F/Y229W mutant could be also attributable to the epistatic effect of the Y229W mutation that involved enzyme catalysis. The epistatic effect is a frequent phenomenon that was, also, ascertained in the BcII enzyme (142,143). Compared to NDM-1, the L209F mutation leads to a decrease in activity; on the contrary, the Y229W single mutant showed an increase in catalytic

efficiency toward penicillins, cefazolin, and meropenem but not for imipenem and cefepime. The interaction of F209 and W229 not only restored the activity of the enzyme (double mutant) but, in the case of benzylpenicillin and meropenem, the L209F/Y229W mutant showed an increase in k_{cat} and k_{cat}/K_m parameters with respect to NDM-1. The Y229W mutation is responsible for a large increase in catalytic efficiency. A noteworthy increase in resistance versus all β-lactams tested was observed in *E. coli*/pET-24-L209F/Y229W with respect to *E. coli*/pET-24-L209F. Specifically, in the L209F/Y229W mutant, an increase of MIC values was observed, in particular, for meropenem and cefepime. In conclusion, we stated that several both loop fluctuations and the epistatic effect of the Y229W mutation could have contributed to the restoration of β-lactam activity in the L209F mutant enzyme.

Chapter 4

New metallo-β-lactamase inhibitor: Taniborbactam

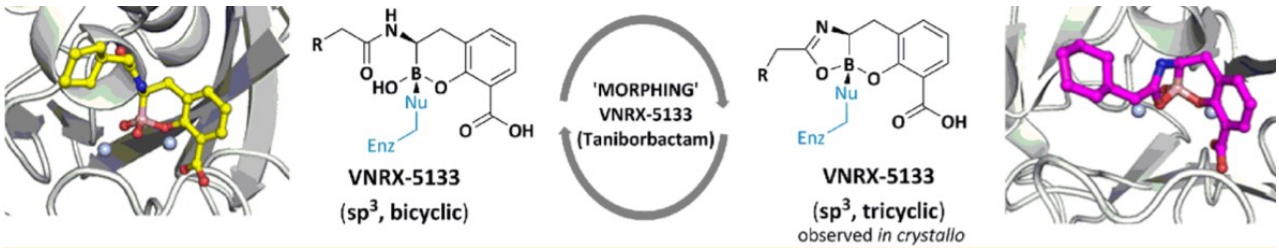

By Krajnc A. et al, 2019

4.1 "Classical" β-lactamase inhibitors and their evolution

The production of β-lactamases is, and has been, the most common resistance mechanism in Gram-negative bacteria (144-146). In the mid-1970s, when the plasmid-encoded TEM-1 β-lactamase evaded from enteric bacteria into *N. gonorrhoeae* and *H. influenzae*, pharmaceutical companies invested to identify a potent inhibitor of the enzyme (147,148). At that time, the key β-lactamases of interest were TEM-1, the staphylococcal penicillinases and the chromosomal AmpC-related cephalosporinases. Clavulanic acid, the first β-lactamase inhibitor introduced into clinical medicine, was isolated from *Streptomyces clavuligerus* in the 1970s. Mechanistically, the inhibitor was shown to be most effective irreversible inactivator of TEM-1, with the initial formation of a transiently inhibited intermediate (E–I) resulting in hydrolyzed clavulanic acid (I*) and free enzyme (E); a competing pathway involved the formation of an irreversibly inactivated enzyme [E–I] $^{\#}$ and fragmented clavulanic acid (I^) (149,150). Generally, in another possible pathway, the acyl enzyme may release intact inhibitor (I) and active enzyme (E), or [E + I]. All reactions may be operative at different rates for the same enzyme–inhibitor combination. Accumulation of [E–I]$^{\#}$ eventually can lead to complete enzyme inactivation (Figure 17) (40).

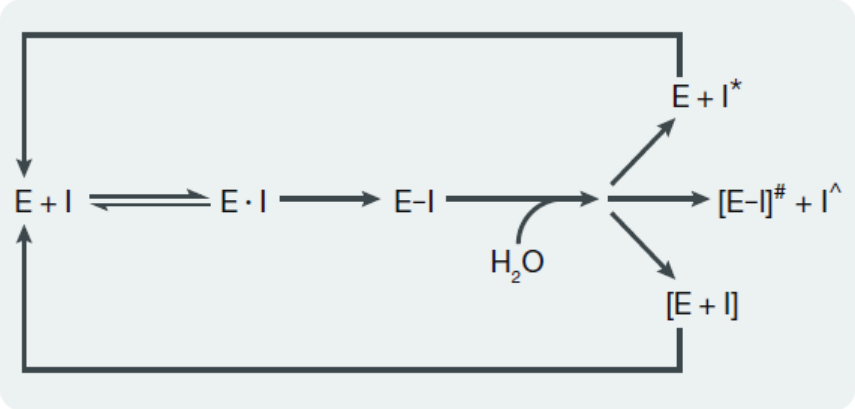

Figure 17: General reaction mechanism for inhibition of a β-lactamase by a mechanism-based β-lactamase inhibitor (40).

Sulbactam and tazobactam are penicillinate sulfones that were later developed by the pharmaceutical industry as synthetic compounds in 1978 and 1980, respectively (151,152). Sulbactam is slightly less potent than clavulanic acid but with modest antibacterial activity against *N. gonorrhoeae* and *Acinetobacter* spp. (153). Tazobactam (Figure 18; Table 13) has no evident antimicrobial activity but greater inhibitory potency than sulbactam and a similar mechanism of inhibition as sulbactam and clavulanic acid (154). All three β-lactamase inhibitor compounds share structural similarity with penicillin; they are efficacious against many susceptible organisms expressing class A/group 2 β-

lactamases. Clavulanic acid and tazobactam have similar inhibitory activities against group 2 enzymes, including CTX-M β-lactamases and the ESBL derivatives of TEM-1, TEM-2 and SHV-1, and both have greater potency than sulbactam (155). Sulbactam and clavulanic acid are generally less effective against KPC and other serine-based carbapenemases. Inhibition of class D/group 2d enzymes is variable (152). Tazobactam, sulbactam and clavulanic acid function as 'suicide' inactivators, rendering the targeted β-lactamase non-functional. Turnover numbers (molecules of inhibitor hydrolyzed for each inactivation event) varied for each inhibitor with each enzyme. Sulbactam usually had higher turnover numbers than clavulanic acid or tazobactam for all the β-lactamases tested (151,156). With the assistance of X-ray crystallography, covalent adducts with inactivated enzymes have been identified to support the biochemically derived mechanisms (Figure 17). For example, a structural analysis of tazobactam-inactivated SHV-1 β-lactamase showed that the active-site S70 was acylated by tazobactam together with a five-atom tazobactam fragment bound to S130 (157).

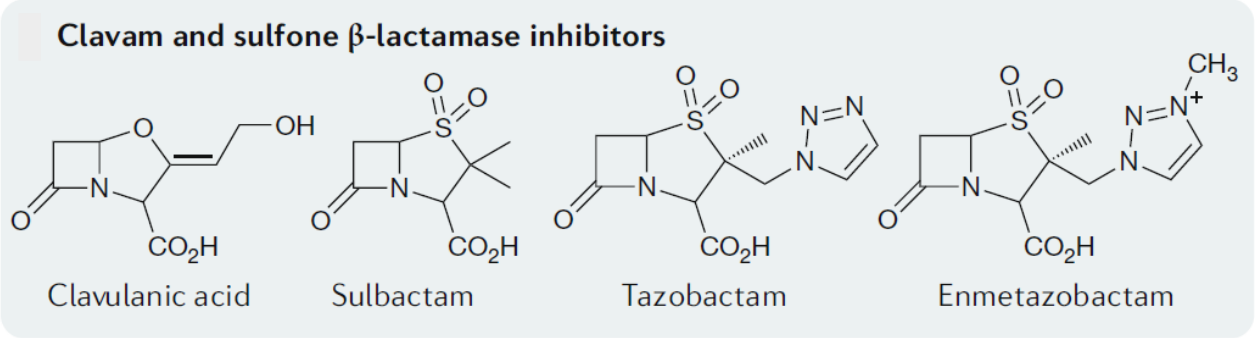

Figure 18: The structure of clavam and the sulfone β-lactamase inhibitors clavulanic acid, sulbactam, tazobactam and enmetazobactam (formerly AAI101).

In developing a BLI combination is important the selection of a β-lactam with similar pharmacokinetic properties as the inhibitor. BLI combinations were introduced into clinical practice in the period of 1984–1993 and includes:

-clavulanic acid-amoxicillin as an orally bioavailable agent;

-clavulanic acid-ticarcillin for Gram-negative infections, including those caused by *P. aeruginosa*;

-sulbactam combined with ampicillin, used parenterally for the treatment of urinary tract infections (UTIs) and intra-abdominal infections;

-tazobactam-piperacillin, with broad-spectrum staphylococcal, Gram-negative and pseudomonal coverage of soft tissue and intra-abdominal and lower respiratory tract infections in hospitalized patients (158).

The amoxicillin–clavulanic acid combination is currently the most frequently used in many paediatric primary care units (159). Piperacillin–tazobactam is still frequently used in empiric therapy for nosocomial infections (160).

Structural group	Inhibitor	β-Lactam partner	Development stage (trade name)	Spectrum of inhibition				
				ESBL	AmpC	KPC	OXA-48	MBL
Clavam	Clavulanic acid	• Amoxicillin • Ticarcillin	• Approved (Augmentin) • Approved (Timentin)	✓	–	–	–	–
Penicillanic acid sulfone	Sulbactam	Ampicillin	Approved (Unasyn)	✓	–	–	–	–
	Tazobactam	• Piperacillin • Cefepime • Ceftolozane	• Approved (Zosyn/Tazocin) • Approved outside the US • Approved (Zerbaxa)	✓	–	–	–	–
	Enmetazobactam	Cefepime	Phase II	✓	–	–	–	–
DBO	Avibactam	Ceftazidime	Approved (Avycaz/ Zavicefta)	✓	✓	✓	✓	
		Aztreonam	Phase III	✓	✓	✓	✓	✓
	Relebactam	Imipenem	Phase III	✓	✓	✓	–	–
	Nacubactam	Meropenem	Phase I	✓	✓	✓	–	–
	Zidebactam	Cefepime	Phase I	✓	✓	✓	–	–
	ETX2514	Sulbactam	Phase II	✓	✓	✓	✓	–
Boronic acid	Vaborbactam	Meropenem	Approved (Vabomere)	✓	✓	✓	–	–
	VNRX-5133	Cefepime	Phase I	✓	✓	✓	✓	✓
Pyridine-2-carboxylic acid	ANT431	Meropenem	Preclinical	–	–	–	–	✓

✓, useful inhibitory activity shown; –, no useful inhibitory activity shown; DBO, diazabicyclooctanone analogue; ESBL, extended-spectrum β-lactamase; MBL, metallo-β-lactamase.

Table 13: Comparison of β-lactamase inhibitors (40).

More recently, tazobactam has been combined with ceftolozane, and with cefepime providing a broader spectrum of activity but no activity against serine carbapenemases. The major cause of resistance to the older BLI combinations has been high levels of β-lactamase activity in the infecting pathogen. These high levels of activity may be due to increased expression of the targeted enzymes, such as TEM-1 hyperproduction caused by gene amplification in the presence of sub-inhibitory amounts of tazobactam, or to the presence of multiple β-lactamases produced by a single bacterial species. With increasing numbers of ESBLs and carbapenemases that are appearing in multidrug-resistant Gram-negative pathogens, the use of these older combinations is becoming restricted to treating community-acquired respiratory infections with amoxicillin–clavulanic acid or the less serious hospital-acquired infections with ampicillin–sulbactam or piperacillin–tazobactam combinations (161). MBLs are insensitive to most of the clinically available β-lactamase inhibitors and hence represent one of the most worrying bacterial resistance factors. The rise and spread of MBLs in pathogens and the threat they pose to human health make the search for inhibitors of these enzymes an acute clinical need. Like the highly successfull SBL inhibitors, such molecules have the potential to be co-formulated with β-lactam antibiotics to improve drug success in the clinic, even

when infectious organisms harbor an MBL gene. However, the lack of sequence similarity among MBLs, their shallow active sites, the abscence of invariant catalytic residues, and the structural similarity with some human enzymes, conspire to make the identification of broad-spectrum MBL inhibitors a challenge.

4.2 New classes of inhibitors

All three of the BLIs mentioned before, are effective against many class A β-lactamases but do not protect against class B, C and D β-lactamases. However, they are inefficient against strains that expressed multiple ESBLs, plasmid-encoded AmpC-type β-lactamases or serine carbapenemases such as KPC. For this reason, the need for new inhibitors has emerged (162). Several new non-β-lactam inhibitor combination agents have been recently approved for clinical use, with many more in development.

4.2.1 Penicillanic acid sulfone

Entmetazobactam. Enmetazobactam (formerly AAI101), a methylated penicillanic acid sulfone BLI related to tazobactam, is a novel ESBL inhibitor (Figure 18). It exerts potent inhibitory activity toward CTX-M, TEM, SHV, and other class A β-lactamases through a different mechanism of action than tazobactam. The cefepime–enmetazobactam combination was at least eight-fold more potent than piperacillin–tazobactam against ESBL-producing clinical isolates of Enterobacteriaceae (40). Enmetazobactam has completed a phase II study in cUTIs.

4.2.2 Diazabicyclooctanones (DBOs)

DBOs are synthetic non-β-lactam-based β-lactamase inhibitors that were discovered in the early 2000s. Over a period of 15 years, this class of compunds has expanded almost exponentially with most modifications occurring at the C2 side chain. Most studies published to date indicate that DBOs possess class A and class C activity with minor class D activity.

Avibactam: In december 2014, avibactam (formerly known as AVE1330A and NXL104) was the first DBO to be approved by the FDA in combination with ceftazidime for the treatment of complicated UTIs (cUTIs), complicated intra-abdominal infections (cIAIs) and hospital-acquired

infections. Compared with clavulanic acid, sulbactam and tazobactam, avibactam provides excellent inhibition of the clinically relevant class A and class C β-lactamases such as CTX-M-15, KPC-2 and AmpC β-lactamases from *Enterobacter* spp. and *P. aeruginosa* (163,164). In addition, avibactam follows a different mechanism of inhibition than the previous BLIs in that avibactam binds in a covalent, but reversible, manner to most β-lactamases tested, followed by the regeneration of active enzyme and intact inhibitor via deacylation and recyclization of the five-membered urea ring of avibactam (Figure 1 with the product being [E + I]) (165). In the case of KPC-2 enzyme, however, a reaction similar to that observed with clavulanic acid and tazobactam occurs (Figure 1), in which the (E–I) complex leads to the hydrolysis of avibactam (I*) and regeneration of free enzyme (E). The combination avibactam-ceftazidime has broad activity against many isolates of Enterobacteriaceae and *P. aeruginosa* that express one or multiple β-lactamases, including ESBLs, KPC, OXA-48 and AmpC-type enzymes (20). Compared with ceftazidime alone, ceftazidime–avibactam is not considered to have sufficient anti-anaerobic activity against *Bacteroides fragilis*, *Clostridium perfringens*, *Prevotella* spp. and *Porphyromonas* spp (166). Avibactam is also in development in combination with aztreonam, which provides activity against Enterobacteriaceae that express both serine β-lactamases and MBLs (167). In fact, aztreonam is not hydrolyzed by MBLs. Aztreonam–avibactam is currently in phase III clinical trials (168).

Relebactam Relebactam (formerly known as MK-7655) is another DBO that differs from avibactam with the addition of a piperidine ring (Figure 19; Table 13). It is currently in development in combination with imipenem and the renal dehydropeptidase inhibitor cilastatin. When combined with imipenem, relebactam is effective against Enterobacteriaceae with known KPC carbapenemases, AmpCs, and/or ESBLs (169,170). Imipenem-relebactam also demonstrates potent activity against Enterobacteriaceae that express AmpCs or ESBLs and that have impermeability phenotypes (e.g., loss of porins) (171). The imipenem-relebactam combination was found to be very effective in a hollow-fiber infection model due to a KPC-producing *K. pneumoniae* strain. By contrast, this combination was not effective in restoring susceptibility to Enterobacteriaceae that express OXA-48 or any of the metallo-carbapenemases (172). In addition, relebactam did not restore the activity of imipenem against *A. baumannii*. The combination of imipenem-cilastatin- relebactam is currently being studied in a phase III comparative trial for the treatment of hospital-acquired pneumonia and ventilator-associated bacterial pneumonia (168).

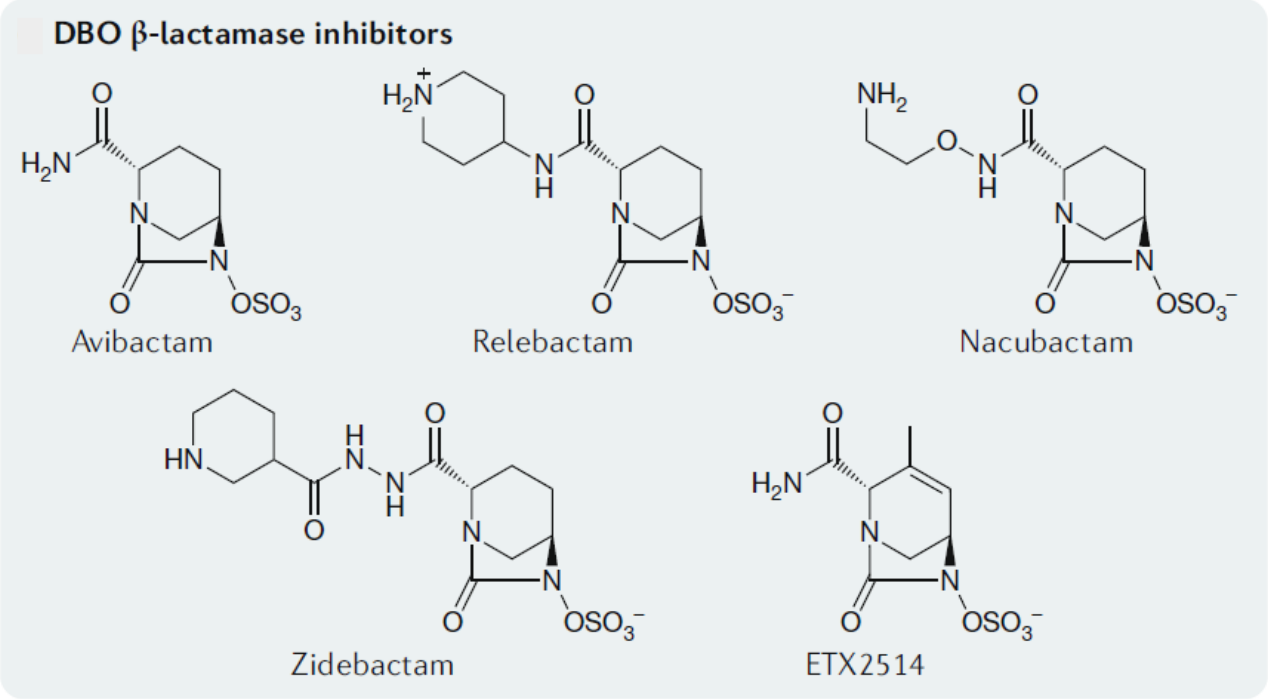

Figure 19: Structures of the diazabicyclo [3.2.1] octanone (DBO) β-lactamase inhibitors avibactam, relebactam, nacubactam, zidebactam and ETX2514 (40).

Nacubactam. Nacubactam (RG6080, OP0595) is a diazabicyclooctanone (non--lactam–-lactamase inhibitor) that differs from avibactam with the addition of an aminoethoxy group to the carbamoyl side chain present on avibactam (Figure 19). This addition is likely responsible for the significant intrinsic antibiotic activity of nacubactam alone. Nacubactam is currently being combined with meropenem for the treatment of serious Gram-negative bacterial infections. It inhibits class A and class C β-lactamases, in addition to minor class D activity. Nacubactam alone has proven antibacterial activity via PBP2 inhibition of several Enterobacteriaceae isolates (173). When is combined with β-lactams, its efficacy expands to most Enterobacteriaceae isolates producing extended-spectrum β-lactamases (ESBLs), AmpCs, KPCs, metallo-β-lactamases (MBLs), and OXA-48. Nacubactam is currently in phase I clinical studies (174).

Zidebactam. Zidebactam (formerly known as WCK 5107) is another DBO inhibitor with PBP2 binding activity that inhibits class A and C serine β-lactamases (Figure 19; Table 13). In combination with cefepime, zidebactam is currently under clinical development for infections caused by MDR Gram-negative organisms, including *P. aeruginosa*, that express ESBLs, AmpC, KPC and OXA-48 β-lactamases (175). Zidebactam is currently in phase I clinical trials (176).

ETX2514. ETX2514 is a reversible DBO inhibitor that was rationally designed as a novel and more versatile inhibitor with increased reactivity and improved binding to β-lactamases, resulting from the addition of a double bond between C3 and C4 and a methyl group at the C3 position compared to avibactam (177). It inhibits class D β-lactamases, in addition to the class A and C enzymes included in the spectrum of activity of the other DBOs (Figure 19; Table 13). The inhibition of OXA-type β-lactamases allows ETX2514 to be used to target *Acinetobacter* spp. as OXA β-lactamases are commonly produced in that species. ETX2514 is in combination with sulbactam, which takes advantage of the unique property of sulbactam to bind to essential PBPs in *Acinetobacter* spp., *N. gonorrhoeae* and *H. influenzae*. Sulbactam–ETX2514 has completed a phase II study and will be developed as a narrow-spectrum agent targeting *Acinetobacter* spp. (178).

4.2.3 Boronic acid

Boronic acid compounds are potent inhibitors of serine proteases and, therefore, have been investigated for their potential to be combined with a β-lactam.

Vaborbactam (formerly known as RPX7009), the first boronic acid BLI to be developed, was designed as a potent inhibitor of class A serine carbapenemases, such as KPC, NMC-A and SME-2, as well as other class A (e.g. CTX-M, SHV) and class C β-lactamases (Figure 20; Table 13) (179). Class B (e.g. NDM, VIM) and class D (e.g. OXA-48) carbapenemases are not inhibited by vaborbactam. Vaborbactam protects meropenem from degradation by serine carbapenemases via a novel mechanism of enzyme inhibition. This involves the formation of a covalent adduct between the catalytic serine residue of β-lactamases and the boron moiety of vaborbactam, which mimics the tetrahedral transition state of β-lactamase hydrolysis, therefore functioning as a competitive inhibitor. Meropenem–vaborbactam completed phase III trials for UTIs and all infection types against CRE (180). Meropenem/vaborbactam (Vabomere™) is the first carbapenem/BLI combination approved in the USA for use in patients with cUTI, including pyelonephritis (181).

VNRX-5133. VNRX-5133 is a novel boronic acid BLI in clinical development with direct inhibitory activity against class A, C and D serine β-lactamases and VIM and NDM class B MBLs in CRE and *P. aeruginosa* (Figure 20; Table 13). The X-ray crystal structure of two clinically relevant β-lactamases, CTX-M-15 and VIM-2, complexed with VNRX-5133 showed that the inhibitor was covalently bound to the catalytic serine residue of CTX-M-15 and that the boron hydroxyl groups interacted with Zn1 and the conserved N233 of VIM-2. The cefepime–VNRX-5133 combination has shown both in vitro and in vivo activity against molecularly characterized ESBL-producing and

carbapenemase-producing Enterobacteriaceae and *P. aeruginosa* isolates. VNRX-5133 is currently in phase 3 trial for patients with complicated urinary tract infections (cUTIs).

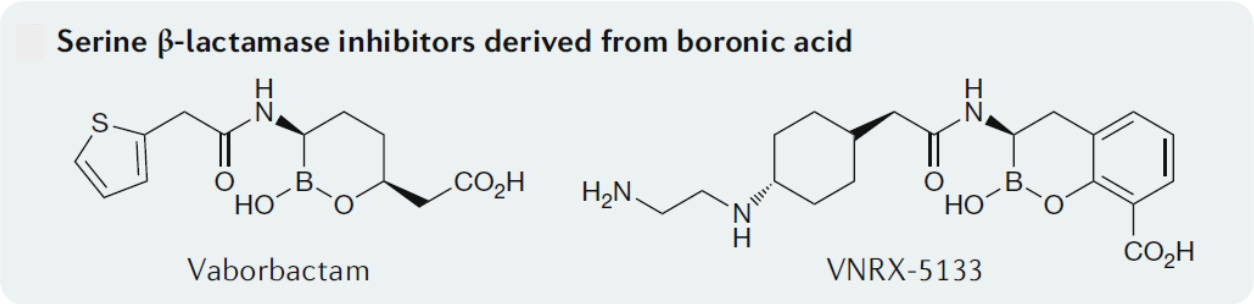

Figure 20: The structures of serine β-lactamase inhibitors vaborbactam and VNRX-5133, which are derived from boronic acid (40).

4.2.4 Pyridine-2-carboxilic acid

ANT431. ANT431, a novel pyridine-2-carboxylic acid that was specifically designed to inhibit MBLs, is currently in preclinical development (Figure 21; Table 13). When combined with meropenem, ANT431 showed good activity against many clinical isolates in a large panel of Enterobacteriaceae that contain NDM-1, but it demonstrated less potentiation against other MBL-producing variants. The compound will probably not be developed as a clinical candidate due to its limited range of MBLs that are inhibited, but it may function as a prototype for future MBL inhibitors (182).

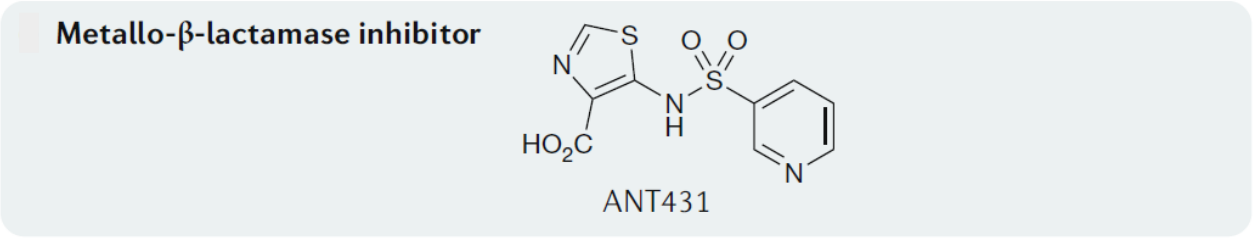

Figure 21: The structure of the metallo-β-lactamase inhibitor ANT431 (40).

4.3 Aim of the study

Examine the impact of a new boronic acid inhibitor, VNRX-5133, in combination with cefepime, against NDM-1 and engineered NDM-1 variants. The cefepime/VNRX-5133 combination (Taniborbactam) was also tested against NDM-1-producing Enterobacteriaceae clinical strains.

4.4 Activity of a new bycyclic boronic acid against engineered NDM-1 variants and NDM-1 producing clinical strains.

4.4.1 Background

Our laboratory generated six laboratory mutants of NDM-1 metallo-β-lactamase and characterized the corresponding kinetic properties of recognition and hydrolysis of β-lactams (183). The six variants examined six substitutions at position 119 (Q119C, Q119F, Q119E, Q119Y, Q119V, Q119K - BBL numbering). Glutamine 119 is located in the L5 Loop adjacent to important residues involved in zinc coordination and catalysis such as H116, H118 and D120 respectively (Figure 22). These NDM-1 variants were able to hydrolyze carbapenems, penicillins and first-, second-, third-, and fourth-generation cephalosporins very efficiently, relative to NDM-1, with significant increases in k_{cat} and k_{cat}/K_m values for most β-lactams tested, including cefepime (Table 14).

Substrates	k_{cat}/K_m (Q119X variants)/k_{cat}/K_m (NDM-1)					
	Q119C	Q119F	Q119E	Q119Y	Q119V	Q119K
Benzylpenicillin	3.36	4.43	47.62	10.11	12.14	65.71
Carbenicillin	2.31	3.18	34.21	18.34	21.95	69.84
Imipenem	0.75	1.17	0.56	1.44	1.92	2.39
Meropenem	2.68	6.33	0.59	5.68	14.31	10.26
Cefazolin	2.08	2.98	7.50	2.54	6.40	1.86
Cefoxitin	4.89	8.23	3.16	5.68	12.18	1.34
Cefotaxime	4.29	6.87	1.40	2.45	1.40	20.75
Ceftazidime	1.18	1.68	0.26	89.47	6.13	25.37
Cefepime	1.97	11.32	1.22	20.27	19.20	9.00

Table 14: Comparison of k_{cat}/K_m ratio between NDM-1 and Q119X mutants (183).

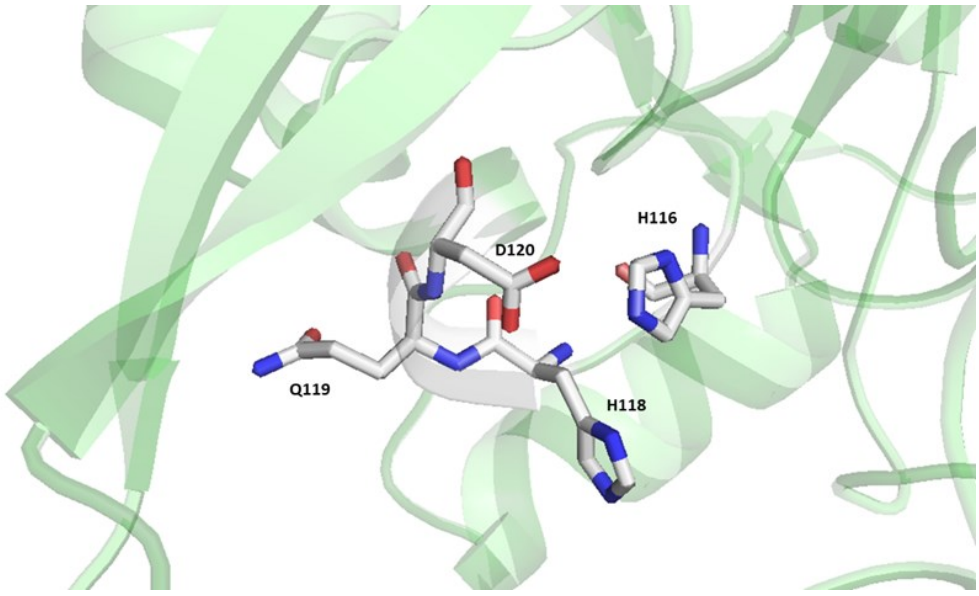

Figure 22: Molecular modeling of NDM-1

4.4.2 Materials and methods

Strains

The clinical strains were from collection of Clinical Molecular Biology and Biochemistry Laboratories, University of L'Aquila.

Antibiotics/inhibitor

Cefepime and VNRX-5133 were kindly provided by VenatoRx Pharmaceuticals Inc, Malvern, Pennsylvania, USA.

Antimicrobial susceptibility tests (MIC)

The phenotypic profile was characterized by broth microdilution using a bacterial inoculum of 5 x 10^5 CFU/mL according to standard Clinical and Laboratory Standards Institute (CLSI) methods (127). The MH broth used as medium was supplemented with 0.4 mM of IPTG. Three experiments were performed to define cefepime MIC alone or in combination with VNRX-5133 at fixed concentrations of 4, 6 and 8 mg/L.

Enzyme kinetic assays

Steady-state kinetic experiments were performed under initial-rate conditions using Hanes plot linearization with purified enzymes (NDM-1, Q119C, Q119F, Q119E, Q119Y, Q119V, Q119K). Competitive inhibition studies with VNRX-5133 were monitored directly by using 50 μM cefepime as reporter substrate, using 80 nM of each enzyme. The experiments were performed at the following conditions:

$v_0/v_i=1+ (K_m \times I) / (K_m +S) \times K_i$

were v_i and v_0 represent the initial rates of hydrolysis of cefepime with or without inhibitor, respectively; I is the concentration of inhibitor or poor substrate, K_i is the inhibition constant, K_m value is Henri-Michaelis constant and S is the concentration of reporter substrate. The plot v_0/v_i versus [I] yielded a straight line of slope $K_m/ (K_m+S) \times K_i$.

4.4.3 Results

All the data obtained were presented at the 29th European Congress of Clinical Microbiology and Infectious Diseases (ECCMID) in Amsterdam, Netherlands (2019) (184). The antibacterial activity of cefepime alone and in combination with VNRX-5133 was evaluated in both engineered *E. coli* BL21(DE3) carrying NDM-1 variants (Table 15) and multidrug resistant clinical isolates of Enterobacteriaceae (Table 16) (184). As shown in Table 15, *E. coli* BL21(DE3)/pET-24-NDM-1 exhibited high-level resistance to cefepime with MIC values ranging from 32 mg/L to > 64 mg/L. Addition of VNRX-5133 at 4 mg/L was able to restore the antibacterial activity of cefepime to MIC values of 0.25-0.5 mg/L for the Q119C, and 1-2 mg/L for all other Q119X variants and NDM-1. Potentiation of cefepime antibacterial activity by VNRX-5133 was also examined in NDM-1 producing *C. freundii*, *E. coli* and *K. pneumoniae* clinical strains. At a fixed concentration of 4 mg/L, VNRX-5133 was able to restore antibacterial activity of cefepime to MIC values ranging from 0.25 mg/L to 4 mg/L. NDM-1, along with the six Q119X variants (Q119E, Q119K, Q119C, Q119F, Q119V and Q119Y) were purified to determine the kinetic parameters (K_m, k_{cat}, k_{cat}/K_m) for cefepime as well as the associated IC_{50} and K_i values for VNRX-5133.

Strains	Cefepime	Cefepime+ VNRX-5133 (4mg/L)	Cefepime+ VNRX-5133 (6mg/L)	Cefepime+ VNRX-5133 (8mg/L)
NDM-1	32-64	1-2	1-2	1
Q119E	32-64	1-2	1	1
Q119K	>64-64	1	1	1
Q119C	64	0.25-0.5	0.25-0.5	0.25-0.5
Q119F	32-64	2	2	2
Q119V	32-64	1-2	1-2	1-2
Q119Y	32-64	2	1	1

Table 15: Antimicrobial susceptibility tests of recombinant strains (184).

Strains	N° isolates	Cefepime	Cefepime+ VNRX-5133 (4mg/L)	Cefepime+ VNRX-5133 (6mg/L)	Cefepime+ VNRX-5133 (8mg/L)
C. freundii/NDM-1	2	>64	0.25-0.125	0.25-0.125	0.25-0.125
E.coli/NDM-1	2	>64	4	4	2
E. coli/NDM-1	3	>64	0.5-0.25	0.25-0.125	0.25-0.125
K.pneumoniae/NDM-1	2	>64	2-1	2-1	0.5

Table 16: Antimicrobial susceptibility tests of clinical strains (184).

As shown in table 17, the K_m values for cefepime remain low for all enzymes. The catalytic efficiency (k_{cat}/K_m) of cefepime hydrolysis by all Q119X variants was increased relative to NDM-1, whereas inhibitory potency (K_i) of the competitive inhibitor VNRX-5133 was relatively unchanged by these substitutions and ranged between 0.003 and 0.023 μM relative to NDM-1 at 0.016 μM.

Enzymes	Cefepime			K_i (nM)	IC_{50} (nM)
	K_m (μM)	k_{cat} (s^{-1})	k_{cat}/K_m (μM s^{-1})		
NDM-1	35±5	13	0.37	16±1.5	41±2
Q119E	40±3	18	0.45	6±0.03	17±1
Q119K	18±2	60	3.33	23±1	95±3
Q119C	30±1	22	0.73	11±1	32±2
Q119F	16±1	67	4.19	19±2	86±4
Q119V	10±1	71	7.10	3±0.5	19±2
Q119Y	4±0.4	30	7.50	5±0.5	110±7

Table 17: Kinetic inhibition assays (184).

VNRX-5133, a new broad spectrum serine- and VIM/NDM metallo-β-lactamase inhibitor, maintains inhibitory activity in the context of Q119X variants of NDM-1 that exhibit increased cefepime hydrolytic efficiency. Addition of VNRX-5133 restored cefepime antibacterial activity in NDM-producing recombinant strains of *E. coli* and in clinical isolates of Enterobacteriaceae.

Concluding remarks

The increasing prevalence of antibiotic resistance and the lack of new antibiotic drug development has gradually reduced the treatment options for bacterial infections. The production of β-lactamases by Gram-negative and Gram-positive bacteria still remains one of the most significant threats to human health. In this study we focalized our attention on class A (GES) and class B (NDM) carbapenemases. Carbapenemases are β-lactamases with a substrate spectrum that includes not only carbapenems but also penicillins and most cephalosporins. In recent years, carbapenem resistance has gradually increased and it has reached high rates in many areas of the world, becoming a public health problem of global importance. Although rare, GES carbapenemases have now been identified worldwide. The majority of GES variants are categorized as ESBLs without any carbapenem-hydrolyzing activity. These enzymes are worrisome, since extensive use of carbapenems to treat ESBLs infections may select for GES-variants capable of hydrolyzing sufficiently carbapenems with a low susceptibility to commercially available inhibitors. Among the known GES variants most of them with G170N or G170S mutations display carbapenemase activity. In the present study we have demonstrated that the position 170 play an important role in the carbapenems activity. Thus, on the basis of data obtained, we can assert that position 170 play a pivotal role in the carbapenems activity but this depend of the kind of the replacement. The proline at position 174 is well conserved in all GES-variants and in more class A carbapenemases. The replacement of proline with glutamic acid does not affect the secondary structural content of the enzymes and improves the activity of GES mutants toward carbapenems. Our data have demonstrated that not only 170 residue is important in the carbapenems catalysis but also residue 174. On the basis of our results, we can speculate that, in GES-enzymes, the hydrolysis of carbapenems could be attributed to the Ω-loop residues. Because of the rapid spread all over the world and its ability to be expressed by numerous Gram-negative pathogens, NDM is poised to become the most commonly isolated and distributed carbapenemase worldwide. Two important loops surround the active site of NDM-1 enzyme: Loop 3 (residues 67-73) and Loop 10 (residues 210-230), which have a greater flexibility and facilitate the entrance of the substrates. In the present study, we have focused the attention on hydrophobic residues of leucines located in the Loop 10. In detail, we mutagenized L218, L221 and L269 residues. The replacement of leucines 218 and 221 with threonine reduces the activity of NDM-1 toward penicillins, cephalosporins and carbapenems. This confirmed that in NDM-1 the hydrophobicity of the enzyme is important in the substrate hydrolysis. On the contrary, L269H mutant showed K_m and k_{cat} values very similar to NDM-1. Probably, this could be due to the different position of 269H respect to the

catalytic zinc ions. We have also demonstrated that Y229W substitution plays an important role in restoring hydrolytic activity in our laboratory variant with a drastic reduction in β-lactamase activity (L209F). The lack of clinical inhibitors for metallo-β-lactamases has encouraged researchers to find new molecules. In this context, VNRX-5133, a new bycyclic boronic acid in combination with cefepime (Taniborbactam), was tested in NDM-1 laboratory mutants and in Enterobacteriaceae clinical strains. This compound showed a high inhibitory efficiency “in vitro” toward NDM-1 and engineered variants and against clinical strains. Site-directed mutagenesis studies are very important to elucidate the role of some non catalytic residues that could be the good target for new molecules with inhibitory activity.

Antibiotic resistance has the potential to affect people at any stage of life, as well as the healthcare, veterinary, and agriculture industries, making it one of the world’s most urgent public health problems. Each year in the U.S., at least 2 million people are infected with antibiotic-resistant bacteria, and at least 23,000 people die as a result. According to the World Health Organization (WHO) predictions, if antibiotic resistance continues to increase at this rate, infections caused by resistant bacteria will become the top cause of death worldwide, ahead of cancer, diabetes and cardiovascular diseases.

How to cope with antibiotic resistance: this is our “Infinity War”.

Acknowledgments

I would like to thank Prof. Gianfranco Amicosante for supporting me during these years, for the availability demonstrated during the whole period.

A wish to thank Prof. Mariagrazia Perilli, for guiding me every single day, giving me the opportunity to grow and test myself. Thank you for making me a better person. I'll always be grateful to you.

I wish to thank also Prof. Moreno Galleni and Dr. Paola Mercuri, Laboratoire de Macromolecules Biologiques, Centre d'Ingénierie des Proteines, Université de Liège, Liège, Belgium, for the hospitality in their laboratory to perform part of the experiments included in GES enzymes characterization.

References

1.Bush K, Bradford PA. 2016. β-Lactams and β-Lactamase Inhibitors: An Overview, p 23–44. *In* Silver LL, Bush K (ed), Antibiotics and Antibiotic Resistance. Cold Spring Harbor Laboratory Press, Cold Spring Harbor, NY.

2. Waxman DJ, Yocum RR, Strominger JL. 1980. Penicillins and cephalosporins are active site-directed acylating agents: evidence in support of the substrate analogue hypothesis. Philos Trans R Soc Lond B Biol Sci 289(1036):257-71.

3. Georgopapadakou N, Hammarstrom S, Strominger JL. 1977. Isolation of the penicillin-binding peptide from D-alanine carboxypeptidase of *Bacillus subtilis*. Proc Natl Acad Sci 74:1009–1012.

4. Frère JM, Joris B. 1985. Penicillin-sensitive enzymes in peptidoglycan biosynthesis. CRC Crit Rev Microbiol 11:299–396.

5. Bush K. 2013. Proliferation and significance of clinically relevant β-lactamases. Ann NY Acad Sci 1277:84–90.

6. Kahan FM, Kropp H, Sundelof JG, Birnbaum J. 1983. Thienamycin: Development of imipenem–cilastatin. J Antimicrob Chemother 12:1–35.

7. Wang X, Zhang F, Zhao C, Wang Z, Nichols WW, Testa R, Li H, Chen H, He W, Wang Q, Wang H. 2014. In vitro activities of ceftazidime–avibactam and aztreonam–avibactam against 372 Gram-negative bacilli collected in 2011 and 2012 from 11 teaching hospitals in China. Antimicrob Agents Chemother 58:1774–1778.

8. Drawz SM, Bonomo RA. 2010. Three decades of β-lactamase inhibitors. Clin Microbiol Rev 23:160–201.

9. Chambers HF. 1999. Penicillin-binding protein-mediated resistance in pneumococci and staphylococci. J. Infect. Dis. 179 (Suppl. 2):S353–S359.

10. Page MG. 2007. Resistance mediated by penicllin-binding proteins, p. 81–99. *In* Bonomo RA and Tolmasky ME (ed.), Enzyme-mediated resistance to antibiotics: mechanisms, dissemination, and prospects for Inhibition. ASM Press, Washington, DC.

11. Bowler LD, Zhang QY, Riou JY, Spratt BG. 1994. Interspecies recombination between the *penA* genes of *Neisseria meningitidis* and commensal *Neisseria* species during the emergence of penicillin resistance in *N. meningitidis*: natural events and laboratory simulation. J Bacteriol 176:333–337.

12. Papp-Wallace KM, Endimiani A, Taracila MA, Bonomo RA. 2011. Carbapenems: Past, present, and future. Antimicrob Agents Chemother 55:4943–4960.

13. Doumith M, Ellington MJ, Livermore DM, Woodford N. 2009. Molecular mechanisms disrupting porin expression in ertapenem-resistant *Klebsiella* and *Enterobacter* spp. clinical isolates from the UK. J Antimicrob Chemother 63:659–667.

14. Li XZ, Ma D, Livermore DM, and Nikaido H. 1994. Role of efflux pump(s) in intrinsic resistance of *Pseudomonas aeruginosa*: active efflux as a contributing factor to β-lactam resistance. Antimicrob Agents Chemother 38:1742–1752.

15. Li XZ, Nikaido H, Poole K. 1995. Role of MexA-MexB-OprM in antibiotic efflux in *Pseudomonas aeruginosa*. Antimicrob Agents Chemother 39:1948–1953.

16. Li XZ, Zhang L, Poole K. 2000. Interplay between the MexAMexB-OprM multidrug efflux system and the outer membrane barrier in the multiple antibiotic resistance of *Pseudomonas aeruginosa*. J Antimicrob Chemother 45:433–436.

17. Hall BG, Barlow M. 2004. Evolution of the serine β-lactamases: past, present and future. Drug Resist Updat 7:111–123.

18. Barlow M, Hall BG. 2002. Phylogenetic analysis shows that the OXA β-lactamase genes have been on plasmids for millions of years. J Mol Evol 55:314 –321.

19. Mittl PR, Luthy L, Hunziker P, Grutter MG. 2000. The cysteine-rich protein A from *Helicobacter pylori* is a β-lactamase. J Biol Chem 275:17693–17699.

20. Rammelkamp CH, Maxon T. 1942. Resistance of *Staphylococcus aureus* to the action of penicillin. Proc Soc Exp Biol Med 51:386–389.

21. Kirby WM. 1944. Extraction of a highly potent penicillin inactivator from penicillin resistant staphylococci. Science 99:452–453.

22. Massova I, Mobashery S. 1998. Kinship and diversification of bacterial penicillin-binding proteins and β-lactamases. Antimicrob Agents Chemother 42:1–17.

23. Bush K. 2018. Past and present perspectives on β-lactamases. Antimicrob Agents Chemother 62(10).

24. Fisher JF, Meroueh SO, Mobashery S. 2005. Bacterial resistance to β-lactam antibiotics: compelling opportunism, compelling opportunity. Chem Rev 105(2):395-424.

25. Knott-Hunziker V, Waley SG, Orlek BS, Sammes PG. 1979. Penicillinase active sites: labelling of serine-44 in β-lactamase I by 6betabromopenicillanic acid. FEBS Lett 99:59–61.

26. Zhang HM, Hao Q. 2011. Crystal structure of NDM-1 reveals a common β-lactam hydrolysis mechanism. FASEB J 25:2574 –2582.

27. Ambler RP. 1980. The structure of β-lactamases. Philos Trans R Soc Lond B Biol Sci 289(1036):321-331.

28. Bush K, Jacoby GA, Medeiros AA. 1995. A functional classification scheme for β-lactamases and its correlation with molecular structure. Antimicrob Agents Chemother 39:1211–1233.

29. Bush K, Jacoby GA. 2010. Updated functional classification of β-lactamases. Antimicrob Agents Chemother 54:969–976.

30. Reading C, Cole M. 1977. Clavulanic acid: a β-lactamase inhibitor from *Streptomyces clavuligerus*. Antimicrob Agents Chemother 11:852–857.

31. Stachyra T, Pechereau MC, Bruneau JM, Claudon M, Frère JM, Miossec C, Coleman K, Black MT. 2010. Mechanistic studies of the inactivation of TEM-1 and P99 by NXL104, a novel non-β-lactam β-lactamase inhibitor. Antimicrob Agents Chemother 54:5132–5138.

32. Saino Y, Kobayashi F, Inoue M, Mitsuhashi S. 1982. Purification and properties of inducible penicillin β-lactamase isolated from *Pseudomonas maltophilia*. Antimicrob Agents Chemother 22:564 –570.

33. Bevan ER, Jones AM, Hawkey PM. 2017. Global epidemiology of CTX-M β-lactamases: temporal and geographical shifts in genotype. J Antimicrob Chemother. 72:2145-2155.

34. Sader HS, Mendes RE, Pfaller MA, Shortridge D, Flamm RK, Castanheira M. 2017. Antimicrobial activities of aztreonam-avibactam and comparator agents against contemporary (2016) clinical *Enterobacteriaceae* isolates. Antimicrob Agents Chemother 62(1).

35. Kazmierczak KM, Biedenbach DJ, Hackel M, Rabine S, de Jonge BL, Bouchillon SK, Sahm DF, Bradford PA. 2016. Global dissemination of *bla*KPC into bacterial species beyond *Klebsiella pneumoniae* and in vitro susceptibility to ceftazidime-avibactam and aztreonam-avibactam. Antimicrob. Agents Chemother 60(8):4490-500.

36. Frase H, Shi Q, Testero SA, Mobashery S, Vakulenko SB. 2009. Mechanistic basis for the emergence of catalytic competence against carbapenem antibiotics by the GES family of β-lactamases. J Biol Chem 284, 29509–29513.

37. Queenan AM, Bush K. 2007. Carbapenemases: the versatile β-lactamases. Clin Microbiol Rev 20:440–458.

38. Kazmierczak KM, Rabine S, Hackel M, McLaughlin RE, Biedenbach DJ, Bouchillon SK, Sahm DF, Bradford PA. 2016. Multiyear, multinational survey of the incidence and global distribution of metallo-β-lactamase-producing *Enterobacteriaceae* and *Pseudomonas aeruginosa*. Antimicrob Agents Chemother 60(2):1067–1078.

39. Lauretti L, Riccio ML, Mazzariol A, Cornaglia G, Amicosante G, Fontana R, Rossolini GM. 1999. Cloning and characterization of blaVIM, a new integron-borne metallo-β-lactamase gene from a *Pseudomonas aeruginosa* clinical isolate. Antimicrob Agents Chemother 43(7):1584-90.

40. Bush K, Bradford PA. 2019. Interplay between β-lactamases and new β-lactamase inhibitors. Nat Rev Microbiol 17(5):295-306.

41. Livermore DM, Canton R, Gniadkowski M, Nordmann P, Rossolini GM, Arlet G, Ayala J, Coque TM, Kern-Zdanowicz I, Luzzaro F, Poirel L, Woodford N. 2007. CTX-M: Changing the face of ESBLs in Europe. J Antimicrob Chemother 59:165-174.

42. Bush K. 2010. Alarming β-lactamase-mediated resistance in multidrug-resistant Enterobacteriaceae. Curr Opin Microbiol 13:558-564.

43. Matagne A, Lamotte-Brasseur J, Frère JM. 1998. Catalytic properties of class A β-lactamases: efficiency and diversity. Biochem J 330:581-598.

44. Knox JR, Moews PC. 1991. Beta-lactamase of Bacillus licheniformis 749/C. Refinement at 2 Å resolution and analysis of hydration. J Mol Biol 220: 435-55.

45. Jelsch C, Lenfant F, Masson JM, Samama JP. 1992. B-lactamase TEM-1 of *E. coli*. Crystal structure determination at 2.5 Å resolution. FEBS Lett 299: 135-42.

46. Guillaume G, Vanhove M, Lamotte-Brasseur J, Ledent P, Jamin M, Joris B, Frère JM. 1997. Site-directed mutagenesis of glutamate 166 in two β-lactamases. Kinetic and molecular modeling studies. J Biol Chem 272: 5438-44.

47. Imtiaz U, Billings E, Knox JR, et al. 1993. Inactivation of class A β-lactamases by clavulanic acid: the role of arginine244 in a proposed nonconcerted sequence of events. J Am Chem Soc; 115: 4435-42.

48. Imtiaz U, Billings E, Knox JR, Mobashery S. 1994. A structure-based analysis of the inhibition of class A β-lactamases by sulbactam. Biochemistry 33(19): 5728-38.

49. Strynadka NCJ, Martin R, Jensen SE, et al. 1996. Structure-based design of a potent transition state analogue for TEM1 β-lactamase. Nature Struct Biol 3(8): 688-95.

50. Poirel L, Le Thomas I, Naas T, Karim A, Nordmann P. 2000. Biochemical sequence analyses of GES-1, a novel class A extended-spectrum β-lactamase, and the class 1 integron In52 from *Klebsiella pneumoniae.* Antimicrob Agents Chemother 44:622-32.

51. Jeong SH, Bae IK, Kim D, Hong SG, Song JS, Lee JH, Lee SH. 2005. First outbreak of *Klebsiella pneumoniae* clinical isolates producing GES-5 and SHV-12 extended-spectrum β-lactamases in Korea. Antimicrob Agents Chemother 49:4809-4810.

52. Bae IK, Lee YN, Jeong SH, Hong SG, Lee JH, Lee SH, Kim HJ, Youn H. 2007. Genetic and biochemical characterization of GES-5, an extended spectrum class A β-lactamase from *Klebsiella pneumoniae*. Diagn Microbiol Infect Dis 58:465−468.

53. Bebrone C, Bogaerts P, Delbruck H, Bennink S, Kupper MB, Rezende de Castro R, Glupczynski Y, Hoffmann KM. 2013. GES-18, a new carbapenemhydrolyzing GES-type β-lactamase from *Pseuodomonas aeruginosa* that contains Ile80 and Ser170 residues. Antimicrob Agents Chemother 57:396-401.

54. Bogaerts P, Naas T, El Garch F, Cuzon G, Deplano A, Delaire T, HuangTD, Lissoir B, Nordmann P, Glupczynski Y. 2010. GES extendedspectrum-β-lactamases in *Acinetobacter baumannii* isolates in Belgium. Antimicrob Agents Chemother 54:4872-4878.

55. Al-Agamy MH, Jeannot K, El-Mahdy TS, Shibl AM, Kattan W, Plesiat P, Courvalin P. 2017. First detection of GES-5 carbapenemase-producing *Acinetobacter baumannii* isolate. Microb Drug Resist 23:556 −562.

56. Bonnin RA, Nordmann P, Potron A, Lecuyer H, Zahar JR, Poirel L. 2011. Carbapenem-hydrolyzing GES-type extended spectrum β-lactamase in *Acinetobacter baumannii*. Antimicrob Agents Chemother 55:349-354.

57. Moubareck C, Bremont S, Conroy MC, Courvalin P, Lambert T. 2009. GES-11, a novel integron-associated GES variant in *Acinetobacter baumannii*. Antimicrob Agents Chemother 53:3579 −3581.

58. Cuzon G, Bogaerts P, Bauraing C, Huang TD, Bonnin RA, Glupczynski Y, Naas T. 2016. Spread of plasmids carrying multiple GES variants. Antimicrob Agents Chemother 60:5040-5043.

59. Smith CA, Caccamo M, Kantardjieff KA, Vakulenko S. 2007. Structure of GES-1 at atomic resolution: insights into the evolution of carbapenemase activity in the class A extended- spectrum β-lactamases. Acta Crystallogr Sect D 63:982–992.

60. Smith CA, Frase H, Toth M, Kumarasiri M, Wiafe K, Munoz J, Mobashery S, Vakulenko SB. 2012. Structural basis for progression toward the carbapenemase activity in the GES family of β-lactamases. J Am Chem Soc 134:19512–19515.

61. Stewart NK, Smith CA, Frase H, Black DJ, Vakulenko SB. 2015. Kinetic and structural requirements for carbapenemase activity in GES-type β-lactamases. Biochemistry 54:588–597.

62. Raquet X, Lamotte-Brasseur J, Bouillenne F, Frere JM. 1997. A disulfide bridge near the active site of carbapenem-hydrolyzing class A β-lactamases might explain their unusual substrate profile. Proteins 27:47–58.

63. Majiduddin FK, Palzkill T. 2003. Amino acid sequence requirements at residues 69 and 238 for the SME-1 β-lactamase to confer resistance to β-lactam antibiotics. Antimicrob Agents Chemother 47:1062–1067.

64. Smith CA, Nossoni Z, Toth M, Stewart NK, Frase H, Vakulenko SB. 2016. Role of the conserved disulfide bridge in class A carbapenemases. J Biol Chem 291:22196–22206.

65. Ho SN, Hunt HD, Horton RM, Pullen JK, Pease LR. 1989. Site-directed mutagenesis by overlap extension using a polymerase chain reaction. Gene 77:51-59.

66. Clinical and Laboratory Standards Institute. Methods for Dilution Antimicrobial Susceptibility Tests for Bacteria that Grow Aerobically: Approved Standard, 11th ed.; CLSI document M07; Clinical and Laboratory Standards Institute: Wayne, PA, USA, 2018.

67. Laemmli UK. 1970. Cleavage of structural proteins during the assembly of the head of bacteriophage T4. Nature 227:680–685.

68. Bradford MM. 1976. A rapid and sensitive method for the quantitation of microgram quantities of protein utilizing the principle of protein-dye binding. Anal Biochem 72:248–254.

69. De Meester F, Joris B, Reckinger G. 1987. Automated analysis of enzyme inactivation phenomena. Application to β-lactamases and DDpeptidases. Biochem Pharmacol 36:2393–2403.

70. Segel IH. 1976. Biochemical calculations, 2nd ed, p 236–241. John Wiley & Sons, New York,NY.

71. Van Der Spoel D, Lindahl E, Hess B, Groenhof G, Mark AE, Berendsen HJC. 2005. GROMACS: fast, flexible and free. J Comput Chem 26:1701–1718.

72. Van Gunsteren WF, Billeter SR, Eising AA, Hunenberger PH, Kruger P, Mark AE, Scott WRP, Tironi IG. 1996. Biomolecular simulation: the GROMOS96 manual and user guide. Vdf Hochschulverlag AG an der ETH Zurich, Zurich, Switzerland.

73. Schaftenaar G, Noordik JH. 2000. Molden: a pre- and post-processing program for molecular and electronic structures. J Comput Aided Mol Des 14:123–134.

74. Darden TA, York DM, Pedersen LG. 1993. Particle mesh Ewald: an $N \cdot \log(N)$ method for Ewald sums in large systems. J Chem Phys 98:10089.

75. Bussi G, Donadio D, Parrinello M. 2007. Canonical sampling through velocity rescaling. J Chem Phys 126:014101.

76. Hess B, Bekker H, Berendsen HJC, Fraajie JGEM. 1997. LINCS: a linear constraint solver for molecular simulations. J Comput Chem 18:1463–1472.

77. Frisch MJ, Trucks GW, Schlegel HB, Scuseria GE, Robb MA, Cheeseman JR, Scalmani G, Barone V, Mennucci B, Petersson GA, Nakatsuji H, Caricato M, Li X, Hratchian HP, Izmaylov AF, Bloino J, Zheng G, Sonnenberg JL, Hada M, Ehara M, Toyota K, Fukuda R, Hasegawa J, Ishida M, Nakajima T, Honda Y, Kitao O, Nakai H, Vreven T, Montgomery JA, Jr, Peralta JE, Ogliaro F, Bearpark M, Heyd JJ, Brothers E, Kudin KN, Staroverov VN, Kobayashi R, Normand J, Raghavachari K, Rendell A, Burant JC, Iyengar SS, Tomasi J, Cossi M, Rega N, Millam JM, Klene M, Knox JE, Cross JB, et al. 2009. Gaussian 09, Revision E.01, Gaussian, Inc., Wallingford, CT.

78. Amadei A, Linssen ABM, Berendsen HJC. 1993. Essential dynamics of proteins. Proteins 17:412– 425.

79. Piccirilli A, Mercuri PS, Galleni M, Aschi M, Matagne A, Amicosante G, Perilli M. 2018. P174E Substitution in GES-1 and GES-5 β-Lactamases Improves Catalytic Efficiency toward Carbapenems. Antimicrob Agents Chemother 62(5).

80. Lim HM, Pene JJ, Shaw RW. 1988. Cloning, nucleotide sequence, and expression of the Bacillus cereus 5/B/6 β-lactamase structural gene. J. Bacteriol. 170: 2873–2878.

81. Walsh TR, Hall L, Assinder SJ, Nichols WW, Cartwright SJ, MacGowan AP, Bennett PM. 1994. Sequence analysis of the L1 metallo-β-lactamase from *Xanthomonas maltophilia*. Biochim Biophys Acta 1218:199–201.

82. Laraki N, Galleni M, Thamm I, Riccio ML, Amicosante G, Frère JM, Rossolini GM. 1999. Structure of In31, a *bla*IMP-containing *Pseudomonas aeruginosa* integron phyletically related to In5, which carries an unusual array of gene cassettes. Antimicrob Agents Chemother 43: 890–901.

83. Bennett PM. 2008. Plasmid encoded antibiotic resistance: acquistion and transfer of antibiotic resistance genes in bacteria. Br J Pharmacol 153: S347–S357.

84. Mojica MF, Bonomo RA, Fast W. 2015. B1-metallo-β-lactamases: Where do we stand? Curr Drug Targets 17:1029–1050.

85. Ullah JH, Walsh TR, Taylor IA, Emery DC, Verma CS, Gamblin SJ, Spencer J. 1998. The crystal structure of the L1 metallo-β-lactamase from *Stenotrophomonas maltophilia* at 1.7 A° resolution. J Mol Biol 284: 125–136.

86. Concha NO, Rasmussen BA, Bush K, Herzberg O. 1996. Crystal structure of the wide-spectrum binuclear zinc β-lactamase from *Bacteroides fragilis*. Structure 4: 823–836.

87. Garau G, Garcia-Saez I, Bebrone C, Anne C, Mercuri P, Galleni M, Frère JM, Dideberg O. 2004. Update of the standard numbering scheme for class B β-lactamases. Antimicrob Agents Chemoter 48:2347-9.

88. Felici A, Amicosante G, Oratore A, Strom R, Ledengt P, Joris B, Fanuel L, Frère JM. 1993. An overview of the kinetic parameters of class B β-lactamases. Biochem J 291:151-5.

89. Segatore B, Massidda O, Satta G, Setacci D, Amicosante G. 1993. High specificity of CphA-encoded metallo-β-lactamase from *Aeromosan hydrophila* AE036 for carbapenems and its contribution to β-lactam resistance. Antimicrob Agents Chemoter 37:1324-8.

90. Rasmussen BA, Gluzman Y, Tally FP. 1990. Cloning and sequencing of the class B β-lactamase gene (ccrA) from *Bacteroides fragilis* TAL3636. Antimicrob Agents Chemoter 34:1590-2.

91. Rossolini GM, Franceschini N, Riccio ML, Mercuri PS, Perilli M, Galleni M, Frere JM, Amicosante G. 1998. Characterization and sequence of the Chryseobacterium (Flavobacterium) meningosepticum carbapenemase: a new molecular class B β-lactamase showing a broad substrate profile. Biochem J 332 (Pt 1):145-52.

92. Bebrone C. 2007. Metallo-β-lactamases (classification, activity, genetic organization, structure, zinc coordination) and their superfamily. Biochemical pharmacology 74(12):1686 701.

93. Poirel L, Heritier C, Nordmann P. 2005. Genetic and biochemical characterization of the chromosome-encoded class B β-lactamases from *Shewanella livingstonensis* (SLB-1) and *Shewanella frigidimarina* (SFB-1). J Antimicrob Chemother 55(5): 680-5.

94. Wommer S, Rival S, Heinz U, Galleni M, Frere JM, Franceschini N, Amicosante G, Rasmussen B, Bauer R, Adolph HW. 2002. Substrate-activated zinc binding of metallo-β-lactamases: physiological importance of mononuclear enzymes. J Biol Chem 277: 24142–24147.

95. Hall BG, Salipante SJ, Barlow M. 2004. Independent origins of subgroup Bl + B2 and subgroup B3 metallo-β-lactamases. J Mol Evol. 59:133-41.

96. Fonseca F, Bromley EH, Saavedra MJ, Correia A, Spencer J. 2011. Crystal structure of Serratia fonticola SFH-I: activation of the nucleophile in mono-zinc metallo-β-lactamases. J Mol Biol 411: 951–959.

97. Garau G, Bebrone C, Anne C, Galleni M, Frère JM, Dideberg O. 2005, A metallo-β-lactamase enzyme in action: Crystal structures of the monozinc carbapenemase CphA and its complex with biapenem. J Mol Biol 345:785–795.

98. Massidda O, Rossolini GM, Satta G. 1991. The *Aeromonas hydrophila* CphA gene: molecular heterogeneity among class B metallo-β-lactamases. J Bacteriol 173:4611–7.

99. Walsh TR, Gamblin S, Emery DC, MacGowan AP, Bennett PM. 1996. Enzyme kinetics and biochemical analysis of ImiS, the metallo-β-lactamase from *Aeromonas veronii* 163a. J Antimicrob Chemother 37:423–31.

100. Saavedra MJ, Peixe L, Sousa JC, Henriques I, Alves A, Correia A. 2003. Sfh-I, a subclass B2 metallo-β-lactamase from a *Serratia fonticola* environmental isolate. Antimicrob Agents Chemother 47:2330-3.

101. Avison MB, Higgins CS, von Heldreich CJ, Bennett PM, Walsh TR. 2001. Plasmid location and molecular heterogeneity of the L1 and L2 β-lactamase genes of *Stenotrophomonas maltophilia*. Antimicrob Agents Chemother 45(2):413-9.

102. Wachino J, Yoshida H, Yamane K, Suzuki S, Matsui M, Yamagishi T, Tsutsui A, Konda T, Shibayama K, Arakawa Y. 2011. SMB-1, a novel subclass B3 metallo-β-lactamase, associated with ISCR1 and a class 1 integron, from a carbapenem-resistant *Serratia marcescens* clinical isolate. Antimicrob Agents Chemother 55(11):5143-9.

103. Hernandez Valladares M, Felici A, Weber G, Adolph HW, Zeppezauer M, Rossolini GM, Amicosante G, Frère JM, Galleni M. 1997. Zn(II) dependence of the *Aeromonas hydrophila* AE036 metallo-β-lactamase activity and stability. Biochemistry 36:11534–11541.

104. Bebrone C, Delbrück H, Kupper MB, Schlömer P, Willmann C, Frère JM, Fischer R, Galleni M, Hoffmann KM. 2009. The structure of the dizinc subclass B2 metallo-β-lactamase CphA reveals that the second inhibitory zinc ion binds in the histidine site. Antimicrob Agents Chemother 53:4464–4471.

105. Zheng M, Xu D. 2013. New Delhi metallo-β-lactamase 1: substrate binding and catalytic mechanism, J Phys Chem B 117:11596–11607.

106. Yong D, Toleman MA, Giske CG, Cho HS, Sundman K, Lee K, Walsh TR. 2009. Characterization of a new metallo-β-lactamase gene, *bla*NDM-1, and a novel erythromycin esterase gene carried on a unique genetic structure in *Klebsiella pneumoniae* sequence type 14 from India. Antimicrob Agents Chemother 53:5046 −5054.

107. Rahman M, Mukhopadhyay C, Rai RP, Singh S, Gupta S, Singh A, Pathak A, Prasad KN. 2018. Novel variant NDM-11 and other NDM-1 variants in multidrug resistant *Escherichia coli* from South India. J Glob Antimicrob Resist 14:154 −157.

108. Kanzari L, Ferjani S, Saidani M, Hamzaoui Z, Jendoubi A, Harbaoui S, Ferjani A, Rehaiem A, Boutiba Ben Boubaker I, Slim A. 2018. First report of extremely drug resistant *Proteus mirabilis* isolate carrying plasmidmediated blaNDM-1 in a Tunisian intensive care unit. Int J Antimicrob Agents 52:906 −909.

109. Solgi H, Badmasti F, Giske CG, Aghamohammad S, Shahcheraghi F. 2018. Molecular epidemiology of NDM-1- and OXA-48-producing *Klebsiella pneumoniae* in an Iranian hospital: clonal dissemination of ST11 and ST893. J Antimicrob Chemother 73:1517−1524.

110. Kocsis E, Gužvinec M, Butic´ I, Krešic´ S, Crnek SŠ, Tambic´ A, Cornaglia G, Mazzariol A. 2016. *bla*NDM-1 carriage on IncR plasmid in Enterobacteriaceae strains. Microb Drug Resist 22:123−128.

111. Kumarasamy KK, Toleman MA, Walsh TR, Bagaria J, Butt F, Balakrishnan R, Chaudhary U, Doumith M, Giske CG, Irfan S, Krishnan P, Kumar AV, Maharjan S, Mushtaq S, Noorie T, Paterson DL, Pearson A, Perry C, Pike R, Rao B, Ray U, Sarma JB, Sharma M, Sheridan E, Thirunarayan MA, Turton J, Upadhyay S, Warner M, Welfare W, Livermore DM, Woodford N. 2010. Emergence of a new antibiotic resistance mechanism in India, Pakistan, and the UK: a molecular, biological, and epidemiological study. Lancet Infect Dis 10: 597–602.

112. Marrs ECL, Day KM, Perry JD. 2014. In vitro activity of mecillinam against Enterobacteriaceae with NDM-1 carbapenemase. J Antimicrob Chemoter 69:2873-2875.

113. Gonzalez LJ, Bahr G, Nakashige TG, Nolan EM, Bonomo RA, Vila AJ. 2016. Membrane-anchoring stabilizes and favors secretion of New Delhi Metallo-β-lactamase. Nat Chem Biol 12:516 −522.

114. Wailan AM, Paterson DL, Caffery M, Sowden D, Sidjabat HE. 2015. Draft genome sequence of NDM-5-producing *Escherichia coli* sequence type 648 and genetic context of $bla_{\text{NDM-5}}$ in Australia. Genome Announc 3(2).

115. Nordmann P, Poirel L, Walsh TR, Livermore DM. 2011. The emerging NDM carbapenemases. Trends Microbiol. 19:588-595.

116. Bonnin RA, Poirel L, Carattoli A, Nordmann P. 2012. Characterization of an IncFII Plasmid Encoding NDM-1 from *Escherichia coli* ST131. PLoS ONE 7(4): e34752.

117. Kim Y, Cunningham MA, Mire J, Tesar C, Sacchettini J, Joachimiak A. 2013. NDM-1, the ultimate promiscuous enzyme: substrate recognition and catalytic mechanism FASEB J. 27(5):1917-27.

118. Carfi A, Duée E, Paul-Soto R, Galleni M, Frère JM, Dideberg O. 1998. X-ray structure of the ZnII β-lactamase from *Bacteroides fragilis* in an orthorhombic crystal form. Acta Crystallogr D Biol Crystallogr 54:45–57.

119. Carfi A, Pares S, Duée E, Galleni M, Duez C, Frère JM, Dideberg O. 1995. The 3-D structure of a zinc metallo-β-lactamase from *Bacillus cereus* reveals a new type of protein fold. EMBO J. 14:4914–4921.

120. Liénard BM, Garau G, Horsfall L, Karsisiotis AI, Damblon C, Lassaux P, Papamicael C, Roberts GC, Galleni M, Dideberg O, Frère JM, Schofield CJ. 2008. Structural basis for the broad-spectrum inhibition of metallo-β-lactamases by thiols. Org Biomol Chem 6:2282–2294.

121. Chen J, Chen H, Shi Y, Hu F, Lao X, Gao X, Zheng H, Yao W. 2013. Probing the effect of the non-active-site mutation Y229W in New Delhi metallo-β-lactamase-1 by site-directed mutagenesis, kinetic studies, and molecular dynamics simulations. PLoS One 8(12):e82080.

122. Marcoccia F, Leiros HKS, Aschi M, Amicosante G, Perilli M. 2018. Exploring the role of L209 residue in active site of NDM-1 a metallo-β- lactamase. PLoS One 13:e0189686.

123. Piccirilli A, Brisdelli F, Aschi M, Celenza G, Amicosante G, Perilli M. 2019. Kinetic Profile and Molecular Dynamic Studies Show that Y229W Substitution in an NDM-1/L209F Variant Restores the Hydrolytic Activity of the Enzyme toward Penicillins, Cephalosporins, and Carbapenems. Antimicrob Agents Chemother 27;63(4).

124. Segel IH. 1976. Methods of plotting enzyme kinetics data, p 236 −241. *In* Segel IH (ed), Biochemical calculations: how to solve mathematical problems in general biochemistry, 2nd ed. John Wiley & Sons, New York, NY.

125. Celenza G, Luzi C, Aschi M, Segatore B, Setacci D, Pellegrini C, Forcella C, Amicosante G, Perilli M. 2008. Natural D240G Toho-1 mutant conferring resistance to ceftazidime: biochemical characterization of CTX-M-43. J Antimicrob Chemother 62:991−997.

126. Petersen TN, Brunak S, von Heijne G, Nielsen H. 2011. SignalP 4.0: discriminating signal peptides from transmembrane regions. Nat Methods 8:785−786.

127. Clinical and Laboratory Standards Institute. 2018. Performance standards for antimicrobial susceptibility testing, 28th ed. CLSI document M100. Clinical and Laboratory Standards Institute, Wayne, PA.

128. Berendsen JC, Postma JPM, van Gunsteren WF, Hermans J. 1981. Interaction models for water in relation to protein hydration, p 331. *In* Pullman B (ed), Intermolecular forces. Reidel, Dordrecht, the Netherlands.

129. Aschi M, D′Abramo M, Amadei A. 2016. Photoinduced electron transfer in a dichromophoric peptide: a numerical experiment. Theor Chem Acc 135:132.

130. King DT, Worrall LJ, Gruninger R, Strynadka NC. 2012. New Delhi metallo-β-lactamase: structural insights into β-lactam recognition and inhibition. J Am Chem Soc 134:11362−11365.

131. Hornsey M, Phee L, Wareham DW. 2011. A novel variant, NDM-5, of the New Delhi metallo-β-lactamase in a multidrug-resistant *Escherichia coli* ST648 isolate recovered from a patient in the United Kingdom. Antimicrob Agents Chemother 55:5952–5954.

132. Nordmann P, Boulanger AE, Poirel L. 2012. NDM-4 metallo-β-lactamase with increased carbapenemase activity from *Escherichia coli*. Antimicrob Agents Chemother 56: 2184–2186.

133. Tomatis PE, Fabiane SM, Simona F, Carloni P, Sutton BJ, Vila AJ. 2008. Adaptive protein evolution grants organismal fitness by improving catalysis and flexibility. Proc Natl Acad Sci U S A. 105(52):20605-10.

134. Oelschlaeger P, Schmid RD, Pleiss J. 2003. Insight into the mechanism of the IMP-1 metallo-beta-lactamase by molecular dynamics simulations. Protein Eng. 16:341–350.

135. Brown MC, Verma D, Russell C, Jacobs DJ, Livesay DR. 2014. A case study comparing quantitative stability-flexibility relationships across five metallo-β-lactamases highlighting differences within NDM-1. Methods Mol Biol 1084:227–238.

136. Murphy TA, Catto LE, Halford SE, Hadfield AT, Minor W, Walsh TR, Spencer J. 2006. Crystal structure of *Pseudomonas aeruginosa* SPM-1 provides insights into variable zinc affinity of metallo-β-lactamases. J Mol Biol 357:890–903.

137. Guo Y, Wang J, Niu G, Shui W, Sun Y, Zhou H, Zhang Y, Yang C, Lou Z, Rao Z. 2011. A structural view of the antibiotic degradation enzyme NDM-1 from a superbug. Protein Cell 2:384-394.

138. King D, Strynadka N. 2011. Crystal structure of New Delhi metallo-β-lactamase reveals molecular basis for antibiotic resistance. Protein Sci 20:1484 −1491.

139. Zhang H, Ma G, Zhu Y, Zeng L, Ahmad A, Wang C, Pang B, Fang H, Zhao L, Hao Q. 2018. Active site conformational fluctuations promote the enzymatic activity of NDM-1. Antimicrob Agents Chemother 62:e01579-18.

140. Lisa MN, Palacios AR, Aitha M, Gonzalez MM, Moreno DM, Crowder MW, Bonomo RA, Spencer J, Tierney DL, Llarrull LI, Vila AJ. 2017. A general reaction mechanism for carbapenem hydrolysis by mononuclear and binuclear metallo-β-lactamases. Nature Commun 8:538.

141. Feng H, Liu X, Wang S, Fleming J, Wang DC, Liu W. 2017. The mechanism of NDM-1 catalyzed carbapenem hydrolysis is distinct from that of penicillin or cephalosporin hydrolysis. Nature Commun 8:2242.

142. Meini MR, Tomatis PE, Weinreich DM, Vila AJ. 2015. Quantitative description of a protein fitness landscape based on molecular features. Mol Biol Evol 32:1774 −1787.

143. Gonzalez MM, Abriata LA, Tomatis PE, Vila AJ. 2016. Optimization of conformational dynamics in an epistatic evolutionary trajectory. Mol Biol Evol 33:1768 −1776.

144.Neu HC. 1990. β-Lactamases β-lactamase inhibitors, and skin and skin-structure infections. J Am Acad Dermatol 22:896–904.

145. Prabaker K, Weinstein RA. 2011. Trends in antimicrobial resistance in intensive care units in the United States. Curr Opin Crit Care 17:472–479.

146. Harris P, Paterson D, Rogers B. 2015. Facing the challenge of multidrug-resistant gram-negative bacilli in Australia. Med J Aust 202:243–247.

147. Eisenstein BI, Sox T, Biswas G, Blackman E, Sparling PF. 1977. Conjugal transfer of the gonococcal penicillinase plasmid. Science 195:998–1000.

148. Medeiros AA, O'Brien TF. 1975. Ampicillin-resistant *Haemophilus influenzae* type B possessing a TEM-type β-lactamase but little permeability barrier to ampicillin. Lancet 1:716–719.

149. Fisher J, Charnas RL, Knowles JR. 1978. Kinetic studies on the inactivation of *Escherichia coli* RTEM β-lactamase by clavulanic acid. Biochemistry 17:2180–2184.

150. Charnas RL, Fisher J, Knowles JR. 1978. Chemical studies on the inactivation of *Escherichia coli* RTEM β-lactamase by clavulanic acid. Biochemistry 17:2185–2189.

151. English AR, Retsema JA, Girard AE, Lynch JE, and Barth WE. 1978. CP-45,899, a beta-lactamase inhibitor that extends the antibacterial spectrum of β-lactams: initial bacteriological characterization. Antimicrob Agents Chemother 14:414–419.

152. Fisher J, Belasco JG, Charnas RL, Khosla S, Knowles JR. 1980. β-Lactamase inactivation by mechanism-based reagents. Philos Trans R Soc Lond B Biol Sci 289:309–319.

153. Kitzis MD, Goldstein FW, Labia R, Acar JF. 1983. Activity of sulbactam and clavulanic acid, alone and combined, on *Acinetobacter calcoaceticus* [French]. Ann Microbiol 134a, 163:168.

154. Aronoff SC, Jacobs MR, Johenning S, Yamabe S. 1984. Comparative activities of the β-lactamase inhibitors YTR 830, sodium clavulanate, and sulbactam combined with amoxicillin or ampicillin. Antimicrob Agents Chemother 26:580–582.

155. Payne DJ, Cramp R, Winstanley DJ, Knowles DJ. 1994. Comparative activities of clavulanic acid, sulbactam, and tazobactam against clinically important β-lactamases. Antimicrob Agents Chemother 38:767–772.

156. Shapiro AB. 2017. Kinetics of sulbactam hydrolysis by β-lactamases, and kinetics of β-lactamase inhibition by sulbactam. Antimicrob. Agents Chemother 61:e01612–17.

157. Kuzin AP, Nukaga M, Nukaga Y, Hujer A, Bonomo RA, Knox JR. 2001. Inhibition of the SHV-1 β-lactamase by sulfones: crystallographic observation of two reaction intermediates with tazobactam. Biochemistry 40:1861–1866.

158. Charbonneau P. 1994. Review of piperacillin/tazobactam in the treatment of bacteremic infections and summary of clinical efficacy. Intensive Care Med 20, (Suppl. 3):S43–S48.

159. Newton L, Kotowski A, Grinker M, Chun R. 2018. Diagnosis and management of pediatric sinusitis: a survey of primary care, otolaryngology and urgent care providers. Int J Pediatr Otorhinolaryngol 108:163–167.

160. Horita N, Shibata Y, Watanabe H, Namkoong H, Kaneko T. 2017. Comparison of antipseudomonal β-lactams for febrile neutropenia empiric therapy: systematic review and network meta-analysis. Clin Microbiol Infect 23:723–729.

161. Pilmis B, Jullien V, Tabah A, Zahar JR, Brun-Buisson C. 2017. Piperacillin-tazobactam as alternative to carbapenems for ICU patients. Ann Intensive Care 7:113.

162. Drawz SM, Papp-Wallace KM, Bonomo RA. 2014. New β-lactamase inhibitors: a therapeutic renaissance in an MDR world. Antimicrob Agents Chemother 58:1835–1846.

163. Coleman K. 2011. Diazabicyclooctanes (DBOs): a potent new class of non-β-lactam β-lactamase inhibitors. Curr. Opin. Microbiol. 14:550–555.

164. Livermore DM, Mushtaq S, Warner M, Zhang J, Maharjan S, Doumith M, Woodford N. 2011. Activities of NXL104 combinations with ceftazidime and aztreonam against carbapenemase-producing Enterobacteriaceae. Antimicrob Agents Chemother. 55:390–394.

165. Ehmann DE, Jahić H, Ross PL, Gu RF, Hu J, Kern G, Walkup GK, Fisher SL. 2012. Avibactam is a covalent, reversible, non-β-lactam β-lactamase inhibitor. Proc. Natl Acad. Sci. USA 109:11663–11668.

166. Citron DM, Tyrrell KL, Merriam V, Goldstein EJ. 2011. In vitro activity of ceftazidime-NXL104 against 396 strains of β-lactamase-producing anaerobes. Antimicrob Agents Chemother 55:3616–3620.

167. Biedenbach DJ, Kazmierczak K, Bouchillon SK, Sahm DF, Bradford PA. 2015. In vitro activity of aztreonam-avibactam against a global collection of Gram-negative pathogens from 2012 and 2013. Antimicrob Agents Chemother 59:4239–4248.

168. US National Library of Medicine. 2019. ClinicalTrials.gov https://clinicaltrials.gov/ct2/show/NCT03329092.

169. Blizzard TA, Chen H, Kim S, Wu J, Bodner R, Gude C, Imbriglio J, Young K, Park YW, Ogawa A, Raghoobar S, Hairston N, Painter RE, Wisniewski D, Scapin G, Fitzgerald P, Sharma N, Lu J, Ha S, Hermes J, Hammond ML. 2014. Discovery of MK-7655, a β-lactamase inhibitor for combination with Primaxin(R). Bioorg Med Chem Lett 24:780 –785.

170. Hirsch EB, Ledesma KR, Chang KT, Schwartz MS, Motyl MR, Tam VH. 2012. In vitro activity of MK-7655, a novel β-lactamase inhibitor, in combination with imipenem against carbapenem-resistant Gram-negative bacteria. Antimicrob Agents Chemother 56:3753–3757.

171. Livermore DM, Warner M, Mushtaq S. 2013. Activity of MK-7655 combined with imipenem against Enterobacteriaceae and Pseudomonas aeruginosa. J Antimicrob Chemother 68:2286 –2290.

172. Lapuebla A, Abdallah M, Olafisoye O, Cortes C, Urban C, Landman D, Quale J. 2015. Activity of imipenem with relebactam against Gram-negative pathogens from New York City. Antimicrob Agents Chemother 59: 5029–5031.

173. Papp-Wallace KM, Bonomo RA. 2016. New β-lactamase inhibitors in the clinic. Infect Dis Clin North Am 30:441– 464.

174. US National Library of Medicine. 2018. ClinicalTrials.gov https://clinicaltrials.gov/ct2/show/NCT03182504.

175. Livermore DM, Mushtaq S, Warner M, Vickers A, Woodford N. 2017. In vitro activity of cefepime/zidebactam (WCK 5222) against Gram-negative bacteria. J Antimicrob Chemother 72: 1373–1385.

176. US National Library of Medicine. 2016. ClinicalTrials.gov https://clinicaltrials.gov/ct2/show/NCT02674347.

177. Durand-Reville TF, Guler S, Comita-Prevoir J, Chen B, Bifulco N, Huynh H, Lahiri S, Shapiro AB, McLeod SM, Carter NM, Moussa SH, Velez-Vega C, Olivier NB, McLaughlin R, Gao N, Thresher J, Palmer T, Andrews B, Giacobbe RA, Newman JV, Ehmann DE, de Jonge B, O'Donnell J, Mueller JP, Tommasi RA, Miller AA. 2017. ETX2514 is a broad-spectrum -lactamase inhibitor for the treatment of drug-resistant Gram-negative bacteria including Acinetobacter baumannii. Nat Microbiol 2:17104.

178. US National Library of Medicine. 2019. ClinicalTrials.gov https://clinicaltrials.gov/ct2/show/NCT03445195.

179. Hecker SJ, Reddy KR, Totrov M, Hirst GC, Lomovskaya O, Griffith DC, King P, Tsivkovski R, Sun D, Sabet M, Tarazi Z, Clifton MC, Atkins K, Raymond A, Potts KT, Abendroth J, Boyer SH, Loutit JS, Morgan EE, Durso S, Dudley MN. 2015. Discovery of a cyclic boronic acid β-lactamase inhibitor (RPX7009) with utility versus class A serine carbapenemases. J Med Chem 58:3682–3692.

180. Kaye KS, Bhowmick T, Metallidis S, Bleasdale SC, Sagan OS, Stus V, Vazquez J, Zaitsev V, Bidair M, Chorvat E, Dragoescu PO, Fedosiuk E, Horcajada JP, Murta C, Sarychev Y, Stoev V, Morgan E, Fusaro K, Griffith D, Lomovskaya O, Alexander EL, Loutit J, Dudley MN, Giamarellos-Bourboulis EJ. 2018. Effect of meropenem-vaborbactam versus piperacillin-tazobactam on clinical cure or improvement and microbial eradication in complicated urinary tract infection: the TANGO I randomized clinical trial. JAMA 319:788–799.

181. US Food & Drug Administration. Highlights of prescribing information. 2018. Vabomere™ (meropenem and vaborbactam) for injection, for intravenous use. FDA.gov https://www.accessdata.fda.gov/drugsatfda_docs/label/2017/209776lbl.pdf.

182. Everett M, Sprynski N, Coelho A, Castandet J, Bayet M, Bougnon J, Lozano C, Davies DT, Leiris S, Zalacain M, Morrissey I, Magnet S, Holden K, Warn P, De Luca F, Docquier JD, Lemonnier M. 2018. Discovery of a novel metallo-β- lactamase inhibitor that potentiates

meropenem activity against carbapenem-resistant Enterobacteriaceae. Antimicrob Agents Chemother 62:e00074–18.

183. Marcoccia F, Mercuri PS, Galleni M, Celenza G, Amicosante G, Perilli M. 2018. A Kinetic Study of the Replacement by Site Saturation Mutagenesis of Residue 119 in NDM-1 Metallo-β-Lactamase. Antimicrob Agents Chemother. 62(8).

184. Piccirilli A, Segatore B, Daigle D, Amicosante G, Perilli M. 2019. VNRX-5133 maintains potent inhibitory activity in engineered NDM-1 variants with increased cefepime hydrolytic efficiency. [abstract P1178]. Presented at the 29th European Congress of Clinical Microbiology and Infectious Diseases (ECCMID) in Amsterdam, Netherlands.

"If you think you are beaten, you are,

If you think you dare not, you don't

If you like to win, hut you think you can't,

It is almost certain you won't.

If you think you'll lose, you're lost

For out of the world we find,

Success begins with a fellow's will-It's all in the state of mind.

If you think you are outclassed, you are,

You've got to think high to rise,

You've got to be sure of yourself before

You can ever win a prize.

Life's battles don't always go

To the stronger or faster man,

But soon or late the man who wins

Is the man WHO THINKS HE CAN!"